MICROSTRUCTURE AND MECHANICAL PROPERTIES OF LOW CARBON LOW ALLOY MARTENSITE

A THESIS

submitted in fulfilment of the requirements

for the award of the degree

of

DOCTOR OF PHILOSOPHY

in

METALLURGICAL ENGINEERING

by

ARUN KUMAR PATWARDHAN

DEPARTMENT OF METALLURGICAL ENGINEERING

UNIVERSITY OF ROORKEE

ROORKEE-247672 INDIA

JULY, 1979

TO

THE ALMIGHTY

Lord:

Ganesh

Shanidev

Sai Baba of Shirdi

Venkateswara of

Tirupati

TO

THE REVERED MEMORY

OF

MY FATHER

AND

TO

THE CONSTANT INSPIRATION

OF

MY MOTHER

CERTIFICATE

This is to certify that the thesis entitled MICROSTRUCTURE AND MECHANICAL PROPERTIES OF LOW CARBON LOW ALLOY MARTENSITE being submitted by Mr. A.K. Patwardhan

PAPERS PUBLISHED/ACCEPTED FOR PUBLICATION BASED ON PART OF THE RESULTS REPORTED IN THE THESIS

1. Trans. Iron and Steel Instt. of Japan; 16, 297 (1976).
2. Scripta Metallurgica; 10, 677 (1976).
3. 'Structural Studies in Some Extra Low-Carbon Manganese - Silicon and Manganese -Silicon - Niobium High Strength Steels' -
   To appear in Archieves für das Eisenheutenwesen in 1979.

Certified that [illegible] Thesis/ Dissertation has been [illegible] for the award of [illegible] or of Philosophy [illegible]

No. Ex/452/E-10/79. 22.01.79.

Assistant Registrar (Exam.)

A C K N O W L E D G E M E N T

I am indebted to Dr. M.L.Mehta, Professor and Head of the Department of Metallurgical Engineering, University of Roorkee, for his continued interest, supervision and for useful suggestions during the course of this investigation.

I am extremely thankful to :

- Prof. G.W.Greenwood, Department of Metallurgy, University of Sheffield (U.K.) for providing laboratory facilities, Dr. J.A.Whiteman of the same department for useful discussions and Association of Commonwealth Universities, London for financial support.
- Prof. M.N.Saxena for interest in the early stages of the work.
- Dr. V.G.Paranjpe Ex-Director, R and D, TISCO, Jamshedpur for helping with melts and for critical suggestions.
- Dr. M.K.Asundi, Head Physical Metallurgy Section of the Metallurgy Division, BARC, Bombay, for providing facilities for testing and electron microscopy.
- M/S Bombay Forge and Bharat Forge for providing forging facilities.

- Prof. P.K.Rao and Prof. K.M.Pai of the Met. Engg. Deptt. I.I.T., Bombay for providing laboratory facilities including ESR.

I wish to record my sincerest thanks to Dr.M.L.Kapoor, Professor Metallurgical Engineering Department, Dr.R.K.Sinha and Dr.S.Ray for helpful discussions, Mr.V.N.S.Mathur for suggesting modifications and for helping in the correction work and Mr.R.P.Ram for critical suggestions and help. Encouragement and help from my colleagues, Dr.D.B.Goel and Dr.Satya Prakash is greatly appreciated.

The help rendered by Mr.Imran Ahmed, Mr.S.K.Seth, Mr.S.P.Kush, Mr.S.S.Gupta, Mr.R.P.Gupta and Mr.M.C.Vaish is greatfully acknowledged. Thanks are also due to Mr.U.K.Mishra, who typed the manuscript.

A.K.PATWARDHAN

S Y N O P S I S

A critical survey of the literature on low alloy high strength (LAHS) steels revealed that they are most usefully employed in the proof strength range of 775-850 MN/m^2 whereever a combination of high strength coupled with good ambient - temperature and sub-zero temperature toughness is an essential requirement. Steels which normally cater to this range of proof strength are,(a) aircooled bainitic steels and, (b) quenched and tempered (Q and T) steels alloyed with Ni, Cr, Mo, V and Mn. Ausformed steels which could also be employed have been excluded since ausforming is confined only to those steels having transformation characteristics leading to 'bay' formation. The main drawback with the bainitic steels is that the stipulated level of toughness may not be attained because of the formation of unintended microconstituents such as (i) elongated carbides surrounding the bainitic ferrite regions and, (ii) the austenite-martensite (A-M) constituent. Although the toughness can be improved upon by tempering, the effective proof strength is lowered to $\sim$700 MN/m^2. The major problem with the Q and T steels is the necessity of making adjustments in the composition for toughening the ferrite matrix and for eliminating temper-embrittlement. Further, the difficulty in exercising control over carbide size, shape

and distribution can lead to an unexpected deterioration in the ambient and sub-zero temperature toughness.

There is thus a definite scope to explore the possibility of developing high strength steels in the proof strength range of 775-850 MN/m^2 in which the stipulated levels of ductility and particularly the toughness can be unfailingly attained. This forms the main theme of the present investigation. The alternative approach suggested to achieve the objective is based on the utilization of extra low-carbon lath (martensite) structure. Fundamentally, the investigation was carried out in two distinct stages : (a) experimentation with the sole purpose of designing an air-hardening base composition and, (b) assessment of the mechanical properties that would result when airhardening steels are subjected to control-hot forming (rolling and forging). Emphasis was laid on attaining high strength in combination with appropriate levels of ductility and toughness. Experimental techniques, relevant to the requirements, were employed.

On the basis of the information available in the literature, the effect of carbon content and alloying elements on the parameters of design interest particularly hardenability, strength, ductility and toughness was evaluated. A critical analysis of this data served as the basis for postulating a large number of manganese

bearing alloy systems which were likely to prove useful in designing new high strength steels. One such system, Fe-Mn-Si, was investigated by employing vacuum induction melts, in the composition range C = 0.01 to 0.03%, Mn = $\sim$2 to 5%, Si = $\sim$1 to 2.6%. Manganese promotes the formation of lath structure at a moderate cost and also improves low temperature toughness. Silicon was chosen since it delays the breakdown of martensite and raises the temperature of breakdown, reduces volume changes associated with the α to γ and reverse transformations. Further, it decreases the absorption of electrolytic hydrogen in low carbon steels, does not adversely affect the toughness even when present in amounts $>$ 0.3 % provided the nitrogen content is low and reduces the lattice parameter of ferrite thereby giving additional strengthening.

During the initial part of the study, the steels investigated were in the form of hot-swaged bars. Subjecting them to different heat treatments revealed that in most cases the microstructure observed was lath-like in nature although other microstructures namely high-dislocation-density-ferrite, polygonal-ferrite and an aggregate consisting of polygonal ferrite and lath constituent were also observed. A correlation between the microstructures and the resulting mechanical properties was qualitatively established. Two compositional

extremities for obtaining lath structure existed at 0.03% carbon level. The first, having a composition Fe-2.6% Mn-1.0% Si, yielded lath structure only on quenching from temperatures upwards of 900°C and exhibited proof strength in excess of 900 MN/m^2 and good toughness even at - 70°C in 1000°C water-quenched (WQ) condition. The other, having a composition Fe-5% Mn - 1.5% Si, yielded lath structure on annealing or quenching from 800°C upwards. When identically heat-treated as the previous alloy, it had a proof strength $\sim$ 1000 MN/m^2 and good toughness down to - 18°C. The room temperature ductility values of the two alloys were in excess of 20%. Other compositions investigated revealed that although the general mechanical properties were exceedingly good, their toughness precluded their general applications.

From the point of view of using minimal alloying elements, the composition Fe-2.6 Mn-1.0Si was promising. It was rendered air-hardening by altering its manganese content to arrive at a base composition Fe-3.7Mn-1.0Si. This was investigated at 0.022% and 0.055% carbon levels without and with $\sim$ 0.045% Nb in the as-rolled ($\sim$ 17 mm dia) condition. The first of the two carbon levels ensured that the precipitated carbides were at a minimum. The second level was chosen with a view to develop the

composition from carbon steels. Niobium was preferred since it acts as a grain refiner and also supresses the formation of polygonal ferrite. In terms of mechanical properties, the best results in the control-rolled condition were obtained with the composition containing 0.022% C and 0.042% Nb, which exhibited a proof strength ~ 780 MN/m^2, UTS of ~900 MN/m^2, percent elongation value ~ 27%. The overall toughness was exceedingly high, the ambient temperature toughness being in excess of 270J and impact transition temperature (ITT), based on 54J (40ft-lbs), around - 90°C. Raising the carbon content to 0.055% resulted in an increase in strength and a deterioration in toughness e.g. the 0.055% C, 0.042% Nb alloy exhibited PS ~930 MN/m^2, UTS ~1090 MN/m^2, USE ~170J and ITT of -30°C. The studies in the as-rolled condition thus provided information on the range of mechanical properties that can be achieved from the base composition Fe-3.7% Mn -1.0%Si.

A modification of the aforesaid airhardening base composition and containing Fe-4% Mn-0.4%Si-0.4% Mo-0.074% Nb-0.03%C was air induction melted and investigated as before in the as-forged ($17\frac{5}{7}$ mm square) condition. Molybdenum additions are useful in (a) eliminating harmful effects associated with grain boundary precipitation and segregation and therefore, can suitably counteract

the likely adverse effect on toughness if carbon content were to exceed the critical limit(~0.06%) and, (b) reducing volume changes associated with the α to γ and reverse transformations. The results obtained reveal that (a) the minimum value of the ambient temperature toughness in the control-forged condition is comparable to that obtained in forging quality high strength steels only after normalizing, normalizing and tempering (N and T) or N and T + Q and T heat treatments, (b) toughness of the stock, forged with intermediate reheating was much lower in comparison to that obtained on control forging but improved, on normalizing from 850°C, to a value comparable to that obtained on control forging. These observations, which reveal the strong dependence of the ambient temperature toughness on grain size, are of considerable theoretical and practical interest. The UTS and ductility were independent of the forging schedule, the levels obtained being 900-950 MN/m^2 and 20% respectively.

The lath structures obtained in the present study can be classified into two groups, (i) having hardness in the range of ~250 to ~300 HV_{30} and, (ii) having hardness in the range of ~300 to ~370 HV_{30}. Lath structures observed in the Fe-Mn, Fe-Ni and Fe-Ni-Co-Mo-Ti systems conform to the former. On the basis of (i) the results obtained so far and, (ii) the data available in the literature, a comprehensive model for the strengthening

the likely adverse effect on toughness if carbon content were to exceed the critical limit(~0.06%) and, (b) reducing volume changes associated with the α to γ and reverse transformations. The results obtained reveal that (a) the minimum value of the ambient temperature toughness in the control-forged condition is comparable to that obtained in forging quality high strength steels only after normalizing, normalizing and tempering (N and T) or N and T + Q and T heat treatments, (b) toughness of the stock, forged with intermediate reheating was much lower in comparison to that obtained on control forging but improved, on normalizing from 850°C, to a value comparable to that obtained on control forging. These observations, which reveal the strong dependence of the ambient temperature toughness on grain size, are of considerable theoretical and practical interest. The UTS and ductility were independent of the forging schedule, the levels obtained being 900-950 MN/m^2 and 20% respectively.

The lath structures obtained in the present study can be classified into two groups, (i) having hardness in the range of ~250 to ~300 HV_{30} and, (ii) having hardness in the range of ~300 to ~370 HV_{30}. Lath structures observed in the Fe-Mn, Fe-Ni and Fe-Ni-Co-Mo-Ti systems conform to the former. On the basis of (i) the results obtained so far and, (ii) the data available in the literature, a comprehensive model for the strengthening

in alloys based on lath structure was put forward. While doing so, due consideration was given to the sub-structural features constituting the lath structure.

In order to investigate the factors responsible for additional strengthening in the latter type of lath structures mentioned above, a detailed structural examination of the different alloys was carried out by X-ray diffraction using the Debye-Scherrer method. The results obtained revealed that although in most cases the structure was single phase α' (bcc), in some instances it consisted of α' (bcc) + retained γ (fcc) and α' (bcc) + $M_{23}C_6$ (sc). However, once, a diamond cubic structure (dc) was also observed. These results, which did not provide a direct clue to the reasons for the additional strengthening in the latter type of the lath structures, none the less proved useful in arriving at a better understanding of the structure-property aspect of steels based on lath structures.

The present investigation has thus revealed that by utilizing lath structures formed in Fe-Mn-Si, Fe-Mn-Si-Nb and Fe-Mn-Si-Mo-Nb systems, over the composition range already specified, proof strength in the range of 780-1080 MN/m^2, UTS in the range of $\sim$900 to $\sim$1150 MN/m^2, percentage elongation values $\sim$20% can be easily attained. Although the extra low-carbon lath structure is intrinsically tough, the ambient temperature and sub-zero temperature toughness would depend upon the heat-treatment and

the hot forming schedules employed. From the point of view of employing minimal yet optimum amount of alloying elements, the useful proof strength attainable from lath structures appears to be 800-850 MN/m^2.

P R E F A C E

The first chapter deals with the existing low alloy high strength steels out of which those, relying on precipitation hardening and bainite microstructure for their properties, were chosen for further discussion. For such steels, the properties most usefully lie in the range of 775-850 MN/m^2 with adequate toughness at ambient and subzero temperatures. The limitations of these steels were highlighted.

The second chapter is a critical assessment of the fundamental parameters involved in developing strong and tough steels to evaluate if it is possible to evolve an alternative approach overcoming the limitations of the bainitic and precipitation strengthened steels. From such a discussion it emerged that utilization of low carbon martensites may lead to the attainment of very useful mechanical properties.

Based on considerations, discussed in chapter-II an alternative approach to developing new steels is outlined in chapter 3 which led to the planning of new very low carbon alloys containing low cost elements manganese and silicon in place of the conventionally employed nickel etc.

The experimental techniques and procedures outlined in Chapter-III involved the examination of very low carbon Fe-Mn-Si, Fe-Mn-Si-Nb and Fe-Mn-Si-Mo-Nb alloys over a composition range C = 0.01 to 0.055, Mn = 1.8 to 5%, Si=0.4 to 2.6%, Mo = 0.4%, Nb = 0.04% and 0.07% with a view to establish an air-hardening base composition containing a minimum of alloying elements. Different alloys were examined in detail by mechanical testing, dilatometry, X-ray diffraction and optical microscopy and to a limited extent by replication, thin foil and scanning electron microcopy.

Experimental results and the analysis of the existing data has been spread out over four chapters.

The fifth chapter deals with the transformation behaviour and mechanical properties of extra low carbon Mn-Si steels in the heat-treated condition. This part of the study was undertaken primarily with a view to obtain clues for developing an air-hardening composition containing a minimum of alloying elements.

The sixth chapter deals in section 'A' with the effect of controlled mechanical working (rolling) on properties of Fe-Mn-Si and Fe-Mn-Si-Nb air-hardening steels at two different Nb and carbon contents. Section 'B' is devoted to a study of the effect of forging on the properties of an air-hardening steel based on Fe-Mn-Mo-Si-Nb system.

Chapter seven has been devoted to an analysis of the strengthening mechanisms in the alloys currently investigated and also in other alloys based on lath structure.

In eighth chapter results of structural investigations carried out by X-ray diffraction have been reported.

Conclusions drawn are enumerated in the nineth chapter.

ABBREVIATIONS

ppm	Parts per million
Wt. %	Weight percent
At. %	Atomic percent
FC	Furnace cooled
CC	Cooled at a controlled rate
AC	Air cooled
WQ	Water quenched
HV	Vickers hardness
HV_{30}, HV_{10}, HV_5	Vickers hardness at 30 kg, 10 kg and 5 kg loads respectively
YS	Yield strength
PS	Proof strength at 0.2% offset
UTS	Ultimate Tensile Strength
El	% Elongation
RA	% Reduction in Area
USE, ATT	Upper shelf energy, Ambient temperature toughness
ITT	Impact transition temperature
bcc	Body centred cubic
fcc	Face centred
dc	Diamond cubic
Sc	Simple cubic
Shear Transformation Structure	Microstructure formed by shear transformation

Acicular Microstructure	Microstructure with a plate/needle like appearance normally associated with shear transformation structures
σ_s	Increase in flowstress due to solid solution hardening
σ_{sub}	Increase in flowstress due to sub-structural strengthening

2 Mn or 2% Mn convey the same meaning.

CR	Control-Rolling
CF	Control-Forging
vvw	very very weak
vw	very weak
w	weak
m	medium
ms	Medium strong
s	Strong

Unless otherwise stated, composition is in weight percent.

C O N T E N T S

C H A P T E R - I

LOW ALLOY HIGH STRENGTH STEELS

1.1 INTRODUCTION

The term 'high strength steel' has varying interpretations. In its simplest form, it represents any steel which has strength higher than mild steel. Similarly, the term 'low alloy', which in a broad sense, conveys that the amount of major alloying element/ elements in a steel is around 5%, is very popular and widely acceptable. High strength steels are next only to mild steels as far as the total annual world consumption of different grades of steels is concerned (1). The most important reason for their development was the need for attaining higher strengths.

During the early days of their development, the use of high strength steels was based entirely on tensile strength as the main design criteria. Weldability and resistance to brittle failure were not considered essential requirements (2). A 0.3% carbon steel alloyed with 1.2 - 1.5% Mn and a small amount of silicon was very popular and was specified for a tensile strength range of 37-43 tsi $\sim$ 600 MN/m^2 (2). It soon emerged that the steel had very poor weldability and resistance to brittle failure which was traced essentially to its

high carbon content (2). The carbon content was, therefore, brought down to around 0.2% and the resulting loss in strength was made up by marginally raising the manganese and silicon contents (2).

With an increase in the demand for steels with higher yield strength and improved weldability, incorporation of alloying elements such as nickel, chromium, vandium and molybdenum and a further reduction in the carbon content was actively considered while designing new compositions. This, however, led to the attainment of unintended intermediate temperature acicular microstructures in place of the desired ones - the alloy compositions tended to be semi-airhardening type. This tendency was, therefore, used to advantage in attaining the maximum permissible hardening in a given grade by resorting to quenching. Tempering such a steel facilitated the attainment of any desired combination of mechanical properties. The quenched and tempered (Q and T) steels were thus developed (2). More or less simultaneously, a better understanding of (i) the effect of alloying elements in general and, (ii) the beneficial effect of boron additions, in supressing the formation of polygonal ferrite, in particular, led to the development of commercial bainitic steels, in which bainite was formed on continuous cooling. As a consequence of these developments, the useful level of yield/proof stength had been extended to about 45 tsi-around 700 MN/m^2 (2).

A significant development over the last 10-15 years has been the introduction of grain refined precipitation hardened-GRPH ferrite-pearlite steels (2). Low carbon (- 0.15%) - manganese steels microalloyed with Nb, V, Al and Ti have been shown to exhibit yield/proof strength in the range of 21-23 tsi (~ 342 MN/m^2) with good ductility and impact transition temperature in the as-rolled condition (2-4). Commercial HSLA steels containing Nb, V, and Al (2-4) and more recently titanium (5) have been developed and are quite popular. Pearlite reduced steels (PRS), in view of their improved weldability and toughness (without practically any reduction in strength), represent a further improvement over the GRPH ferrite-pearlite steels (6).

The advent and utilization of thermomechanical treatments for processing steels (7,8) and a better understanding of the effect of alloying elements on mechanical properties made it possible to extend the level of proof strength attainable in low alloy steels from ~ 50 tsi (~ 800 MN/m^2) to about 100 tsi (~ 1500 MN/m^2). Suitable examples in this regard are Ni-Cr-Mo and Mn-Mo steels used in the quenched and tempered condition (9), 3% Cr and 3%Co steels (10) and many steels in the ausformed condition (7,8). The versatility of low alloy steels vis-a-vis the attainment of proof strength over a large range from about 342 MN/m^2 to as high as

$\sim$ 1500 MN/m^2) is, therefore, evident.

Factors which will determine whether high strength steels in general can be used for increasing number of applications are (a) service conditions (b) availability of standard specification for design and (c) information on actual performance under service conditions. Weldability is considered an equally important factor in this regard (11). Information envisaged in (c) is difficult to obtain in structural applications e.g. ships and bridges and more readily obtainable in the field of transportation with the help of simulated laboratory tests. It is for this reason that high strength steels have gained and are gaining wider acceptability in the field of transportation as structural members and in sheet form (11).

Inspite of a general lack of standards and other relevant data, use of high strength steels offers definite advantages (11-13). In the field of structures, there is a reduction in structural weight since smaller sections can be used (11-13). In the field of transportation, the advantages envisaged are (a) a decrease in the dead weight of the vehicle and hence an increase in vehicle capacity, (b) possible improvement in the resistance to mechanical abrasion and corrosion and therefore, a saving in the maintenance cost. In view

of the above the use of high strength steels is considerably increasing. More important areas of their application are bridges and construction of buildings, transporration and earth moving equipment, ship and marine appliances, storage tanks and vessels, gas transmission pipe lines, communication and power distribution, heavy construction equipment and fastners and material handling equipment (11,13).

1.2 USER REQUIREMENTS

As has been stated earlier, the main requirements of the earlier high strength steels were a high yield strength, resistance to brittle failure and adequate weldability. In view of the extremely diverse and stringent service conditions to which the present day high strength steels have to cater to, the user requirements have become more diverse and exacting and can be summarised as follows:

a) A high yield/tensile ratio (12,14,15)

b) Adequate ductility at high strength (11,12,15,16-18)

c) Hardenability (11,12,15,16)

d) Notch toughness and resistance to crack propagation (11,12,15,16,18).

e) Resistance to fatigue failure (11,12,15,17)

f) Weldability (11-13,15,16,18)

g) Other properties such as: i). resistance to softening

at high temperatures (19,20),

ii) improved dimensional stability (19-24)

iii) corrosion and abrasion resistance (11,12,16) and,

iv) freedom from hydrogen embrittlement.

A majority of these requirements could be met at least in part through a combination of alloying and through the experience gained in different thermal and mechanical treatments. Many of the above parameters operate in a manner counter to each other e.g. an increase in strength in general is accompained by a decrease in ductility and toughness. Most often in practice a compromise has to be struck between various properties desirable and certain minor requirements have to be sacrified or met with only partly in preference to the major ones. So, also, many of the requirements are related with high strength and good ductility e.g. high fatigue resistance is related to the presence of adequate ductility coupled with high strength. Thus, the user requirements essentially reduce down to the economic attainment of high strength and appropriate ductility and toughness with the emphasis on improving ductility and toughness as much as possible.

1.3 CLASSIFICATION

Based on their development, high strength steels can be classified as

i) PHGR F-P STEELS - Useful yield strength $\sim$ 360 MN/m^2

ii) Continuously Cooled Bainitic Steels - Max. attainable proof strength $\sim$ 900 MN/m^2. Useful proof strength range $\sim$ 360 to 700 MN/m^2.

iii) Quenched and Tempered (Q and T) Steels - Max. attainable proof strength $\sim$ 1500 MN/m^2. Useful proof strength range $\sim$ 775 to 850 MN/m^2.

iv) Ausformed Steels - Max. attainable proof strength $\sim$ 1500 MN/m^2.

Amongst the above grades, a brief mention of the ausformed steels is necessary since they have not been discussed while outlining the development of high strength steels in sec. 1.1. Ausforming essentially involves imparting controlled mechanical deformation to metastable austenite prior to its undergoing phase transformation and therefore has limited applicability (7,8). In view of the permissible upper limit upto which alloying elements may be present in a given composition, the optimally useful proof strength range in LAHS steels (appropriate ductility, toughness and transition temperature being assured) appears to be 775 - 850 MN/m^2. Therefore, only two of the above mentioned categories of steels namely (a) bainitic steels and, (b) Q and T steels qualify for a further detailed discussion.

1.3.1 Quenched and Tempered Steels

Majority of these steels contain nickel, manganese, and carbide forming elements such as chromium, molybdenum or

vanadium in varying amounts (9,10,25-27). These alloys are used in the overaged condition to attain optimum ductility and toughness levels. The microstructure consists of ferrite matrix, toughened by nickel additions and containing a dispersion of carbide particles. Their nature would depend upon the composition of steel. The carbides formed in the overaged condition, in general, can be represented by a formula Mx Cy where M represents [Fe,A,B etc.], A and B being the alloying species present e.g. in the presence of molybdenum the carbide precipitate has a formula $[Fe\ Mo]_6C$ or simply M_6C (28-30). Mechanical properties are primarily governed by the carbide size, shape and distribution.

Besides carbide precipitate, steels can also be strengthened by the precipitation of intermetallic compounds. Depending upon the carbon content and steel composition, intermetallic precipitation may take place from polygonal ferrite (30-33), massive ferrite (33), ferrite-pearlite (34) or martensitic matrices (31-33). For strengthening it is desirable to obtain fine spherical precipitate particles having (a) a low matrix mismatch (b) a cube face coincidence relationship with the ferrite matrix and (c) a lattice parameter which is an integral multiple of the ferrite lattice parameter (34-36). The main problem with these steels is that ductility and toughness levels are low. These can be improved upon by

refining grain size (30-33) and by keeping the carbon content as low as possible (33, 37).

A yet another method of strengthening alloy steels is by elemental precipitation. Copper additions are most useful in this regard (38). Low alloy copper bearing steels are used either in the normalized or in the normalized and tempered condition (23,38-42). A proprietory copper bearing steel called NICUTEN has extensive applications in the form of quenched and tempered plates (42).

Strengthening in these steels results from the precipitation of copper in elemental form as a fine dispersion with some solid solution hardening effect (23,34,38-42). There is evidence that the precipitation occurs in lines in ferrite which possibly indicates an interphase precipitation similar to the one for the precipitation of V_4C_3 and Nbc in steels (43). Strengthening has been observed to be independent of the microstructure of the matrix (38). The ductility and toughness of these steels can be improved upon by lowering the carbon content (38), choosing an optimum amount of copper and by controlling the prior austenite grain size by the addition of carbide forming elements (38).

1.4 BAINITIC STEELS

Bainite in them is formed on air cooling. In

order to obtain a fully bainitic microstructure on continuous cooling, over a wide range of cooling rates, it is necessary that the transformation to polygonal ferrite is totally suppressed and the transformation to martensite avoided (44-46). The former is achieved through 0.5 Mo-B additions to a low or a high carbon iron base (3,47) and the latter through proper alloying(44-46).

Two basic morphologies exist in bainites. In the upper bainite, large dislocated ferrite laths are bounded by cementite (carbide) while in lower bainite, carbides precipitate inside these ferrite laths at an angle of 55-60°. There is no clear cut evidence for twinned ferrite in lower bainite. Possibility of the carbide being epsilon carbide exists. The temperature for the change from the lower to upper bainite rises steeply with carbon content reaching a maximum value - 550°C around 0.5% carbon(Fig.1.1). Thereafter it drops to 350°C around - 0.55% C and levels off at higher carbon contents as shown in Fig. 1.1(46-48).

The factors affecting the strength of bainites are bainitic ferrite grain size, carbide dispersion, dislocation density, internal stresses and carbon dissolved in bainitic ferrite (46). All these parameters are primarily affected by the transformation temperature on cooling. It's effect on the tensile strength of bainites is shown in Fig. 1.2. In general lower bainites are

~~more~~ stronger than upper bainites.

From ductility and toughness considerations the bainite morphology assumes a considerable significance. Upper bainite is an undesirable constituent since low ductility and toughness are inherent to its morphology. This is because the bainitic ferrite lath width is relatively large and carbides are present along lath boundaries. As a result, arresting crack propagation is rendered difficult. Contrary to this, the lower bainite microstructure consisting of dispersed carbides, [and in view of its similarity with the tempered structure, is beneficial from the point of view of ductility and toughness(46).

The variation in the impact transition temperature as a function of tensile strength is shown in Fig. 1.3. Initially, the curve rises steeply with the tensile strength in the region where the structure is upper bainite. The transition from upper to lower bainite is characterized by a sudden drop in the impact transition temperature (Fig. 1.3). This is attributed to a change in the carbide dispersion (46). Thereafter, an increase in the tensile strength results in a gradual increase in the transition temperature in the region where the structure is lower bainite (Fig. 1.3).

From purely theoretical considerations, best ductility and toughness with upper bainites would be obtained when the strength is low (3,46,47). At a given strength level, ductility and toughness can be improved upon by refining the prior austenite grain size. This is brought about by adding grain refiners such as Al or Nb and by employing low roll finishing temperatures(3,46).

Lower bainite microstructure offers advantage in that it exhibits good ductility and toughness in addition to high strength. It is, therefore, possible to temper these structures to a desired level and yet maintain the beneficial microstructure consisting of dispersed carbides (46). A lowering of strength on tempering would result in a further improvement in toughness. In order that the ductility and toughness levels are appropriate, tempering has to be carried out to an extent that proof strength drops to about 45 tsi or 700 MN/m^2 (46).

1.5 CONCLUSION

The development of high strength steels with special reference to the bainitic (46) and the Q and T steels has been reviewed. Their drawbacks pertaining to the difficulties encountered in achieving the desired levels of ductility and toughness have been discussed.

The useful range of proof strength attainable in low alloy steels, without sacrificing toughness, appears to be in the range of 775-850 MN/m^2. In order to develop steels in this range of proof strength with improved ductility and toughness, it is necessary to consider the different microstructural parameters affecting mechanical properties of low alloy steels. This has been discussed in the next Chapter.

C H A P T E R - II

FUNDAMENTALS IN DEVELOPING STRONG AND TOUGH STEELS

2.1 INTRODUCTION

The main factors to be considered in developing a high strength steel are the attainment of high strength in useful sections, appropriate ductility and good impact properties at room and sub-zero temperatures.

It is most beneficial to obtain high strength in the as-transformed condition. For this, the transformation must be one involving shear and occuring at sufficiently low temperatures. This ensures that the transformation induced sub-structure, which contributes significantly to strength, does not anneal out during the later stages of cooling. By doing so an additional heat treatment involving tempering or ageing is eliminated. From hardenability considerations, it is important to obtain shear transformation product at slow cooling rates without polygonal ferrite being formed. Rapid quenching can supress the formation of polygonal ferrite during cooling from austenite but would lead to problems such as quench-cracking. Therefore, from practical considerations, it is desirable that shear transformation in large sections are obtained at relatively slow cooling rates. This ensures sub-structural strengthening in useful sections and to a very large extent eliminates the

possibility of polygonal ferrite formation.

The other important factors to be considered are ductility and toughness. An increase in strength in general affects them in an adverse manner. In steels, an increase in carbon content increases strength. Thus, for optimization of properties, a close control over carbon content is vital. Lowering carbon content improves ductility and toughness only at the expense of hardenability and strength. The loss in hardenability and strength would have to be made up by appropriate alloying additions. Attainment of a useful combination of strength, ductility and toughness would only then be ensured.

Mechanical properties depend upon microstructure which in turn is a function of the composition and thermal/mechanical treatments. The following discussion is related to the effect of different microstructural features on strength, ductility and toughness.

2.2 MICROSTRUCTURAL FEATURES AFFECTING STRENGTH

2.2.1 Transformation Induced Strengthening

The most effective transformation in this regard is change the austenite to martensite transformation. Depending upon carbon and nitrogen content and stacking fault energy of austenite, the resulting product is either

an internally twinned plate martensite or a heavily dislocated lath martensite (29,49-59). The plate martensite forms at carbon contents $>$ 0.6 wt.% (52-57) and has a tetragonal lattice (60). As a result of this teragonality, it has fewer available slip planes than normal ferrite lattice (13). The transformation itself generates numerous dislocations in addition to twinning and this inhibits the movement of other dislocations (13). All these factors coupled with a limited deformation inherent to a twinned structure (61), result in an extremely strong material with very poor toughness and ductility. The strength in the astransformed condition is mainly governed by carbon in solution, more than three quarters of the effect coming from carbide precipitation during quenching and the remainder from the carbon still retained in solution in martensite (51). The carbon level at which twinned martensite forms and the associated brittleness precludes the possibility of this structure being used for developing high strength steels.

Lath martensite forms towards lower carbon contents ranging from about zero to 0.6 wt% (52-57) and has a bcc lattice (60). There is a high a dislocation density within laths capable of a restricted movement under an applied stress (62). This micro-constituent thus offers a better combination of strength, ductility, and toughness

compared to its plate-like morphology and should therefore, prove useful. As before, the strength is governed by carbide precipitation during quenching, interstitial solid solution hardening and sub-structural contribution. The contribution of sub-structure to strength is of the order of 10-20 tsi - 155 to 310 MN/m^2 (51), and the relative contributions of the other two factors are governed by carbon content.

Results reported in more recent investigations on the transition of lath to twinned martensite, as influenced by carbon content, are at variance with the earlier observations. In one of the investigations it is reported that lath martensite are formed at $C < 0.3\%$, and twinned martensite at $C > 0.6\%$, the microstructure being partly lath and partly twinned in the carbon range 0.3 - 0.6% (52, 63-65). However, in another study it is reported that lath martensite forms at $C < 0.4\%$ and twinned martensite above 0.4% C (66).

2.2.2 Grain-Size Strengthening

The most successful quantitative relationship between lower yield stress and grain size is the one given by Petch (67, 68):

$$\sigma_y = \sigma_i + K_y d^{-1/2} \text{ , where,}$$

σ_y = lower yield stress

σ_i = frictional stress needed to move a dislocation through the lattice.

K_y = grain boundary locking term

d = grain diameter

The Petch parameter $K_y = m^2.\tau_c.\rho^{1/2}$, where,

m = a factor governing the number of operating slip systems

τ_c = stress required to operate a dislocation source

ρ = radius of the tip of a blocked slip band.

For a mild steel (0.11%), it can be calculated that for a grain diameter = 0.25 mm (ASTM-1), an yield stress = 7 tsi or 110MN/m^2 is obtained while for d = 0.01 mm (just above ASTM 10), an yield stress of 20 tsi or 310 MN/m^2 is obtained (68). If the grain diameter is reduced to 1 μm, a minimum yield stress in excess of 40 tsi - 620 MN/m^2 could be obtained. This is more of a theoretical possibility and so far no commercially feasible methods have been developed to obtain such fine grain sizes at least in low alloy compositions. However, recent evidence suggests that grain sizes of the order of 1 μm diameter can be obtained in high alloy steels by a combination of mechanical and thermal treatments (31, 32).

The value of m increases as the ease of cross slip diminishes resulting in a rapid increase in K_y (13). Therefore, techniques of reducing cross slip in ferrite would enhance the effect of grain size and hence are worthy of examination. Boron has been shown to exert such an effect (69) and, therefore, its small additions may prove very useful.

The tensile strength does not increase to the same extent with grain refinement as the yield strength. Thus a high YS/UTS ratio would be attained. This is in keeping with the present day thinking on the user requirements of high strength steels (sec. 1.2) and does not raise any problems.

2.2.2.1 Control by Deformation and Precipitation

Grain refinement depends upon producing a fine grained austenite structure. This is achieved by restricting recrystallization and grain growth in the austenite (13,70) or by controlled recrystallization of austenite without allowing grain growth to occur (71). Methods of affecting grain refinement are (i) thermal and thermo-mechanical treatments, and, (ii) restriction of boundary migration by particles of second phase. In the former, austenite grain size is governed by the distribution of deformation with time and temperature (70,71) and cooling rate from austenitizing temperature after

deformation (71). A more detailed discussion on this follows in a later section (2.4).

The theory and mechanism underlying grain refinement by second phase particles is now well understood(72-77). In this method, the recrystallization kinetics of austenite are controlled by precipitation of carbides, nitrides and carbonitrides in it. Thus, parameters such as reheating temperature, time at soaking temperature, net amount of deformation, deformation per pass, and deformation finishing temperature normally associated with hot working schedules are of immense importance (70). Based on the above discussion, it can be inferred that the thermo-mechanical technique would be more effective in the presence of second phase particles.

Elements commonly used for grain refinement are aluminium, niobium and vanadium (4,13) though in principle other elements such as titanium can also be used (4,5). With aluminium additions, the grain refining precipitate is AlN (4,13). The particles of AlN, precipitated by a prior treatment, begin to redissolve on reheating at temperatures around 1000°C, solution is rapid around 1200°C and virtually complete around 1300°C (4,13). The nature of these particles around 900 - 1000°C is most suitable for grain refinement since coarsening is very rapid above this temperature range. Therefore, aluminium

bearing steels are usually normalized from temperature around 900 -1000°C (950°C) to develop fine grained structures (4,13). AlN particles can also give rise to grain refining during rolling provided the reheating temperature is around 1150°C (13). A sufficient number of AlN particles are still available at this temperature for grain refinement. This is further enhanced by using low finish-rolling temperatures. Thus, aluminium nitride particles can result in grain refinement both during normalizing and during rolling.

The grain refining action of niobium is due to a complex carbo-nitride, the predominant partner in the precipitate being the carbide (4,13,78). Hence, the precipitate is commonly referred to as niobium carbide. It has been lately established that the composition of this precipitate is $NbC_{0.87}$ rather than NbC (79).

As before, the solubility data of NbC in austenite is of importance, Different quantitative relationships correlating niobium and carbon weight percentages to the solution temperature exist (79). For carbon levels generally used, the carbide starts dissolving at temperatures above 1050°C and the solution is complete around 1250 -1300°C (4,13,79). On cooling, it reprecipitates partly in austenite but mostly in the ferrite (4,13,80). Precipitate suitable for grain refinement by pinning of

grains is produced when steels are normalized from 900 - 950°C (4,13).

Niobium could also act as a grain refiner during rolling provided that an appropriate rolling-schedule is employed. The best starting condition is to have almost the entire niobium as carbide in solution in austenite. Precipitation of niobium carbide occurs during rolling on sub-grain boundaries formed during recovery after each pass (13). These are therefore pinned and recrystallization by sub-grain growth is restricted. These precipitates coarsen during subsequent passes and also help to restrain grain boundary migration (13). The overall rate of recrystallization is thus considerably slowed down in the presence of niobium carbide particles and is extremely sluggish below 900 - 950°C (1,13). This enables retention of beneficial microstructural features produced by controlled hot deformation at the deformation finish temperature, down to room temperature, without the necessity of altering the cooling rate (80).

However, great caution must be excercised in controlled hot working of niobium bearing steels. This is because the recrystallization of austenite in niobium bearing steels is not instantaneous (1,13). Any holding between 1050 - 950°C to achieve the desired roll finishing temperatures would result in mixed grain structure (1).

The disadvantages associated with a variable grain size microstructure are well known.

Vanadium is not a strong grain refiner as aluminium or niobium. This is because the vanadium bearing precipitate has a much lower solution temperature than either NbC or AlN and is therefore more useful in affecting precipitation hardening (13). Vanadium nitride is more effective than carbide and hence the steels require high nitrogen contents. High nitrogen contents may adversely affect ductility and toughness (4,13). Hence vanadium is normally used in combination with a grain refiner-Al or Nb (13).

2.2.3 Sub-Grain Strengthening

Sub-grains play an important role in controlling room temperature mechanical properties of wrought materials. The conditions under which sub-grains form, mechanism of formation and their influence on mechanical properties have been reviewed 70). Hot worked structures are characterized by a more or less equiaxed and uniform sub-grain structure with a three-dimensional dislocation arrangement within these sub-grains. The relationship between high temperature flow stress and sub-grain size is governed by a Petch type of equation (70) :

$$\sigma = \sigma_o + Kd^{-M}$$

where,

σ = flow stress

d = sub-grain size, and, σ_o, K and M are constants

The frictional stress σ_o is usually found to be zero for both pure metals and dilute solid solutions (81-84). The constant 'M' generally has a value of 1 (83-86), although values of 1.5 (82) and 2 (87) have also been reported.

Several workers have observed that room temperature hardness (83,84,88), microhardness (87,89) and yield strength (81) are related to the sub-grain size by an equation of the form:-

$$S = S_o + K (d)^{-1/2}$$

where, s = property being measured

d = sub-grain size and S_o and K are constants.

Thus, when sub-grains are present, ambient temperature properties depend only on sub-grain size and are independent of the temperature and strain rate at which sub-grains were formed (70). It is, therefore, possible to produce materials with improved properties by controlling deformation and temperature in a way so as to obtain a specific sub-grain size and preventing recrystallization by rapid cooling (70).

2.2.4 Precipitation Strengthening

The most popular mode of strengthening currently used is precipitation or dispersion hardening. In this method, barriers to dislocation movement are provided by precipitate particles. In steels, coherent precipitates do not result in marked strengthening. However, incoherent particles provide strong barriers to dislocation movement by preventing dislocation movement either past them or through them until very high stresses are applied (13). This results in considerable strengthening. The theoretical model for the strengthening effect in the presence of incoherent particles is due to Orowan (90):

$$\tau_y = \tau_s + \frac{Gb}{4} \cdot \frac{2\varphi}{(d-2r)} \cdot \ln\left(\frac{d-2r}{2b}\right)$$

where, $$\varphi = \frac{1}{2}\left(1 + \frac{1}{1-\mu}\right)$$

τ_y = shear stress at yielding

τ_s = yield stress of the matrix

G = shear-modulus

b = burger's vector

d = particle-spacing

r = particle radius, and, μ = poisson's ratio.

The Orowan equation suggests that if the inter-particle spacing is halved the strength can be doubled and if the spacing approaches particle diameter, obtaining infinite strength is theoretically possible. This goes

to show that this mode of strengthening is capable of producing very large increment in strength. It follows, therefore, that this must be accompanied by a considerable decrease in ductility and toughness. This aspect will be dealt in section 2,3 and methods of reducing this intense strengthening effect to reduce brittleness discussed.

The precipitate, most effective in hardening steels, is niobium carbide. Normalizing from 1250°C produces maximum strengthening (4,13). During cooling, the carbide in solution at 1250°C, reprecipitates mostly in the ferrite as 100 A° diameter particles 500 A° apart(4,13,80).

2.2.5 Other Strengthening Mechanisms

Many other strengthening mechanisms such as interstitial solid-solution hardening, substitutional solid solution hardening, order hardening, work hardening are well known and would be reviewed in brief.

In interstitial solid solution hardening, carbon and nitrogen atoms occupy interstitial sites in the ferrite lattice. As a result of this, asymmetric distortions are produced in the parent lattice and the dislocation motion severely retarded resulting in strengthening(13). However, the movement of dislocations is restricted to an extent that new dislocations are created which become entangled with other dislocations giving rise to crack

nuclei (13). Thus, although a large increase in strength is obtained, but ductility and toughness are adversely affected.

Strengthening brought about by substitutional alloy addition is much less compared to that obtained with interstitial elements. This is because the presence of substitutional solute atoms causes relatively smaller distortions in the parent lattice. Therefore, the increase in strength is comparatively smaller and ductility and toughness are not greatly impaired.

In order-hardening, solute atoms occupy positions with a definite periodicity throughout the parent lattice (91). This is a stable configuration and hence more energy is required for slip to occur in such a configuration compared to a random array (4,13). Ordering, however, requires a high alloy content and is uneconomical in developing new steels. Spinodal decomposition is another phenomenon which has received considerable attention (92). The principle involved is to obtain a precipitating phase distributed throughout the lattice with definite periodicity at the stage of precipitation where it is still coherent with the matrix. Thus, such a configuration would not provide severe barrier to the movement of dislocations in the classical sense (as in precipitation hardening), but slip is rendered more difficult

from energy considerations. Thus, strengthening is obtained without ductility and toughness being greatly impaired. However, for reasons discussed earlier, the applicability of this method is limited.

In strengthening by work-hardening, dislocations are generated as a result of deformation to a stage where tangles and net-works of dislocations form. These retard movement of other dislocations resulting in a large increase in strength which is accompanied by a considerable decrease in ductility and toughness.

2.3 MICROSTRUCTURAL FEATURES AFFECTING DUCTILITY AND TOUGHNESS

2.3.1 Introduction

A high strength steel should exhibit 'appropriate ductility' in order that it performs its engineering functions satisfactorily. Its magnitude is governed by service requirements and strength level.

Ductility is the property which governs the ability of a material to undergo enough plastic deformation prior to failure. It, therefore, ensures that stress concentrations in structural components are relieved to an extent that sudden catastrophic failures are avoided. Ductility is also important for achieving resistance to fatigue failure (25). It has been shown that uniaxial tests for measuring ductility are not always reliable and

may give misleading results particularly at very high strengths (14). The use of more elaborate tests which give biaxial stresses at the region where failure occurs has been recommended.

Toughness indicates the ability of a material to withstand suddenly applied loads and is expressed as the energy a material absorbs prior to failure. A material which is ductile and tough at ambient temperatures may undergo an abrupt transition to a brittle state at some temperature or a narrow range of temperature known as the impact transition temperature (ITT). Uniaxial tests which give an indirect measure may yield misleading results e.g. a material exhibiting a large area under the load extension curve in a tensile test, implying a good toughness value, may fail in a brittle manner if the transition temperature is at or above room temperature. The reporting on this parameter is thus complete and meaningful only when impact transition data is provided. In applications where low temperature toughness is an essential requirement, the nature of variation of toughness with temperature may be more important than the actual value itself e.g. a material 'A' possessing a lower impact value at room temperature than material B but showing a more gradual decrease as the test temperature is lowered is more likely to be chosen for cryogenic applications in comparison to a material B which shows an

abrupt decrease in impact value on lowering test temperature. Therefore, the three important aspects of toughness are (a) ambient temperature toughness (Upper Shelf Energy) (b) the nature of its variation with temperature, and, (c) transition temperature. Their relative importance is governed by the service requirements. A better assessment of this parameter is now available at room temperature with the advent of techniques for measuring fracture toughness (93,94). However, as stated earlier, the reporting on this parameter is complete only when the transition data is available. Thus, classical methods of impact testing are still very useful.

It is difficult to isolate ductility from toughness and vice versa as they are interrelated. Appropriate levels of these parameters are usually obtained in steels by a combination of alloying and thermal/mechanical treatments. Various factors influencing ductility and toughness are discussed below:

2.3.2 Purity

In order to extract maximum benefit in terms of properties, steel specifications must have severe control on impurities. Elements such as S,P, and oxygen which adversely affect toughness should be kept down to the lowest possible levels (14). Sulphur adversely affects

ductility and particularly toughness through harmful low melting constituents at grain boundaries (4,95). Phosphorus segregates to grain boundaries in elemental form and causes grain boundary decohesion (96). However, there is evidence that phosphorus is not particularly harmful at very low carbon levels (96). Oxygen causes grain boundary embrittlement and promotes intergrannular failure at sub-zero temperatures (14).

Inclusions are usually present in some form or the other in steels. Their influence on ductility and toughness depends upon their nature, size and distribution. An improvement in ductility can be obtained by avoiding stringer inclusions (14). The fewer and smaller the non-metallic inclusions and the more even their distribution, higher is the ductility, particularly in the transverse direction (97). Disc shaped sulphides are far more detrimental than sulphides which are elongated parallel to the tensile axis (98). Pearlitic carbides are less harmful than sulphides and spheroidal carbides less detrimental than lamellar carbides (98). According to a more recent study, anisotropy in wrought steels is because of the presence of inclusions, their shape being of prime importance (99). Tensile ductility and notch toughness are highly direction dependent. Anisotropy increases with deformation, its influence being mainly related to the presence of inclusions (99). Increase in

sulphur content generally increases anisotropy. Banding also increases anisotropy, and there is some evidence that banding and inclusions accentuate the effect of each other (99). The shape of inclusions also significantly affects fatigue strength (97).

Residual hydrogen causes embrittlement and thus adversely affects ductility which eventually may lead to brittle failure. Transverse specimens are more susceptible than longitudinal test specimens (100).

All these factors amply indicate the importance of purity. The higher the strength requirements, the more pronounced the harmful effects associated with impurities. A low gas content, and a reduction in the amount of S,P, and O_2 would result in an overall improvement in mechanical properties. This can be achieved by employing vacuum melting and casting methods (101, 102) and refining methods such as electro-slag remelting. The use of these techniques is restircted to specialised applications. Therefore, under normal melting and casting conditions it is difficult to avoid inclusions in steels. In their presence, an improvement in ductility can be brought about by (i) lowering their size, controlling their shape and, (ii) obtaining a more uniform distribution. The latter can be achieved by an appropriate selection of thermal and or mechanical treatments/schedules.

2.3.3 Carbon Content

Effect of carbon on the strength of steels is well-known. An increase in carbon content results in an increase in strength in both the as-transformed as well as in the quenched and tempered conditions (103-111). The strength and ductility of quenched and tempered martensitic steels are inversely related (104-111). An increase in hardness (equivalent to increasing carbon content) results in a considerable decrease in ductility and toughness. This could assume unacceptable proportions at very high strength levels.

A reduction in carbon would considerably improve ductility and toughness at the expense of strength. However, this possibility may yield useful results at the strength levels currently under consideration.

2.3.4 Nature of Martensite

It has been seen earlier (Sec. 2.2.1) how twinned martensite undergoes limited deformation and is, therefore, an undesirable microconstituent from the point of view of ductility and toughness. However, it is possible to obtain adequate ductility and toughness coupled with high strength by employing lath martensite as a primary constituent. It is, therefore, considered a useful microconstituent. A further improvement in ductility and toughness can be brought about by lowering the carbon content because the interstitial solid solution

hardening effect and the volume fraction of auto-tempered carbides is considerably reduced. The resultant loss in strength and hardenability can be made up by balanced additions of substitutional alloying elements. This approach appears promising and could prove very useful in developing new high strength steels.

A further disadvantage with twinned martensite is its susceptibility to hydrogen embrittlement and stress corrosion cracking (112,113). It was suggested that the susceptibility of some low carbon (0.18 - 0.2%), low alloy steels to hydrogen embrittlement in the quenched and tempered condition might be the result of formation of localized patches of twinned martensite. This is possible if segregation occurred so as to raise the carbon content in some localized regions to a value high enough to promote the formation of twinned martensite (113). The use of lath martensite structure in transformable alloys which may be further strengthened by age hardening has, therefore, been advocated (112).

2.3.5 Nature of Precipitates

In section 2.2.4, it has been shown how incoherent particles could lead to considerable strengthening. The disadvantage of precipitation hardening is that dislocation multiplication and pile up can easily occur at stresses well below those required to move dislocations

through or past the precipitate particles. This leads to the formation of crack nuclei, thus adversely affecting ductility and toughness (13,114). One method of improving toughness is to alter the dispersion of particles in a way that the number of dislocations between adjacent precipitates is below that needed for a pile of critical length for crack nucleation to occur (114). A second method is to reduce the precipitate size so that they are easily cut or engulfed by dislocations (114). It has been shown through extensive experimentation that an increase in 1 tsi (15.5 MN/m^2) yield strength produced by dispersion strengthening raises the impact transition temperature by approximately $4^{o}C$ (115).

2.3.6 Grain-Size

Fine grains in addition to increasing the lower yield strength also improve both toughness and ductility. The transition temperature, Tc, is related to the grain size by Petch equation (67,68) :

$$\beta . Tc = \ln \beta - \ln C - \ln d^{-1/2}$$

where, Tc = transition temperature

β = measure of resistance to lattice distortion and depends directly upon σ_1 i.e. the frictional stress

C = measure of difficulty of crack propagation, and,

d = grain diameter.

Thus, the ductile to brittle transition in a fine-grained material occurs at a lower temperature compared to that in a coarse-grained material. When the above equation is considered alongwith the relationship, $\sigma_y = \sigma_i + K_y d^{-1/2}$, two important factors emerge. If strengthening is obtained as a result of grain refinement, then an improvement in ductility and toughness occurs. On the other hand, if strengthening occurs by raising σ_i, brittleness would be induced.

The different methods of affecting grain refinement in steels have already been discussed (Sec. 2.2.2). Quantitatively, an increase in 1 tsi (15.5 MN/m^2) yield strength produced by grain refinement results in a decrease in impact transition temperature by about 10°C(115). It has been shown that a 200°C drop in finish rolling temperature can cause a reduction in transition temperature by 110°C with a 0.06 wt.% niobium in low carbon, 1.5% manganese steel (1). In an equivalent niobium free steel, a similar drop in roll finishing temperature resulted in a lowering of transition temperature by only 20°C (1). The advantage of employing low finish rolling temperatures in the presence of a grain refiner is, therefore, evident.

2.3.7 Sub-Grain Size

The role of sub-grains in controlling ambient temperature mechanical properties has already been discussed (Sec. 2.2.3). Interest in the behaviour of sub-grains has significantly increased and it has been suggested by some that refinement of austenite grain size by controlled hot deformation is not the only mechanism of improving toughness (116). Provided that a large number of stable sub-grains are present within a grain, the net effect then would be similar to that of a fine grained microstructure. This condition could apply despite a relatively large grain size. Thus a microstructure consisting of stable sub-grains could in principle bring about an overall improvement in mechanical properties in a way brought about by a fine grained microstructure. Work on isoforming (116-118) amply supports this view.

2.3.8 Carbide Morphology Size and Distribution

Cementite is an essential constituent in continuously cooled steels (bainitic steels) even when carbon content is low. Irvine and Pickering were two of the earliest investigators to conclude, on the basis of fractographic studies, that cementite morphology had an important bearing on the impact properties of molybdenum-boron steel(3).This has since been further substantiated (119). It was shown that in Mo-B steels, large

elongated areas of cementite formed along bainitic ferrite grains and that their distribution was not uniform resulting in poor toughness and ductility. An improvement in impact properties resulted by employing faster cooling rates and was attributed to a decrease in the size of the cementite areas and the bainitic ferrite sub-grains. Contrary to the observation in Mo-B steels, a more general dispersion of cementite particles was obtained in a low carbon Mn-Mo-Nb steel. Spherical particles of cementite precipitated along bainitic ferrite lath boundaries and since the number of lath boundaries was large, the dispersion of particles throughout the structure was uniform resulting in an improvement in toughness (119).

The effect of size, shape and distribution of carbides, on ductility and toughness is therefore clear. If a close control is not exercised over these parameters, their harmful effect is likely to assume large proportions. The mechanism by which carbides lower impact properties is known as carbide cracking mechanism (120,121). When carbides are present, particularly large ones, they tend to crack under stress while blocking slip bands. At low temperatures, the formation of a crack in a carbide particle can in turn nucleate cleavage failure of the ferrite matrix. Even above the brittle range, these particles can lower resistance to ductile failure as

evidenced by a decrease in the upper shelf energy of the Charpy impact curves.

The adverse effect of carbides on impact properties can be best eliminated by attaining carbide free microstructures. This is possible only if carbon is eliminated from the steel compositions or by lowering it to a sufficiently low level so that the volume fraction of carbides is at a minimum. There are indications that superior toughness of maraging steels is probably due to the very low carbon content (0.03 wt.%) present in them (122).

2.3.9 Austenite-Martensite Constituent

The appearance of such a constituent has been reported in air cooled low carbon (0.1 - 0.2 wt.%) molybdenum-boron steel when its B_s temperature is depressed below 625°C by the addition of Cr (119). The martensite associated with this constituent occasionally shows micro-twins thereby indicating that the carbon content of these regions could be around atleast 0.5 - 0.6 wt.% (119). The presence of retained austenite has been confirmed by x-ray diffraction (119,123). It has been suggested that this constituent can form as a result of an increase in the stability of localised carbon enriched regions in parent austenite during cooling(119). These regions remain fully austenitic till they have cooled below the M_s temperature. The M_f temperature of

the carbon enriched regions could be below room temperature thereby resulting in the retention of austenite. The resulting microconstituent is thus a combination of martensite and retained austenite and hence the name.

The appearance of such a constituent adversely affects impact properties of continuously cooled bainitic steels. Its formation can be suppressed by employing rapid cooling. A suitable tempering treatment will reduce the adverse effect, associated with the constituent, to a minimum (119).

2.4 TECHNIQUES FOR DEVELOPING STRONG TOUGH STEELS

The different methods used are:

i) Controlled rolling
ii) Ausforming
iii) Iso-Forming
iv) Hot-Cold Working
v) Thermal cycling
vi) Strain tempering.

2.4.1 Controlled Rolling

This is being increasingly used for producing grain refined precipitation hardened structural steels. The different variables to be considered are (1,4,124-128).

i) Soaking or reheating temperature.

ii) Time at reheating temperature.

iii) Amount and rate of deformation per pass

iv) Finish rolling temperature.

The first two factors determine the solution rate of carbides, the third the amount and mode of deformation and the fourth alters the amount of precipitation and nature of the microstructure on further cooling (4,124). Strengthening occurs due to precipitation during rolling. The grain-size is determined by recrystallization kinetics, which, in turn, is controlled by carbide precipitation in austenite. This, in turn, is controlled by the factors listed above.

Another variable which may be associated with controlled rolling is intermediate holding periods to attain desired roll finishing temperatures. The nature of rolling schedule employed depends upon steel composition and the properties desired.

2.4.2 Ausforming

This technique consists of deformation in a metastable austenite bay before transformation to martensite. The treatment, is, therefore, confined to steels having suitable transformation characteristics leading to 'bay' formation.

The variables associated with ausforming are (111, 129) :

i) Steel composition

ii) Austenitizing temperature

iii) Austenitizing time

iv) Cooling rate to isothermal working temperature

v) Isothermal working temperature

vi) Holding time at working temperature

vii) Degree of working

viii) Rate of working

ix) Cooling rate from isothermal temperature

x) Subsequent treatment.

The ausformed microstructure consists of lath martensite with fine carbide precipitate and ferrite-carbide aggregate in the tempered condition. The main feature of this treatment is that considerable strengthening occurs without a substantial decrease in ductility and toughness. Reasons for obtaining an overall improvement in mechanical properties are:

i) Precipitation of carbides in metastable austenite inherited by lath martensite formed (130-132).

ii) Improved dispersion of carbide after tempering (130)

iii) Increase in dislocation density (133,104)

The requirement of a transformation 'bay' and large degree of deformation limits the application of this

process to only a few steels.

2.4.3 Isoforming

In this process, deformation is applied during isothermal transformation to pearlite (117,118). Temperatures involved in this treatment are higher than those used in ausforming. The process oonsists of quenching the bar from the austenitizing temperature into a lead bath and holding at the temperature of deformition. After each pass, reheating is done. The process, thus, involves the use of several cycles of alternate deformation and reheating and could be considered too slow for large scale production.

The iso-formed microstructure consists of a fine sub-grain structure in ferrite matrix containing a dense dispersion of spherical carbides (118). The impvovement in strength and toughness is due to the presence of spherical carbide particles which besides strengthening also contribute to the stability of subgrain structure in the ferrite matrix (118).

2.4.4 Hot-Cold Working

In this process, steel is heated to the lowest temperature of complete austenitization, severally deformed and then transformed to martensite (71,116). The rate of cooling after deformation is critical and should be such so as to cause recrystallization but no grain growth.

It has been suggested that hot-cold working derives its strengthening mainly from refined austenite grain size produced by recrystallization after deformation e.g. 3 - 5 μm compared with 10 - 60 μm during conventional treatments (71). A fine grained structure also contributes to an improvement in toughness. The degree of grain redinement depends upon the steel composition, deformation and recrystallization kinetics.

This method is useful and could be applied to steels which cannot be iso-formed.

2.4.5 Thermal Cycling

This process involves repetitive austenitizing treatments of short duration (71). The temperature of austenitization is chosen to be the minimum temperature at which a fully austenitic structure can be formed in the time available. In order to minimize grain growth and the time necessary for heat transfer, austenitization should be carried out by quenching into a lead bath or a salt bath.

This process utilises the grain refining effect of austenite decomposition and the tendency for each of the ferrite grains to re-transform to a single austenite grain on re-austenitizing. The minimal holding time and rapid heating and cooling reduce the possibility of grain growth. The degree of grain refinement depends upon the

number of cycles employed and the response of the alloy under consideration. The resulting fine grained structure loads to an overall improvement in mechanical properties.

2.4.6 Strain Tempering

It consists of straining martensitic structure prior to tempering treatment. This leads to a finer carbide dispersion than normally obtained (135-138). An improvement in dispersion results in an overall improvement in mechanical properties.

2.5 CONCLUSION

A critical analysis of the above sections reveals that unintended microstructural features, which adversely effect ductility and toughness and which have their origin in carbon content, do generally form in steels. Their formation can, therefore, be avoided only by maintaining the carbon content at the lowest permissible levels.

From strengthening considerations, the parameters of interest are (a) transformation induced strengthening from lath martensite and, (b) precipitation hardening. Foreseeing the different problems associated with precipitation hardening vis-a-vis obtaining appropriate levels of ductility and toughness, it emerges that low carbon lath martensite has potential as a 'primary' constituent. The next chapter is therefore, devoted to outlining the alternative approach leading to the design of new steel compositions based on low carbon lath martensite.

C H A P T E R - III

METALLURGICAL CONSIDERATIONS IN THE DESIGN OF NEW COMPOSITIONS

3.1 THE ALTERNATIVE APPROACH

Certain deductions of design interest emerge from an analysis of the preceeding sections. Unintended micro-constituents (secondary constituents) may form during the attainment of the desired microstructure. Their formation cannot be predicted with certainty from thermodynamic and kinetic considerations. In most cases they have their origin in the carbon content. Secondary constituents adversely affect durcility and toughness and are difficult to investigate. The remedy is to either eliminate carbon in totality or to have it present in amounts such that the possibility of obtaining unintended microconstituents is reduced to a minimum.

From strengthening considerations, three mechanisms are of interest. Grain refinement improves (i) yield strength and (ii) toughness, particularly at sub-zero temperatures. However, grain sizes obtained in commercial practice do not result in significant strengthening. Presence of precipitate particles can lead to a large increase in strength, thereby adversely affecting toughness. Transformation strengthening from low-carbon lath martensite structure may be

said to occupy a position in-between these two extremes i.e. grain refinement and precipitation hardening. Utilization of a combination comprising of transformation hardening and grain refinement was most likely to result in properties envisaged earlier (section 1.3) and forms the basis of the present investigation. The existing practice is to utilize a combination of precipitation hardening and grain refinement.

The alternative approach can be best utilized if lath martensite structure is attained in useful sections over a wide range of cooling rates resulting in an air-hardening steel. Controlled hot forming of a such a steel would facilitate the attainment of the properties envisaged. The usefulness of this approach can be justified as follows:

a) Possibility of obtaining a combination of high strength and toughness from lath martensite.

b) Superior crack propagation characteristics of lath martensites compared to lower bainite.

c) Lath martensite exhibiting a much better resistance to delayed failure compared to twinned-martensite.

d) Elimination of quenching and tempering.

e) Attainment of end requirements, particularly the toughness, by controlled hot-forming, and,

f) Possibility of using one or more controlled hot-forming processes.

In developing steels based on the above approach, due consideration can also be given to :

a) Possibility of substituting costlier elements.

b) Improvement in dimensional stability.

c) Eliminating the possibility of twinned martensite forming in welded joints.

d) Oxidation Resistance.

e) Fatigue strength, and,

f) Weldability.

Factors (b), (c), (d) and (f) are related to the carbon content and alloying elements present and therefore can be controlled by choosing a proper composition. Fatigue strength is related to toughness (section 3.2.2.5). The implementation of the idea envisaged in (a) would lead to a saving in the production cost.

Having thus outlined the alternative approach, it would of interest to acquire comprehensive information on the physical metallurgy of low carbon martensites (the microconstituent of interest) in the as-transformed state. Other aspects e.g. structure-property correlation in the

tempered state have not been considered. This has been discussed in the next section. Wherever information on the physical metallurgy of low carbon martensite is not readily available, relevant data on lath martensites forming in other carbon-free systems has been utilized.

3.2 PHYSICAL METALLURGY OF LOW CARBON LATH MARTENSITES RELEVANT TO DEVELOPING NEW STEEL COMPOSITIONS

3.2.1 Formation and Morphology

Lath martensite is formed athermally at low carbon contents (section 2.2.1). In view of this, the M_s temperature is high (52-57,139,140) and results in the retention of a negligibly small amount of austenite (52,58,141). Presence of low carbon content necessitates addition of appropriate substitutional alloying elements to ensure the formation of fully martensitic structure in useful sections with relative ease.

The microstructure of low carbon lath martensite has been differently described as massive or blocky martensite (52,142,143), bainite (144), bainitic ferrite (3), self-accommodating (49,50,145), need-like (103,146), and 'scheibung' martensite (147). The most commonly accepted description is, however, simply 'lath-like' or lath structure (146-148).

Prepolished specimen surfaces, on being transformed, show characteristic surface tilts. A surface tilt, unlike in high-carbon martensites, corresponds to a packet of shear plates. The jagged boundaries outlining the massive packets or slabs result from different packets impinging on one another (145). The surface tilts on prepolished specimen surfaces do not merely represent surface martensite phenomenon (149,150) but are indicative of boulk transformations (145). Each massive slab or packet consists of a bundle of elongated platelets or laths which are approximately parallel and of one single orientation (58,103,142, 151,152). The laths which do not always have planar interfaces and which may dove-tail together to fill space (52, 145), are several microns long and may vary in width from 0.2 μm to 2.0μm (52,103,145).

The most complete description of the fine structure of massive (lath) martensites, observed in Fe-C and Fe-Ni systems, can be summarized as follows (52,153):

a) The basic structure is packet of massive martensite and corresponds to a packet of a large number of shear plates.

b) Blocks of different orientations constitute a packet,

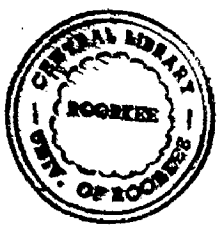

c) Blocks are separated by high angle boundaries and may occassionally be twin related.

d) Each block contains an array of parallel laths of a single orientation called the 'matrix laths', and,

e) There is a possibility of another set or sets of laths existing in a block having an orientation different from the matrix laths.

The earliest model conceived the formation of lath martensite as occurring by platelet-by-platelet shear that has propagated through the austensite matrix (52). This effect was considered analogous to that produced by a wave-front moving through austenite. Experimental observations supporting this hypothesis were (a) the change in direction of lath formation across a prior annealing twin in austenite, and, (b) an almost complete transformation of parent austenite (52,141). Subsequent to this hypothesis, partitioning effect was observed in austenite with additional shear plates forming in partitioned austenite(153). In view of this observation a modified hypothesis was proposed. According to this, the laths no longer formed adjascent to one another. The net effect still remained that of a phasefront moving through austenite with the actual process now consisting of parallel partitioning of austenite and subsequent transformation (153). Whether the shear plates formed singly or in pairs was not commented upon (153). A systematic study of Fe-Ni

massive martensites using hotstage microscopy, showed that laths formed in groups of at least two self accommodating plates (145). This experimental observation confirmed a theoretical prediction that laths usually formed in pairs (50). Hence the name 'self accommodating' martensite was conceived (49,50,145). Interferometric studies revealed that the interface between pairs of self accommodating plates is undistorted thereby confirming the observation that laths formed in pairs (145). For a further confirmation of the above hypothesis, the progress of the transformation was observed by hot stage microscopy employing cinematographic technique. This revealed that the austenite to martensite transformation progressed by lengthwise growth of initially formed plates and also by subsequent formation and growth of new plates (153). Formation and growth of additional plates occurred in discontinuous 'bursts' with several shear plates making up a single burst. Occurrence of the transformation in discontinuous bursts acted as a strong evidence of block formation (153).

It is now well accepted that the habit plane of martensite bundles or slabs, surface shear markings and individual laths is very close to $\{111\}_\gamma$ or close to $\{110\}_\alpha$ and the long axis along $<110>_\gamma$ (49,50,146, 154-156) although in some instances irrational habit planes - $\{213\}_\alpha$ have also been reported (157,158).

$\{111\}_\gamma$ or $\{110\}_\alpha$ being slip planes, it is to be expected that lath martensites will deform relatively easily in comparison to a microconstituent which has an irrational habit plane e.g. $\{225\}_\gamma$ or $\{259\}_\gamma$ in twinned martensite.

The sub-structural laths contain a high density of random dislocations or net works of low angle dislocation cell walls (49,103,151,156). The dislocation cell structure may represent an early stage in the recovery of transformation induced deformation (159). Until recently, it was believed that lath martensite is always dislocated and plate martensite twinned but this may not be so (160,161). It was pointed out that driving force alone is not a sufficient criterion to explain the transition from dislocated to twinned martensite in steels. This idea was conceived while explaining a similar transition in Fe-C and Fe-N systems (142). In addition to the effect of composition on driving force, it was equally vital to consider the effect of composition on critically resolved shear stress (CRSS) for slip and twinning (160). If CRSS for twinning is less than that for slip at the temperature of martensite formation, twinned martensite would almost certainly form and vice-versa irrespective of the martensite morphology. Thus, it was no longer possible to assume that lath martensite would be dislocated and the plate morphology twinned.

In fact there is evidence of twinning occurring in lath martensites in the literature (52,146,160-162).

3.2.2 Strengthening Mechanisms

Different factors controlling the strength of martensites may be summarized as (162):

a) Carbon content - i) Interstitial solid solution Hardening
ii) Precipitation during quenching

b) Substitutional elements

c) Sub-structure - i) Dislocation
ii) Twinning

d) Plate or lath size.

The effect of interstitial carbon content on strength is very large. It is now well accepted that the 'carbon effect' is made up of two components - solution hardening and precipitation during quenching, their contribution to the strength being nearly similar (138,163-165). Considering the solution hardening component first, although a linear relationship between flow stress and cube root of carbon content was initially proposed (138,163-165), the square-root relationship, suggested later, is regarded as more authentic since it fits in with the experimental observations better (166). This relationship has since been confirmed by many investigators (103,167-169). The slope of the linear plot for twinned martensite is slightly higher than that for lath

martensite (51,151,169). Short range interactions involving carbon atoms and dislocations give rise to solution hardening in both lath and twinned martensites (168).

The remaining half of the contribution from the carbon content arises from precipitation during quenching (165). The extent of precipitation is governed by the M_s temperature and cooling rate (169). In view of high M_s temperatures associated with lath martensites, extensive precipitation or segregation occurs during quenching and this would make a major contribution to the strength of lath martensites (169). The marked increases in strength is associated with very small particles of cementite which appear to form on dislocations (169). The particles have been related to the matrix by the Bagaryatski/Pitsch and Schrader orientation relationship (170,171).

The martensite plate/lath size is important in relation to strength and could contribute significantly at low carbon contents (159). Martensite cell thickness was shown to be influenced by carbon content. At very low carbon contents (0.001-0.002%), the cell-thickness decreased from 0.5 μm, observed in the carbon-content range of 0.02 to 0.2%, to a value around 0.25 μm (103). The deviation of the hardness data from the $(C)^{1/2}$

relationship (110) and a sudden change in cell size(103), occurred in the same carbon content range. This data reflects the strong dependence of martensite strength on the cell or lath size particularly towards very low carbon contents, similar to the dependence of the strength of cold worked iron on cell size (159). A similar range of cell sizes (0.25 - 0.5 μm) exists for martensite (lath and twin) in Fe-Ni system at all concentrations of nickel below 33%. This indicates that the lath size is more or less constant and appears to be independent of composition and thermal treatment. Considering the likely carbon contents attainable in conventional practice, martensitic lath/plate size strengthening is not unduly important (51,138,163).

A yet another factor to be considered is the presence of substitutional elements in solution. Earlier studies indicated that this contribution was very small in magnitude (165). In a subsequent study on an Fe-20 Ni alloy showing lath martensite structure, it was shown that solid solution hardening effect of nickel accounted for three quarters of its strength, the remaining contribution coming from the presence of substructure (151). Further, investigations on the same alloy, however, showed that the contribution of solid solution hardening is only 35% (172). The discrepency in the two findings arose because the structures reported in the earlier

study (151) were perhaps not fully martensitic (172). A conclusion similar to the one arrived at in one of the studies (172) has also been arrived at by reinvestigating the Fe-20 Ni-0.02C alloy after correcting for cell thickness (103).

The austenite to martensite transformation involves a microscopic change of shape and inhomogeneous shear (49,50). This inhomogeneous deformation results in some form of deformation sub-structure within the martensite plates/laths. Normally, the mode of shear in lath martensite is one involving slip (50). This results in a high dislocation density within laths. The dislocation sub-structure is usually arranged in the form of cells (49,103,151) and may represent an early stage of recovery of transformation induced deformation (159). The plate martensite usually has a twinned sub-structure (49,50, 103,145,146,151). Some of the earliest indications that sub-structure may contribute to strength came as early as 1960 (146). It was subsequently shown that in Fe-Ni massive martensites, the contribution of sub-structure to the strength remained fairly constant and was of the order of 25-30% (151). However, later studies revealed that the sub-structural contribution could be well above 40% (103,172). The first quantitative estimates indicated that for low carbon martensites, the contribution from dislocation sub-structure was likely to be of

the order of 50-100 HV, i.e. about 10-20 tsi (51). However, a more recent study has revealed that the role of dislocation density vis-a-vis the strength has been under-rated (173). It was argued that the interstitial solid solution theories based on short range interaction of carbon atoms with dislocations are inadequate because such interactions would provide a thermal barrier rather than an athermal one. Thus the slope of the flow stress vs $(C)^{1/2}$ curve should be temperature dependent whereas this is not supported by experimental evidence. It has also been shown beyond doubt that nearly 90% of carbon in lath martensite is segregated to defects i.e. not in solution (172). This led to the suggestion that an alternative mode of strengthening existed (173). It was proposed that carbon out of solution must be affecting the dislocation density in some way. In fact as the carbon content was varied from 0.01 to 0.1% (increased ten-fold), the amount of carbon in solution was estimated to be nearly constant. Also, the dislocation density varied linearly with carbon content and a plot of flow stress vs dislocation density-$(\rho)^{1/2}$ at 77°K and 250°K showed a linear relationship. The intercept at $\rho = 0$ was not zero and corresponded to the thermal component of the applied stress. These observations confirmed that the strength of martensites depends upon dislocation density which in turn is influenced by

carbon out of solution. The effect of carbon on strength was thus an indirect one. A point in favour of this theory is that if it were to be true, the change in slope of ρ vs $(C)^{1/2}$ curve with temperature, should be very nearly constant. Since the shear modulus varies only 5% between 77° and 250°K, a conclusion consistent with currently available experimental evidence, it is likely that this theory is correct (173).

With the possibility of twinning occurring in lath martensite, a brief mention of the effect of internal twinning on strength is necessary. After several conflicting opinions it has been concluded that twinning is important only in the presence of carbon (51,61,138,163, 165,166,169). At a given carbon content, twinned martensite has higher strength than lath martensite. Twinned martensite, unlike its lath counterpart, can be further strengthened by artificial ageing (169).

3.2.3 Auto-Tempering

As a consequence of the high M_s temperature associated with low carbon steels, the first formed martensite laths temper during quenching. This is known as 'auto-tempering (104,105). Thin foil electron microscopy revealed that cementite is rejected within laths in the form of plates and carbide layers along lath boundaries (105). The auto-tempered cementite appears

as plates 100°A wide and 1500 A° long and disposed in a Widmanstatten pattern (105). Alloying elements generally depress M_s temperature, thereby leading to a decrease in the amount of auto-tempered carbides and to a minimization of sub-boundary carbide films.

3.2.4 Conclusion

Physical metallurgy of low carbon martensites relevant to developing new compositions has been reviewed. The fundamental structure is the 'block' which contains a set of nearly parallel laths. Deformation behaviour of lath martensites would be governed by i) the block size, ii) the lath size, (iii) austenite grain size, and, (iv) the relative mobility of the dislocation substructure within laths which is governed by the volume fraction of autotempered carbides. The habit plane of laths being close to $\{111\}_\gamma$ or $\{110\}_\alpha$ is favourable from the point of view of obtaining an improvement in the ease of deformation. Factors controlling the strength of low carbon lath martensites are - precipitation during quench, solution hardening and sub-structural hardening. At low carbon contents, the magnitude of the solution hardening would be small and the volume fraction of the precipitated carbides, formed during quenching would be at a minimum. Sub-structural strengthening would then become the major source. In order that

low carbon martensites could be beneficially employed, the carbon content should be so adjusted that the possibility of the formation of lath boundary carbides is excluded.

3.3 PARAMETERS IN THE DESIGN OF ALLOYS

3.3.1 Carbon Content

The effect of carbon content on the strength, ductility and toughness in the quenched and quenched and tempered (Q and T) conditions has already been reviewed. Presence of carbon can lead to :

i) Attainment of auto-tempered carbides within laths and along lath boundaries in quenched steels.

ii) Possibility of attaining the undesirable A-M constituent in the air-cooled bainitic steels even when the carbon content is low ($\sim$0.1 - 0.2%).

iii) Possibility of attaining elongated carbides separating bainitic ferrite regions in air-cooled bainitic steels.

iv) Possibility of obtaining a variation in carbide size, shape and distribution in quenched and tempered steels.

v) Possibility of forming twinned martensite in welded joints even when the carbon content is as low as 0.1 - 0.2%.

Factors (i) to (iv) adversely affect ductility and toughness and factor (v) can bring about a premature failure in the welded joints.

From the above, it can be deduced that in order to attain appropriate ductility and toughness in the as-transformed condition carbon should be eliminated from the steel composition. However, this is neither technically feasible nor economically viable. Therefore, carbon should be kept down to as low a level as possible. The basic philosophy involved envisages elimination of auto-tempered carbides (lath boundary as well as the ones precipitated inside laths) from the microstructure and thus reduce their harmful effect on ductility and toughness to a minimum. However, lower the carbon content, higher is the M_s temperature and greater the possibility of obtaining auto-tempered carbides. Thus, two contradictory factors operate simultaneously. Complete elimination of the carbides from the microstructure is, therefore, not possible. All that can be achieved is a reduction in their volume fraction to such a low level that the associated harmful effects are reduced to a minimum. The consequent loss in hardenability would have to be made up through balanced additions of substitutional elements in a way that a large substructural strengthening is achieved without polygonal ferrite forming. There is some evidence that such an approach may

result in steels attaining excellent mechanical properties (122,148,175).

3.3.2 Alloying Elements

Alloying elements influence mechanical properties of steels through their effect on the phase transformation behaviour of austenite. These effects are now fairly well understood (176-180) and enable a proper selection of elements for a desired application.

3.3.2.1 Hardenability considerations

Except aluminium, titanium and cobalt, all other commonly used elements enhance hardenability to a varying degree.

Most carbide forming elements, when in solution, markedly enhance hardenability, small additions of vanadium and tungsten being more effective. Molybdenum contributes to hardenability very significantly and in amounts upto 1% is more effective than either tungsten or vanadium. Niobium in small amounts greatly influences the hardenability of low carbon steels (181). Phosphorus in small amounts has a marked effect on hardenability and since the harmful effects from the presence of phosphorus are greatly reduced at 'low' carbon contents (96), this may be an element of interest. The hardenability contribution of chromium and manganese is similar for the same

amount of alloy addition. However, manganese has a low price and therefore, very useful in enhancing hardenability at a moderate cost. Nickel and silicon influence hardenability only moderately. In fact it is for this reason that nickel is useful in compositions intended to be insensitive to rapid cooling and is a necessary ingredient in low distortion steels.

Boron significantly enhances hardenability when used in very small amounts $\sim$ 0.003% to 0.005% (176). In combination with about 0.25 - 0.5% molybdenum, it completely supresses the formation of polygonal ferrite in continuously cooled bainitic steels (3,47). It is thus a very useful element. Copper also enhances the hardenability of low alloy steels but has more useful applications in the quenched and tempered conditon (section 3.3.2.3).

The discussion so far has been concentrated on shifting the I-T/CCT curves towards slower transformation rates. An equally significant aspect of hardenability control involves an appropriate lowering of the transformation temperatures. Austenite stabilizers, nickel and manganese, which markedly lower A_1 temperature, are worthy of consideration. The extent to which transformation temperature is lowered by manganese and nickel additions can be found out from the corresponding alloy

diagrams. A comprehensive study of the Fe-Mn and Fe-Ni systems reveals that :

i) Thermal hysteresis occurs during the $\gamma \rightarrow \alpha$ transf. in the presence of both manganese (182-187) and nickel (143,151,172,182).

ii) As the alloy content increases the degree of thermal hysteresis increases to an extent that austenite transforms to α' in preference to α.

iii) α' (bcc) is formed by shear and is called as massive/lath martensite , and,

iv) The amount of manganese required to produce martensite in useful sections at moderate cooling rates (185,187) is much less compared with the corresponding amount of nickel (143,151).

The martensite thus formed is much softer and tougher compared with the conventional carbon martensite.

3.3.2.2 Solution strengthening

As has been previously noted (sec. 3.2.3), the strength of martensite is mainly attributed to (a) carbon in solid solution (b) substitutional elements in solid solution,(c) dislocation density,(d) lath or plate size,and,(e) carbide precipitation during quenching. In the present context also, the strength of martensite would depend upon all these factors. The

choice and amount of carbon content and alloying elements is going to be determined by other considerations namely hardenability and toughness. In view of this and the deduction that in low carbon martensites the major contribution to the strength would result from the dense dislocation substructure, it was decided not to make any special attempt to increase the strength of martensite over and above that inherent to the composition being developed.

3.3.2.3 Ductility and Toughness

Different parameters which improve ductility and toughness namely a low carbon content, a fine grain size and sub-grain size, low sulphur, phosphorus, oxygen and hydrogen contents and a uniform carbide size, shape and distribution have already been discussed (Chapter-II).

Nickel and manganese are the only two elements which improve both the notch impact properties as well as room temperature yield strength of low and medium carbon steels. However, there is a basic difference in the mechanism by which manganese and nickel improve low temperature toughness (188). The transition temperature of pure iron was slightly below that of the Fe-1.8 Mn alloy in the absence of carbon. Raising its (Fe-1.8 Mn alloy) carbon content to 0.04%C resulted in a marked reduction of about 70°C in its transition temperature. This was

attributed to the refinement of grain-boundary carbides brought about by manganese additions. However, addition of 3.3% Ni to iron resulted in a decrease in the transition temperature by about 55°C irrespective of whether or not 0.04% carbon was present. Metallographic examination confirmed this result since the nature and size of carbides in Fe-0.04 C and Fe-3.3 Ni-0.04 C alloys ~~was~~ were found to be the same. This observation contradicted an earlier observation that nickel does affect carbide thickness (189).

A further investigation in this direction gave a better insight into the effect of nickel on low temperature toughness (190). The transition temperature of carbon free iron was found to be 60°K and that of carbon free Fe-3.28 Ni alloy 127°K. When corrected for grain size, the difference due to nickel content was of the order of 56°K. More detailed experimentation revealed that Fe-3.28Ni alloy, which was stronger than pure iron at room temperature, had a lower yield strength than pure Fe in the temperature range 200 to 100°K. A similar behaviour was observed with regard to the strain rate dependence of yield point. It was postulated that this effect may be due to the relative ease of cross slip in the Fe-Ni alloy. Wavy slip traces in Fe-Ni alloy, indicative of cross slip, confirmed this reasoning. Wavy-slip traces in Fe-Ni alloy were observed down to

at least 50°K but gave way to planar-slip below 130°K in pure iron. A better ease of cross-slip in Fe-Ni alloy meant a reduction in the temperature dependence of yield stress and a low K_y value in the Hall-Petch relationship. This resulted in an increase in the resistance to brittle failure (31). Presence of stable microcracks in Fe-Ni alloy at temperatures as low as 40°K, supported this reasoning. Such a behaviour was not observed in pure iron. Thus nickel additions improved toughness by improving the ease of deformation at low temperatures. Whereas the beneficial effect of nickel is independent of the carbon content, manganese is effective only in the presence of a minimum of $\sim$0.04% C.

The observation that nickel additions increase the SFE when added to steels (61) indirectly supports the above mentioned experimental observations. If this explanation is accepted, then it is possible that the lack of toughening effect with manganese additions can be similarly explained. Manganese additions infact reduce the SFE (61) thus decreasing the probability and ease of cross slip. This explains the lack of toughening effect when Mn is added to pure iron. In the presence of carbon, a high Mn/C ratio is desirable to improve low temperature toughness.

Molybdenum has been shown to improve the toughness of marageing steels by minimizing the deleterious effect

associated with grain boundary precipitation and segregation (~~189~~ 91). This is relevant to the present context since it is desired that at least the lath boundary carbides be eliminated from the microstructure.

The effect of copper on toughness cannot be separated from its effect on hardenability in low alloy steels. If the alloy content is such so as to encourage transformation to bainite, then impact properties are adversely affected (38). Little effect was observed in martensitic structure (38). In the quenched and tempered structures, the hardenability effect is beneficial in promoting a more complete transformation to martensite (38).

Effect of boron on toughness is not very clearly understood. In Mo-B steels, slow cooling tends to produce poor impact properties through a mechanism of grain boundary decohesion caused by the segregation of boron to the prior austenite grain boundaries (119). The harmful effects of boron appear to be less pronounced at 'low' carbon contents (119). Hence caution must be exercised in using boron although it is a useful element in supressing the formation of polygonal ferrite.

Chromium and silicon increase the σ_i component in the Petch relationship and therefore induce brittleness (192). However, with the application of controlled rolling, silicon may be utilized in relatively

larger proportions (124). Additions of upto 0.4% silicon lowered the impact transition temperature of 0.17%C, 1.0% Mn steel in the 'as-rolled' condition. Larger amounts however, led to a deterioration in toughness. If the nitrogen content was kept low, the limit of usefulness of silicon could be extended to 0.87% without unduly impairing impact properties provided low roll-finishing temperatures were employed (124).

3.3.2.4 Volume changes

Volume change at the Ac_3 temperature has a considerable influence on the susceptibility of a steel to quench-cracking in that it can directly affect the volume expansion at M_s temperature on rapid cooling (22). A decrease in volume contraction at Ac_3 would minimise the susceptibility of a steel to quench-cracking and to surface cracking induced by rapid heating and cooling. Silicon and molybdenum additions are beneficial in this regard (22,164). Manganese, nickel, cobalt and especially chromium have just the opposite effect (22,164).

3.3.2.5 Other Requirements

Weldability is a factor of primary importance. Many cracks which lead to brittle failure in welds begin in the weld or the heat-affected zone HAZ (13, 193-195). Weldability refers to the satisfactory

welding of two pieces and would depend upon a large number of factors such as size, shape, degree of constraint, and welding electrodes. It is determined in a simplified form with the help of the carbon equivalent(CE) formula:

$$CE = C + \frac{Mn}{6} + \frac{Cr + Mo + V}{5} + \frac{Ni + Cu}{15}$$

The CE gives an indirect measure of the embrittling constituents that can form in the HAZ (13,194). This tendency is related to the composition of steel. The higher acceptable level of CE for obtaining satisfactory welds in high strength steels is between 0.41 - 0.45. An important limitation of the carbon equivalent formula is that it is not a universal one and is applicable only to those types of steels which were used for its derivation (194). In developing weldable quality steels, the main criterion is that 'twinned' martensite should not form in the HAZ since it has the highest embrittling index amongst the acicular micro-structures in steels(194). The possibility of twinned martensite forming is ruled out if the carbon content is kept very low. A reduction in volume changes associated with the $\alpha \rightarrow \gamma$ and reverse transformations would also indirectly contribute towards an improvement in weldability.

Appropriate fatigue strength is a desirable requirement for components which are either continuously

operated or intermittently over-loaded. It has been shown that in steels exhibiting brittle fracture, macroscopically visible cracks did not appear until a later stage in the fatigue life (196). However, these cracks were unable to propagate to any significant extent before rapid unstable crack propagation caused complete and catastrophic brittle failure. In steels exhibiting a substantial amount of ductile or tough fracture, fatigue cracks are initiated quite early in the fatigue life but they propagate slowly to considerable depths before final rupture occurs. The fatigue life of tough steels was shown to be almost four times that of steels which exhibited only a small amount of tough fracture (as indicated in the room temperature impact tests). The importance of toughness in relation to the fatigue strength is thus evident (196).

3.4 DESIGN OF FINAL COMPOSITIONS - FORMULATION OF THE PROBLEM

A good martensitic hardenability is the basic requirement in developing an air-hardening composition. At carbon contents low enough to exclude the possibility of (i) any significant amount of auto-tempered carbides, and,(ii) complete elimination of lath boundary carbides, martensite and bainite become structurally indistinguishable. Therefore, elements which normally promote

the formation of bainite and martensite, namely V, Mo, B, Cr and Mn, are useful additions. The main problem with Cr, Mo and V additions is one involving segregation and so a close control over the composition is required (197). The usefulness of Mn in improving hardenability at a moderate cost has already been discussed. Nickel, although not as effective as manganese in reducing the critical cooling rate, is nonetheless useful since it significantly lowers the A_1 temperature. However, keeping the likely carbon level (maximum permissible C $\leq$ 0.05 to 0.06%) in mind, it can be argued that the beneficial effect of ferrite stabilizers on hardenability, irrespective of their carbide forming tendency, would be at a minimum. Thus, the only viable alternative to improve hardenability at very low carbon contents is to incorporate an austenite stabilizer in the composition. The two prominent austenite stabilizing elements are Mn and Ni. From the point of view of improving low temperature toughness, the choice is once again between Mn and Ni. Thus selecting either of them is inevitable. Manganese has been preferred over nickel because (a) the amount of manganese required to produce an air-hardening composition is much less than the corresponding amount of nickel, (b) it would improve toughness at the carbon levels likely to be chosen ($\sim$0.04%), and, (c) has a moderate cost (section 3.3.2.5).

Having thus chosen manganese as the major alloying element, it is now vital to choose other element/elements so as to produce the desired microstructure keeping in mind the property requirements outlined in section 3.1. First preference would be for elements other than Mn and Ni. W, V, Mo, Cr, B, Si and phosphorus are therefore some of the likely additions. Both boron and phosphorus can be actively considered since very low carbon levels are intended to be used. The following are some of the alloy combinations that can be conceived with manganese as the major alloying element :

Mn - Mo

Mn - Si

Mn - Cr

Mn - P

Mn - P - Mo

Mn - Mo - Cr

Mn - Mo - Si

Mn - Si - Cr

It may be mentioned, in general, that the presence of elements other than Mn would also enhance hardenability but only marginally. Different elements in solution would also additionally contribute to the strength although it has been decided not to make any special efforts to raise the strength level ever that

inherent to the composition being developed. Tungsten and Vanadium have not been considered since they are better utilized for more specialized applications such as creep resistance and also because it is not intended to utilize precipitation hardening. From the remaining ones, molybdenum is useful since it reduces volume changes associated with the $\alpha \rightarrow \gamma$ and reverse transformations(22,164) and improves toughness by eliminating the tendency to grain boundary precipitation and segregation (191). The only disadvantage is its high cost. Chromium additions primarily affect solution strengthening. Silicon has been extensively used in low alloy steels (both 'rolled' as well as 'quenched and tempered') in amounts not exceeding 0.3%. However, it now appears that it can be utilized in relatively larger amounts (section 3.3.2.2). In view of this, the other benefits from silicon additions, namely, a delay in the martensite breakdown and an increase in the temperature of breakdown (21,23), a reduction in volume changes associated with the $\alpha \rightarrow \gamma$ and the reverse transformations (22), a decrease in the absorption of electrolytic hydrogen in low alloy steels (198), a reduction in the lattice parameter of ferrite on quenching thus giving additional strengthening (199) and a moderate cost, can be utilized to advantage. Hence the combinations Mn - Mo, Mn - Cr and Mn - Si can be suitably

justified. The utilization of Mo - B combination in supressing polygonal ferrite formation in bainitic steels is already well known. The combination Mn-Mo-B, hence, is relevant to the present context since martensites and bainites are structurally indistinguishable at very low carbon contents. Further, harmful effects associated with boron segregation to grain boundaries are also at a minimum at very low carbon contents. The same is true for phosphorus additions. Therefore, the beneficial effects of a very small amount of boron and phosphorus on hardenability and therefore the strength can be additionally utilized to advantage. The Mn-Mo-B and Mn-P combinations are thus appropriately suggested. Justification for the remaining combinations follows as a corrolary to the above discussion.

Having thus laid down the basic prerequisites for attaining lath structure with relative ease over a range of section sizes, it is now necessary to concentrate on the remaining element of alloy development, namely, grain refinement. As has been outlined earlier, this is primarily aimed at improving toughness over and above that inherent to a very low carbon composition. The simplest way to achieve it is by resorting to controlled hot forming (controlled rolling). The only effective method of retaining the beneficial of control-

rolling at room temperature is by using a grain refiner. The three possible choices are Al, V and Nb. In the presence of Al, it is vital to ensure that 'free' nitrogen is at a minimum (Chapter II). Also, Al can only be added to a 'killed steel' resulting in a reduced yield (Chapter II). Vandium, is not a powerful grain-refiner. The natural choice is therefore, niobium. It can be added to a 'semi-killed' or a 'balanced' steel. A further advantage is that it supresses the formation of polygonal ferrite.

3.5 SUMMARY

The work reported in this thesis relates to the transformation behaviour and mechanical properties of alloys belonging to the Fe-Mn-Si, Fe-Mn-Si-Nb and Fe-Mn-Si-Mo-Nb systems. Main features of these alloy systems have already been highlighted. The work was planned in the following manner:

Phase I

a) To acquire information on the range of mechanical properties that can be obtained in Fe-Mn-Si steels in the heat treated condition, starting with a minimum of carbon, manganese and silicon contents and varying them to an extent admissible in a low alloy composition.

b) Obtain guide-lines for designing air-hardening compositions containing Fe-Mn-Si.

Phase II

a) To study the effect of controlled hot-forming (rolling) on the mechanical properties of air-hardening Fe-Mn-Si steels in the presence and absence of a grain refiner (Nb) at two different carbon levels.

b) Develop a modified air-hardening composition based on the Fe-Mn-Si-Mo-Nb system and to investigate the effect of controlled hot-forging on its mechanical properties.

Phase III

Postulation of strengthening mechanisms based on:

a) A critical analysis of the results obtained and the data already available, and,

b) X-ray diffraction studies.

Experimental techniques employed in the present investigation have been dealt with in detail in the next Chapter.

H A P T E R - IV

EXPERIMENTAL TECHNIQUES AND PROCEDURE

4.1 MELTING

Raw materials used for melting consisted of electrolytic sponge iron or a low-carbon commercial iron, refined nickel shots, manganese flakes, silicon, molybdenum and niobium metals. The analyses of the sponge iron and low carbon commercial iron is reported in Table 4.1. The main impurity in the sponge iron being oxygen (~0.05%), allowance for loss during melting had to be considered.

Both vacuum and air melting techniques were employed for making alloys used in this investigation. The charge was placed in a clean alumina crucible for melting down in a "Radyne" induction furnace. The initial heating prior to melting was carried out under a vacuum of the order of $1 - 2 \times 10^{-3}$ torr. Once melting began, argon was introduced into the furnace to reduce the splashing of the charge. When the charge was fully molten the furnace was reevacuated to allow a boil to take place. Subsequent to the boil, argon gas was readmitted. After holding to allow for homogenization, the alloy was then cast into ~25 mm and ~50 mm diameter chill moulds. The piped materials was cut from the top of the ingot and a section approximately 8-9 mm thick was cut from

the bottom of the ingot for analysis. The air induction melts were made by the argon-oxygen process and cast as ~ 115 mm square ingots (200). As before, the piped material was cut from the top and a thin slice, cut from the bottom, was sent for chemical analysis.

Analysis for carbon was carried out conductimetrically and all other elements were determined by Quantometer and chemical analysis.

4.2 MECHANICAL WORKING

Vacuum melted ingots were reduced in section to a suitable size by hot-rolling and hot-forging.

The preliminary alloys (~ 0.01% C) were homogenized at about 1150°C for two hours prior to being hot rolled to about ~ 10 mm diameter bars. They were further reduced to a 6.5 mm diameter by cold swaging. However, in case of 0.03 C manganese silicon alloys, the reduction from about 10 mm to - 6.5 mm diameter was accomplished in several passes, by hot swaging.

Air hardening compositions containing manganese, silicon, molybdenum and niobium were investigated in the rolled and forged conditions. Details regarding the different variations of hot rolling/forging schedules employed are given in Chapter- 6 .

4.3 HEAT TREATMENT

Heat-treatments employed in the present investigation involved quenching, air-cooling and furnace-cooling from temperatures ranging from 800-1200°C. Controlled cooling experiments were performed on a dilatometer. Heat-treatment of specimens was carried out using either a vacuum-vertical tube furnace or a muffle furnace.

Tensile specimens were heat-treated in batches in metal jigs or in special hangers designed to keep them individually separated.

Temperature was measured using Pt/Pt-13% Rh or Chromel-alumen thermocouples and was controlled to within ±5°C.

4.4 MECHANICAL TESTING

4.4.1 Hardness Testing

Hardness testing was extensively used because it provided a quick and reliable indication of the effect of different heat treatments on mechanical properties. Hardness measurements were carried out on a Vickers' hardness testing machine. The load usually employed was of 30 kg. For very thin specimens, used in the investigation of preliminary alloys, lighter loads had to be

used, these are indicated within brackets by the side of the hardness values obtained. Each hardness value reported is generally the mean of at least five impressions. Whenever the scatter was more than 8-10 HV, the hardness reported represents an average of about 6-8 impressions.

4.4.2 Tensile Testing

Tensile tests were performed on an Instron machine at cross-head speeds of 0.05 cm/min and 1.0 cm/min. Different standard specimens were used during the investigation. For the preliminary alloys, single shouldered Hounsfield No. 10 tensile specimens were employed. However, for further work, double shouldered Hounsfield No. 11 and 13 tensile specimens were used to ensure that fracture occurred over the gauge length. The use of an adapter allowed Hounsfield grips to be used on the Instron machine. In certain instances cylindrical specimens were also employed. These could be tested with the help of standard grips supplied with the machine. For the preliminary alloys, specimens were machined from rolled/swaged bars and then heat-treated as described earlier. No heat treatment was necessary for the final alloy compositions as the specimens were tested in the as-rolled or in the as-forged condition. The yield/proof strength and ultimate tensile strength values were calculated from the load extension curves. Percentage elongation values were obtained by placing the

fractured specimen together and remeasuring the extended gauge length.

4.4.3 Impact Testing

The notched impact values were obtained at ambient, sub-ambient and high temperatures on a standard Charpy machine. In view of the small laboratory melts used to investigate the preliminary alloys, it was necessary to use sub-standard specimens involving a minimum of material. Sections ~ 56 mm long were cut from the bars, heat treated and special sub-standard Charpy specimens (half size) (~~Fig.4.1.~~) machined from them. These were then tested in accordance with the ASTM/BSS/ISI specifications. No loads were used on the hammer striking the specimen being tested. This meant that all the values indicated on the scale were halved to obtain the final values for the energy absorbed. For the final as-rolled and as-forged specimens, the impact values were determined using standard Charpy specimens with the hammer, striking the specimen being tested, fully loaded.

For impact tests involving high temperatures (upto ~200°C), an oil bath was used. This was kept continually stirred so as to ensure a homogeneous temperature distribution throughout. An arbitrary superheat of approximately 5°C was given to all specimens tested above room temperature. For the low temperature work

two types of baths were used; i) one involving a mixture of solid carbon dioxide and industrial methylated spirit in varying amounts was useful in the temperature range extending from room temperature down to - 70°C; ii) between - 70°C and - 150°C a well agitated mixture of Isopentane/ Methyl Cyclohexane and liquid nitrogen in varying amounts was employed, the temperature being measured with an alcohol thermometer. An arbitrary under cooling of approximately - 5°C to - 10°C was given to all specimens tested below room temperature to compensate for heat losses during transfer to the testing machine. The average transfer time from the bath to the testing machine was just over six seconds.

The criterion used for determining the transition temperature with sub-standard and standard specimens has been dealt with in the appropriate sections.

4.5 METALLOGRAPHY

4.5.1 Optical Microscopy

Optical metallography has been extensively used to study various micro-structures obtained under different cooling conditions. Specimens for optical metallography were usually hot mounted and polished in the usual manner.

It is known that martensitic alloys particularly in the quenched condition, prove difficult to etch. The

use of special etching agents such as sodium bisulphite has been lately suggested to reveal sub-structural details in massive martensites (52). The use of this reagent during the present investigation did not give adequate etching. 2% and 5% Nital proved to be the most satisfactory. In some instances, a combination of 2% Nital and acid-ferric chloride gave very good etched surfaces. A better control over etching could be exercised by resorting to swabbing rather than immersion. The time required depended on the nature of the treatment given to the specimens.

Optical metallography was carried out on Vicker's projection, Zeiss ultraphot, Neophot-2 and Olympus microscopes. Grain size measurements were not made in the present study for reasons stated in appropriate sections.

4.5.2 Electron Microscopy

Sub-structural details of the microstructures obtained under different cooling conditions were studied by thin foil electron microscopy, and to a limited extent by replication technique.

4.5.2.1 Replica Preparation

Mostly carbon extraction replicas were employed. The initial part of the specimen surface preparation was similar to that used for optical metallography. The final polishing was, however, carried out on a selvyt pad

impregnated with alumina. This ensured that any lubricant left behind by the earlier polishing operations was removed. After proper cleaning, the specimens were etched as before.

The replicas were prepared by evaporating carbon on to the specimen surface in vacuum at a slight angle. The surface was slightly scribed into 2-3 mm squares and undesired areas blanked off with lacomit. It was then immersed in the stripping etch(- 2% Nital). Scribing facilitated easy stripping of the replicas. After about five minutes, the specimen was removed from the stripping etch and gradually slid into distilled water contained in a small beaker. Replicas floating on the water surface were then picked up on 200 mesh copper grids and suitably stored or directly observed.

4.5.2.2 Thin foil preparation

The preparation of foils in the present investigation was carried out by using the jet profiling and polishing method (201).

This method used disc specimens of the same diameter as the conventional electron microscope specimen

grids i.e. 3.05 mm or 2.30 mm diameter. Two simple operations are combined in the Polaron Unit which finally result in a foil,

i) Profiling or jetting of the disc blank to obtain a double concave disc, and,

ii) Static electropolishing of this disc in a different cell to produce a small perforation near the centre surrounded by thinned material.

The starting material for making foils was 3.00 mm diameter disc. These were cut off from cylindrical rods of material by parting off discs in the parting off unit. These were then mechanically polished in a special jig so as to obtain $\sim$ 0.15 mm thick disc with parallel faces. One of these discs was then placed in the specimen holder assembly for profiling. An electrolyte consisting of 20 parts of perchloric acid and 80 parts industrial methylated spirit was used at 30 V for profiling. The profiling time varied with disc thickness and for the thickness specified above, was approximately 11-12 seconds each side.

The profiled disc was carefully cleaned in methylated spirit and held between a pair of tantalum tweezers and electropolished at 10-12 volts in the porforation cell in a 2% perchloric acid solution maintained at - 30°C to obtain a foil.

Replicas and thin foils were examined in either in the JEM7 or EM6G electron microscopes. For thin foils, an accelerating voltage of 100 KV was used. In order to obtain a clear picture beam tilting was found to be extremely necessary at least on EM6G, otherwise it was very difficult to focus images above a magnification of 20,000 X. For observing replicas a lower accelerating voltage (75 or 80 KV) was used.

4.6 FRACTURE STUDIES

For examination of fractured surfaces of impact specimens, the Cambridge "stereoscan' and Siemen's scanning electron microscopes were used. Specimens were prepared by first slitting them about 3-4 mm away from and parallel to the fracture surfaces. These could be used as such or were further cut down to provide sections sufficiently small to enter the stereoscan.

To ensure a good electrical contact the specimens were glued to the specimen holder using a silver base paint. These were allowed to dry for about 5 minutes or so before being examined. The examination was carried out at 30 KV with a tilt angle close to 45°.

Photographs of the fractured surfaces were first taken on polaroid films until a proper brightness and contrast in the pictures was established. Once this

was achieved, the final photographs were taken using a 35 mm camera.

4.7 DILATOMETRY

Transformation temperatures were determined using an automatic programmed dilatometer capable of recording dilation vs. temperature on an X-Y recorder, during heating and cooling. The specimen size was 7.6 mm long x 4.0 mm in diameter. Simple mechanical dilatometer was also employed. In such a case the dilation was measured with the help of a dial gauge and the temperature recorded with the help of a thermo couple spot welded to the specimen and connected to a potentiometer. Cylindrical specimen 20 mm long x 4.0 mm diameter were used.

4.8 X-RAY DIFFRACTION

A detailed investigation of the structure of different alloys in the heat treated condition was carried out by X-ray diffraction. Norelco X-ray generator (model 120-101-85) employing an iron target and manganese filter was used for this purpose. The operating voltage and current employed were 50 KV and 15 mA respectively.

Debye-Scherrer method employing 114.6 mm and 90 mm diameter cameras was used for obtaining diffraction patterns. The exposure time varied from 5 to 7 hours.

Powder samples for each alloy were prepared by filing. Heat treatments employed comprised of water quenching from different temperatures.

A small amount of the powdered sample was placed inside a transparent silica tube which was subsequently evaluated. The closed end of the silica tube was placed inside a tubular furnace maintained at a predetermined temperature. After holding for the required length of time, quenching of the powder sample was carried out by putting the closed end of the tube in iced brine.

C H A P T E R - V

MECHANICAL PROPERTIES OF HEAT-TREATED EXTRA LOW-CARBON MANGANESE-SILICON STEELS

5.1 PRELIMINARY ALLOYS

5.1.1 Introduction

Lowest admissible carbon and alloy levels were chosen during the initial part of the study. A low carbon iron base ($< 0.01\%$ C) alloyed with manganese and silicon in the ratio of approximately 2 : 1 was considered to be an appropriate starting composition. A manganese/silicon ratio lesser than this would render the attainment of lath martensite difficult. Another alloy similar in nature but containing nickel in place of manganese was also considered. Chemical composition of these alloys is reported in Table-5.1.

The alloys were investigated with a view to assess the possibility of producing lath martensite structure in them by employing different cooling rates. Optical metallography and hardness measurement were extensively used for obtaining the information desired.

5.1.2 Results

5.1.2.1 Microstructure

Since the carbon and alloy levels were low, quenching was considered essential. Small discs, about 4-5 mm thick, were cut from the swaged bars and quenched from 900°C, 1000°C and 1100°C respectively in cold water and the resulting micro-structures examined. In both the alloys, quenching from 1100°C alone produced transformation products associated with some shear. Hence for all subsequent treatments, a temperature of 1100°C was preferred. In order to obtain different cooling rates, small specimens of the two alloys were cold-rolled into strips of varying thicknesses and were quenched as before from 1100°C. Micro-structures thus obtained could be classified as (i) polygonal ferrite, (ii) massive or high dislocation density ferrite, and, (iii) massive martensite.

In the manganese-silicon alloy H1, the micro-structure obtained on quenching a $\tilde{\sim}$5 mm thick strip revealed the absence of any shear transformation product (Fig. 5.1 (a) and (b)). Whereas in a quenched 1.25 mm thick strip, it was massive ferrite (Fig. 5.2), in very thin strips (thickness $\sim$0.4mm), the micro-structure was massive martensite (Fig. 5.3).

In the nickel-silicon alloy H2, the structures from thin specimens ($\sim$0.4 to $\sim$1.2mm thick) were identical with those obtained in the manganese-silicon alloy (Figs. 5.2 and 5.3), whereas in the $\sim$5mm thick specimen, the microstructure was massive ferrite (Figs. 5.4a and b).

5.1.2.2 Mechanical Properties

The effect of austenitizing temperature and cooling rate on the hardness and microstructure was studied in both the alloys and the results obtained are summarized in the Tables 5.2 and 5.3. The pattern of hardness variation was similar in both the alloys. An increase in the austenitizing temperature resulted in an increase in the as-quenched hardness. The overall hardness values obtained in the nickel-silicon alloy were slightly higher than those in the manganese-silicon alloy (Tables 5.2 and 5.3).

Tensile properties were determined for the two alloys in the 1100°C water quenched condition. Results obtained revealed that for the same ultimate tensile strength, the manganese-silicon alloy was more ductile than the nickel-silicon alloy (Table 5.4). Both the alloys exhibited yield point (Fig. 5.5).

5.1.3 Discussion

Phase transformations associated with shear can result in two types of microstructures. If the cooling rate is very high, the high temperature phase could transform martensitically provided that the M_s temperature is above the temperature of the quenching media.

The other type of transformation is commonly known as a 'massive' transformation. Such transformations exhibit nucleation and growth characteristics, are thermally activated and occur during both heating and cooling (202). For transformations of this type to occur, the heating and cooling rate must be sufficiently rapid to suppress processes involving long range diffusion (i.e. to prevent equilibrium phase separation) but slow enough to allow equilibrium reactions to occur only partially. No change in composition occurs in these types of transformations and the reaction product once nucleated proceeds to develop by rapid migration of highly disordered incoherent interface (202). Massive transformations thus represent an intermediate stage between transformations involving nucleation and growth and martensitic transformations.

The two alloys presently investigated have a very low hardenability in view of their very low carbon and alloy contents. This makes it difficult for martensite

to form except under extreme conditions achieved by quenching very thin strips. Barring these extreme conditions, the shear transformation product which can form with relative ease is 'massive ferrite'. This would explain why massive ferrite is so commonly observed in the alloys, presently investigated.

The ease of martensite formation increases with an increase in the austenitizing temperature. In the present context the higher the temperature, the greater would be the amount of shear associated with the transformation product. This explains the increase in the as-quenched hardness with an increase in the austenitizing temperature.

For a given austenitizing temperature, a decrease in the specimen thickness in effect means an increase in the cooling rate and hence in the hardness on quenching. The results reported in Tables 5.2 and 5.3 are in accordance with this reasoning. Comparing the alloys H1 and H2, the slightly higher hardness observed in the latter can be attributed to a larger alloy content and hence to a marginal improvement in the ability to form 'massive' ferrite structure in thicker sections. The difference in the hardness is, however, not large enough to affect the ultimate tensile strength (Table 5.4). It is for this reason that the ultimate tensile strength

of the two alloys is nearly the same.

An important fact emerging here is that the manganese-silicon alloy H1 is more ductile than the nickelsilicon alloy H2 (Table 5.4 and Figs. 5.5). This observation may appear to be in conflict with the finding that manganese additions decrease the stacking fault energy (SFE) of austenite and hence enhance strengthening (61). However, SFE is not the only factor controlling strength and ductility. They are primarily a function of the grain size and the nature of the transformation product. It is evident from Figs. 5.1 and 5.4 that as-quenched microstructures in the alloys H1 and H2 are different. Whereas in the former, it is predominantly polygonal ferrite (Fig. 5.1), in the latter the microstructure is 'massive' ferrite (Fig.5.4) Of the two, the polygonal structure, like the annealed structure, is more ductile and when deformed gives a larger amount of uniform plastic elongation prior to the onset of necking (Fig. 5.5). The higher ductility obtained in the manganese-silicon alloy is thus explained.

5.1.4 Conclusions

Preliminary investigations revealed that useful mechanical properties in the as-quenched condition can be obtained in extra low carbon manganese-silicon

steels. The observation that for an identical ultimate tensile strength, the Mn-Si alloy had better ductility compared with the nickel-silicon alloy, was of considerable significance. This further encouraged the idea of using manganese in preference to nickel in developing new high strength steels. Alloys investigated thus far were deficient in hardenability and strength. This was duly considered while designing further compositions.

5.2 THE HIGHER HARDENABILITY STEELS

5.2.1 Introduction

Preliminary alloys investigated were deficient in strength and hardenability. This problem was overcome by raising carbon as well as manganese and silicon contents. A carbon content $\sim$ 0.03% was considered to be an appropriate level compatible with strength and hardenability requirements without unduly sacrificing toughness (sec. 3.3.2.3). However, the alloy content could be raised in two ways : (a) by increasing the manganese content while keeping the silicon content fixed around 1.0%, and, (b) by increasing both manganese as well as silicon contents. Both these approaches were adopted, the former for maintaining a proper balance of austenite to ferrite stabilizing elements and the latter with a view to utilize the beneficial effects of silicon additions to advantage(section 3.4). Four alloy compositions

with different manganese and silicon contents were produced.

The first two (H3 and H5) had nominal compositions of 3 Mn, 1.0 Si and 5 Mn and 1.0 Si respectively and were designed to establish the lowest admissible manganese level at which lath martensite could be obtained over a wide range of cooling rates. Preliminary investigations on these alloys had revealed that while lath martensite in the ~3 Mn alloy was obtained only on quenching, in the 5 Mn alloy it formed over a wide range of cooling rates. This served as the basis for designing the two latter alloys (H4 and H6) which had nominal compositions of 4 Mn, 2-2.5 Si and 5 Mn, 2-2.5 Si respectively. They were produced to establish whether (a) volume contraction become negligible at high silicon contents, (22,164), and, (b) silicon in larger amounts adversely affected the toughness of very low carbon steels. Compositions of these four alloys ~~is~~ are reported in Table 5.5.

5.2.2 Results

5.2.2.1 Dilatometry

Dilatometric studies were carried out at a pre-determined heating and cooling rate of 40°C per min. to determine the critical temperatures. An austenitizing temperature of 1100°C was used for all such experiments. Transformation temperatures for the different alloys

and volume changes observed are listed in Table 5.6.

Volume changes on heating and cooling were clearly discernable in alloys H3 and H5 and were similar in magnitude (Table-5.6). However, in alloys H4 and H6, instead of getting a clear indication of the volume contraction on heating, only a change in slope of the dilation vs temperature curve was observed. On cooling, however, volume expansions, which set-in at the Ar_3/Ms temperatures, were clearly observed in alloys H4 and H6. As is evident from the results (Table-5.6), volume changes on cooling were smaller in magnitude than the ones normally associated with the $\gamma \rightarrow \alpha$ or $\gamma \rightarrow$ martensite transformation.

5.2.2.2 Microstructure

Disc specimens of each alloy were heat-treated from 800°C, 900°C, 1000°C and 1100°C and the resulting micro-structures examined. Heat treatments chosen involved air-cooling, water-quenching and furnace-cooling from different austenitizing temperatures. In addition, the micro-structures obtained on controlled cooling (40°C/min using a dilatometer) were recorded for each alloy. Micro-structures observed and the corresponding hardness attained are recorded in Tables-5.7 to 5.10.

In alloy H3, lath martensite structure was obtained over a wide range of cooling rates (Figs. 5.6 to 5.9). Structures obtained on furnace-cooling (Fig. 5.8) and controlled-cooling (Fig. 5.9) bore resemblance to the micro-structure described as 'bainitic' (3). It is difficult to distinguish between 'martensites' and 'bainites' in the alloys being currently investigated in view of their very low carbon contents. Therefore, microstructures forming in the low-and intermediate-temperature transformation range can be described as 'lath like'. This terminology will be adhered to while describing similar micro-structures. Other micro-structures observed in alloy H3 agreed well with the description of massive-martensites as given by some of the earlier investigators, with the possible exception of grain size (57,59,103,142,143,145).

Microstructures obtained in alloy H4 were similar to those observed in alloy H3 (Figs. 5.10-5.12), except when the former was furnace-cooled from 1100°C. In this case the resulting microstructure was a mixture of lath like structure and polygonal ferrite (Fig. 5.12).

In alloy H5, the micro-structures obtained were a function of the cooling rate. Quenching from 1100, 1000 and 900°C resulted in the attainment of lath structure (Figs. 5.13 and 5.14). Air-cooling from the

same temperatures however led to the formation of 'massive' ferrite structure (Figs. 5.15a and b). On controlled-cooling (40°C/minute from 1100°C) and on furnace-cooling from 1100°C, the resulting micro-structures consisted of polygonal ferrite with very small amount of lath structure (Fig. 5.16).

Alloy H6 showed transformation characteristics similar to alloy H3 i.e. lath structure was attained over a wide range of cooling rates (Figs 5.17 to 5.20).

5.2.2.3 Mechanical Properties

(i) Hardness

Hardness values obtained for different heat-treatments are listed alloy-wise in the Tables 5.7 to 5.10.

In alloy H3, quenching and air-cooling from different temperatures between 800°C and 1100°C had little effect on the hardness, the range being between 350-360 HV_{30}. Controlled cooling and furnace cooling, however, resluted in hardness of ~320 and ~340 respectively (Table 5.7).

Hardness values obtained in alloy H4 were similar to those observed in alloy H3 except when heat-treatments involving furnace-cooling from 1100°C and quenching and air-cooling from 800°C were employed. Under these conditions, hardness values were found to be in the

range of 305-310 HV_{30} (Table 5.8). A hardness of 305 HV_{30} in the furnace-cooled condition, although lower in comparison to the corresponding hardness value in alloy H3, appeared satisfactory. However, on quenching and air-cooling from 800°C, hardness values obtained were lower than expected (Table 5.8).

Cooling rate had only a marginal effect on hardness in alloy H6, the values being in the range of 320-370 HV_{30} (Table 5.9).

In alloy H5, cooling rate had a marked effect on hardness. In the 'as-quenched' state, hardness ranged from 300-320 HV_{30} (Tables 5.10). In the 'air-cooled' condition, it was between 206 and 225 HV_{30}. The large difference in hardness in the 'as-quenched' and the 'air-cooled' conditions confirms the structural observations (Fig. 5.13 to 5.16). On controlled cooling and on furnace cooling from 1100°C, hardness of 175 HV_{30} and 158 HV_{30} respectively, further confirmed that the micro-structures obtained under these conditions were nearer to the equilibrium micro-structures and different from those obtained on air-cooling or on quenching.

(ii) Tensile Properties

The results obtained, correlating heat treatment with microstructure were further substantiated by employing

tensile testing. Results thus obtained follow the trend indicated by hardness measurements and are summarised in Tables 5.11 to 5.14. In general, the nature of the load-extension curves was similar and their main features shown in Figs. 5.21 to 5.24 are:

a) A high yield to tensile ratio (~0.8 - 0.9) except for heat treatments involving air-cooling and controlled-cooling in alloy H5.

b) A low rate of work-hardening.

c) Pronounced necking in majority of the cases.

d) A large area under the load-extension curve suggesting a high toughness value.

e) A general flattening of the load-extension curve beyond the maximum load on air cooling, thus leading to the attainment of larger values of percentage elongation compared to the 'as-quenched' state.

A comparison of hardness and ultimate tensile strength values in all the alloys indicated that a definite correlation existed involving a conversion factor of $5\ HV_{30} \equiv 1$ tsi ($15.5 MN/m^2$) UTS. On the basis of this correlation, it can be seen that in alloy H3, a minimum ultimate tensile strength of $\sim 975\ MN/m^2$ was ensured even on employing the slowest cooling rate (Table 5.11). At a cooling rate of $40^{\circ}C$/minute which is approximately

equivalent to air cooling a ~63mm round section from 1100°C, the UTS value increased to 1038MN/m^2. On quenching and air cooling from temperatures between 900°C and 1100°C, proof-strength in the range of 1054-1077MN/m^2, ultimate tensile strength in the range of 1085-1147 MN/m^2, percentage elongation ranging between 22-25% and, percentage reduction in area of the order of 68-72% was obtained (Table 5.11). Air cooling gave slightly better ductility (when measured as percentage elongation) compared with the 'as-quenched' state.

Tensile properties of alloys H4 and H6 (Table 5.12 and 5.14) were found to be similar to those of alloy H3.

In alloy H5, a minimum ultimate tensile strength of ~550 MN/m^2 was obtained at the slowest cooling rate (Table 5.13). However, in the air-cooled condition, it increased from ~670 MN/m^2 to 728 MN/m^2 as the austenitising temperature was raised from 900°C to 1100°C. The percentage elongation values ranged between 42-44% and the PS/UTS ratio was around 0.65. In the 'as-quenched' state, deformation behaviour of the alloy was similar to that of the other three alloys except that the maximum attainable ultimate tensile strength was around 990MN/m^2. It is noteworthy that in this alloy (H5), the proof strength level of interest (i.e. around 850MN/m^2) was attainable only on quenching from 1000°C.

(iii) Impact Properties

Impact tests were carried out on sub-standard Charpy specimens in the 1000°C 'as-quenched' condition. This was considered necessary because the proof strength of interest at least in alloy H5, can be unfailingly obtained only on quenching from 1000°C. It is not so for the other alloys. However, quenching from 1000°C ensured that all the alloys were tested under identically heat-treated condition.

Impact values obtained for different alloys, as a function of temperature, are reported in Tables 5.15 and 5.16 and the impact-transition curves are shown in Figs. 5.25 to 5.28. Impact transition temperatures were determined using an arbitrary impact energy criterion of 0.8 kg-m (42) and are reported in Table 5.16.

From the data given above, it is evident that alloy H5 had the best impact properties since the difference between the ambient temperature toughness and that observed at -70°C was small (Fig. 5.27). Alloy H3 underwent the ductile to brittle transition at around -18°C (Fig. 5.25), whereas in alloy H4 and H6 the transition temperature was close to or above the room temperature (Figs. 5.26 and 5.28). Alloys H4 and H6 were thus not useful for low-temperature applications.

5.2.2.4 Sub-structure

In view of the superior impact properties of alloy H5, transmission electron microscopy work was mainly carried out on this alloy. Two types of micro-structures were observed. On air-cooling from 100 and 1100°C, the structure obtained was 'massive' or high dislocation density ferrite (Figs.5.29 and 5.30). Dislocation density within ferrite grains was high (Fig. 5.29), the dislocation configuration was typically planar (148) as shown in Fig. 5.30 and reminiscent of the deformed structures (190,203). The other type of structure was lath-like in nature (Figs.5.31 and 5.32). Dislocations within laths, which were nearly precipitate-free, were arranged in the form of net-works labelled 'A' in Fig. 5.31. The dislocation density was too high to be determined accurately. Lath structure in the other alloys was similar to that observed in alloy H5.

5.2.3 Discussion

Transformation temperatures on cooling for the alloys other than alloy H5 are in the range of 400 - 450°C (Table 5.6). This clearly indicates that resulting micro-structures at the specified cooling rate would be lath-like in nature. A higher transformation temperature on cooling in alloy H5 (690°C) indicates a greater possibility of upper transformation products being

obtained. Micro-structures observed in the four alloys are, therefore, in agreement with the deductions drawn from the dilatometric data. Results obtained on volume changes associated with heating and cooling are in accordance with the earlier observations that volume contraction on heating diminished with an increase in silicon content and was negligible at silicon contents around 2.5% (22).

It has already been stated that Fe-4 Mn alloy yields massive ferrite structure on slow cooling and lath martensite on quenching. In a subsequent study, it has been reported that an Fe-5 Mn alloy yields shear-transformation (lath) structure in any section size on air-cooling (section 3.2.2). In view of the above it is logically expected that lath-structure would be obtained in alloys H3 and H6 over a wide range of cooling rates. This is because the manganese content in them is close to 5% and in addition they also contain significantly high proportions of silicon. Silicon, being a ferrite-stabilizer like Cr and Mo, is expected to enhance hardenability although to a limited extent (185). Structural observations in alloys H3 and H6 are, therefore, in accordance with this reasoning. Although alloy H4 has a manganese content close to 4%, in combination with 2.6% silicon, its effective transformation behaviour would be similar

to that of alloys H3 and H6, except when very slow cooling i.e. furnace-cooling from 1100°C is employed. On doing so, the attainment of a mixed microstructure in alloy H4 (Fig. 5.12) is because of a low manganese to silicon ratio and hence to an imbalance in the ratio of austenite to ferrite stabilizing elements.

The composition of alloy H5 represents a limiting case since any further reduction in the manganese content would not lead to the formation of lath structure on air cooling. Conversely, an increase in the manganese content would considerably increase the possibility of formation of the lath structure over a range of cooling rates. This reasoning is made more explicit when the composition and transformation behaviour of alloys H3 (5 Mn 1.5 Si) and alloy H5 (2.6 Mn, 1.0 Si) are compared. The latter (alloy H5) is deficient in hardenability in comparison to the former or for that matter alloys H4 and H6 which are air-hardening type. To attain lath structure in alloy H5, therefore, a cooling rate faster than air cooling i.e. quenching has to be employed. Experimental finding that the proof strength is raised from $\sim$660 MN/m^2 to $\sim$900 MN/m^2 by altering the cooling rate from air-cooling to quenching from 900°C (Table 5.13), is in accordance with the above reasoning. The lower hardenability of alloy H5 results in a variety of micro-structures, starting from the near-equilibrium

through massive to shear transformation or lath structure. Slower the cooling rate, the more pronounced the tendency for equilibrium microstructures to form. This is confirmed by structural investigations in all the alloys.

In most of the cases the nature of the stress-strain curves for the alloys under investigation is similar to those for deformed metals. High dislocation density introduced during the transformation tends to make the alloy respond as if it were cold-worked. This, alongwith a very low carbon content, explains why a high PS/UTS ratio and a very low rate of work hardening is obtained. A slight flattening of the tensile curves on air-cooling may be attributed to the absence of quenching stresses and hence to an improvement in ductility. In alloy H5, stress-strain curves obtained on air-cooling from 900 and 1000°C and on furnace-cooling from 1000°C show large elongation. This is because microstructure in the air-cooled condition is massive ferrite and in the furnace-cooled condition predominantly polygonal ferrite with very small amount of lath structure. The two microstructures are basically similar except that the former has a higher dislocation density. Further, the carbon content of the alloys, in general, is very low. These two factors have favourably combined to ensure that the mode of deformation is

similar to an annealed microstructure thus accounting for large percentage elongation values.

Considering the impact values, alloys H4 and H6 have transition temperatures above room temperature (Table 5.16). This may primarily be attributed to a large silicon content. a coarser grain size (expected in view of $AC_3 \sim 800^{\circ}C$) and to a lesser extent to the quenching stresses. Another factor adversely affecting the impact properties is an increase in strength. There are indications that an increase in hardness by 10 HV, equivalent to an UTS of 31 MN/m^2, will raise the transition temperature by about $15^{\circ}C$ (115). This observation may also explain, to some extent, the poorer impact properties of alloys H4 and H6. However, on comparing alloys H4 and H6 with alloy H3 (a basis for doing so being a similar strength and transformation behaviour), it appears likely that higher silicon content is largely responsible for the interior impact properties of alloys H4 and H6. Silicon in large amounts induces brittleness by increasing the σ_i (i.e. the friction stress) component of the Petch-equation thereby increasing the transition temperature (192). Comparing the impact properties of the higher silicon alloys H4 and H6, it is evident that the latter has a higher manganese to silicon ratio and therefore, attains a lower transition temperature as

compared to that of alloy H4.

Alloy H3, on the other hand, has large manganese to silicon and manganese to carbon ratios and therefore has a transition temperature (-18°C) much lower than that of alloys H4 or H6. It is, however, necessary to emphasize that heat treatment involving water quenching from 1000°C is far from the best condition for assessing the impact properties of alloy H3 or for that matter alloys H4 and H6. A better comparison of the impact properties of these three alloys could be made by employing the most suitable heat-treatment involving air cooling from 800°C.

Best results related with impact properties have been obtained in alloy H5. It has high manganese to carbon and manganese to silicon ratios, the grain-coarsening at 1000°C is small compared to the other three alloys. Further, the amount of silicon is appropriate and the tensile strength is the least amongst the four alloys. All these factors have contributed to the superior impact properties of alloy H5. Quenching from 1000°C has only ensured that the microstructure is lath-like in nature and does not in any way suggest that quenching has resulted in superior impact properties.

A more elaborate discussion on the strengthening mechanisms is presented in a later section. It may be pointed out here that in absence of precipitated carbides, strengthening in the alloys would result from a combination of high dislocation density and solid solution hardening. The near-absence of precipitated carbides within laths is most useful in bringing about an improvement in ductility and hence the toughness. Maintaining a large Mn/Si ratio is an important factor favouring the attainment of a large ambient temperature toughness and a low impact transition temperature.

5.2.4 Summary

The range of mechanical properties particularly the strength, that can be attained in the extra low carbon manganese-silicon steels in the heat-treated condition, over a composition range C = 0.01 to 0.03%, Mn =~2 to 5%, Si = 1 to 2.6% has been ascertained.

Two compositions of interest emerged from these experiments. The first, having a composition 0.03 C, 2.6 Mn, 1.0 Si, in which lath structure was obtained only on quenching, has a proof strength of ~930 Mn/m^2 (60 tsi) and good toughness even at -70°C in 1000°C WQ condition. The other has a composition 0.03C, 5 Mn 1.5Si and when identically heat treated has a proof

strength ~1024 MN/m^2 (68 tsi) and good impact properties down to $-18^{o}C$. Other higher hardenability compositions investigated revealed that although the strength and ductility values were comparable or better than the ones mentioned above, their toughness did not elicit their further consideration.

From the point of view of using minimal alloy additions, alloy H5 showed promise and was therefore chosen for further studies.

C H A P T E R - VI

EFFECT OF CONTROLLED MECHANICAL WORKING ON THE PROPERTIES OF AIR HARDENING STEELS

(A) INVESTIGATIONS IN THE AS-ROLLED CONDITION

A.6.1 Design of Compositions

Two important conclusions, relevant to developing an air-hardening composition, emerge from the results discussed in the earlier chapter:

i) Maintaining a proper Mn/Si ratio is an important prerequisite for attaining a high USE and a low ITT.

ii) At 1% Si, the manganese content required to produce an air-hardening composition was likely to be between 2.6 and 5%. With the former, lath structure is attained only on quenching while with the latter it is attainable over a wide range of cooling rates starting from annealing to quenching from 800°C upwards.

From the above, it was deduced that an alloy containing 1.0% Si and a manganese content ~4% was likely to be an air-hardening one and formed the basis of arriving at the compositions investigated in the 'as-rolled' condition.

It was necessary to (i) choose an appropriate carbon level, and (ii) decide upon whether or not any

other element needed to be incorporated so as to arrive at the final compositions. Two carbon contents were decided upon viz., (a) 0.02-0.03%, and (b) 0.05-0.06%. The former ensured that the amount of precipitated carbides was at a minimum whereas the latter was chosen with a view to produce these steels from mild steel. Niobium in amounts 0.04-0.05% was also considered as a possible addition since, besides being a grain-refiner (4,13,80), it also enhances hardenability at very low carbon levels (181). Its amount to be incorporated in the composition was based on (a) the volume fraction of the precipitate most likely required to affect grain refinement, and, (b) the possible adverse effect of employing a larger volume fraction of the precipitate on mechanical properties and particularly the toughness. Although niobium was primarily added for grain-refinement, its presence also ensures the attainment of lath structure in larger sections. This led to the design of four alloys having the same base composition but two different niobium and carbon contents (Table 6.1).

A.6.2 Experimental

All the four alloys were homogenized at 1150°C for about 2 hours and rolled from ~50 mm diameter ingot to ~21 mm round bars. These were used as starting material for controlled rolling. The soaking temperatures

ed for reheating prior to control-rolling were based on the formula (204):

$$\ln [(Nb) \cdot (C)] = - \frac{9350}{T} + 4.55$$

where (Nb) and (C) represent weight percent Nb and C respectively and T = temperature in ^{o}K.

For control-rolling niobium bearing steels, it is essential to have almost the entire niobium in solution as NbC, prior to the commencement of hot working (13). Both, the niobium-free and the niobium-bearing steel at 0.022% carbon level(designated as R1 and R2 respectively) were reheated to 990°C for about an hour and rolled from ~21 mm round to ~17 mm round section in three passes. While doing so it was ensured that the net deformation, deformation per pass and the finishing temperature was maintained constant.

At the 0.055% C level, the soaking temperature employed was 1090°C. As before, both the alloys R3 and R4 (Table 6.1) were reheated to the said temperature, soaked for about an hour, cooled to 990°C in air (time taken for cooling approximately 15-17 seconds) and subsequently hot-rolled in a manner similar to the alloys R1 and R2. This way it was ensured that an identical hot rolling schedule was employed for all the four alloys.

A.6.3 RESULTS

A.6.3.1 Microstructure

Microstructures of the alloys R1 and R2 were examined in the as-cast, heat-treated and control-rolled conditions. The results obtained along with the corresponding hardness values are summarized in Table 6.2. From the table, it can be inferred that the alloys R1 and R2 are air-hardening in nature, since the lath structure is formed in them over a wide range of cooling rates with a minimum hardness of $\sim$240 HV_{30}. The sole exception is when R1 is annealed from 1200°C. However, the same alloy on being annealed from 1100°C, attained lath structure (Table 6.2).

Microstructure of the alloys R1 and R2 in the as-rolled condition was lath like in nature (Figs. 6.1 and 6.2). At low magnification (100 X) the microstructure appeared to consist of fine equiaxed grains (Figs. 6.1a and 6.2a). However, the shear nature of the microstructure was clearly revealed at a higher magnification (Figs. 6.1b and 6.2b). Alloy R2 attained a finer grain size than R1 (Figs. 6.1a and 6.2a).

Microstructure in alloys R3 and R4 was similarly lath like (Figs. 6.3 and 6.4), the niobium bearing alloy R4 being finer grained as compared to R3.

A.6.3.2 Mechanical Properties

Mechanical properties of the four alloys in the hot-rolled condition are presented in Tables 6.3 to 6.6 and summarized in Figs. 6.5 to 6.11.

Alloys R1 and R2 attained USE values in excess of 270 J (Table 6.4). Impact transition temperature of the alloys R1 and R2, based on 54J (40 ft-lbs) energy criteria, was found to be -68°C and -95°C respectively (Figs. 6.5 and 6.6). The stress-strain curves resembled those of heavily cold deformed metals with one notable exception - the ductility measured as percentage elongation was appreciably higher in the present instance (Figs. 6.7 and 6.8 and Table 6.3). Proof strength was in excess of 770 MN/m^2 and the UTS ranged between 850-930 MN/m^2 (Table 6.3). Ductility measured as percentage elongation was found to be in excess of 20%, the alloy R2 being more ductile compared with R1 (Table 6.3).

On raising the carbon to 0.055%, both the proof strength and the ultimate tensile strength increased, the increase being more pronounced in case of the latter (Table 6.5). The corresponding decrease in the percentage elongation was small. Proof strength now ranged from 860-950 MN/m^2, UTS from 1000-1100 MN/m^2 while the percent elongation, was $\sim$20% (Table 6.5). Basic nature of the stress-strain curves for the higher

carbon alloys R3 and R4 (Figs. 6.9 and 6.10) was similar to that observed for alloys R1 and R2 (Figs. 6.7 and 6.8)

Raising the carbon content from 0.022 to 0.055% was, however, detrimental to the toughness as a whole (Table 6.6) . Impact transition temperature for the alloy R4 was found to be -25°C (Fig. 6.11). A complete transition curve for the alloy R3, however, could not be established for want of material.

A.6.3.3 Electron Metallography

Transmission electron microscopic work was mostly confined to alloys R1 and R2, in view of their superior impact properties, in the control-rolled condition.

The microstructure of alloy R1 in the as-rolled condition consisted of laths which often appeared in groups of parallel arrays (Fig. 6.12). Occassionally, laths without distinct straight boundaries (distorted lath structure) were also observed (Fig. 6.13). Such laths contained a cell structure delineated ABC in Fig. 6.13. The dark jagged regions represented areas of high dislocation density. Dove-tailing effect normally associated with massive martensites in Fe-Ni system (52,145) was also observed in the lath structure. Nature of the dislocation tangles within laths, although complex when studied at low-magnifications, was

clearly revealed at higher magnifications (Fig. 6.14). Occassionally, very small particles which could be carbides, were also seen to be present within the laths (Fig. 6.11).

Microstructure of the alloy R2 was found to be similar to that of R1 (Figs.6.15 and 6.16). A high disloc. density within the laths is clearly visible (Fig. 6.14).

Carbon extraction replica technique was also employed for investigating the microstructure of the alloys in the control-rolled condition. Such a study revealed that in alloy R3 elongated carbides formed along lath boundaries (Fig. 6.17). Their presence was, however, not detected in the alloys R1, R2 and R4 (Figs. 6.18 and 6.19).

A.6.3.4 Fracture

Fractography was carried out mainly on impact specimens of the alloys R1 and R2 tested at room temperature and at -70°C.

The room temperature fracture in alloy R1 was ductile in nature showing tear dimples (Fig. 6.20). Fracture appearance at -70°C was characteristically brittle showing river-line markings (Fig. 6.21a and b)

Room temperature fracture appearance in alloy R2 was similar to that in alloy R1 (Fig. 6.22). However, the fracture at -70°C was not wholly brittle but contained regions showing tear dimples (Figs.6.23a and b). The brittle regions revealed features showing transgrannular crack propagation as well as intergrannular facets (Figs. 6.23a and b).

A.6.4 Discussion

Results obtained reveal that the base composition Fe-3.7 Mn-1.0 Si with 0.022% C (composition R1) is the limiting composition for attaining lath structure on air-cooling. The attainment of (i) ferrite on annealing R1 from 1200°C, and,(ii) lath structure on annealing the same alloy from 1100°C, shows that the composition Fe-3.7 Mn-1.0 Si-0.022C has a tendency to revert to equilibrium transformation products when cooled slowly from austenitizing temperatures higher then 1100°C. This indirectly confirms the above deduction. A comparison of alloy R1 with alloy H5 (Fe-2.6 Mn-1.0 Si - 0.03C) would indicate that altering the manganese content of the latter by a percent has resulted in an increase in proof strength from 460 MN/m^2 (obtained on air-cooling alloy H5 from 900°C) to about 775 MN/m^2 (obtained on control-rolling R1 followed by air-cooling). Duly accounting for a slight amount of

strengthening that may have resulted from deformation during rolling, this result demonstrates that the major effect of alloying is to impart hardenability and thus strengthen by sub-structural rather than solid-solution hardening. The beneficial effect of manganese and the likely beneficial effects of Si and Nb in promoting the formation of lath structure have already been discussed earlier. The combined beneficial effect of the elements present has ensured that the alloy R1 and its Nb-bearing counterpart-alloy R2 are air-hardening in nature with a minimum attainable hardness of $\sim$240 HV_{30} (Table 6.2). It has been demonstrated that a slight increase in the carbon content in extra low carbon steels enhances hardenability significantly (148,175,205). Compositions R3 and R4, in view of their higher carbon content, therefore, represent an improvement over R1 and R2 respectively, in their ability to form lath structure with ease. Thus the compositions R3 and R4 are automatically air-hardening in nature. In view of the above it can be postulated that, in general, the CCT curve for the alloys under investigation would show the absence of polygonal ferrite.

Considering the toughness values of R1 and R2, the attainment of USE in excess of 250J in these alloys is of considerable significance and highlights the usefulness of the alternative approach. The near-

absence of precipitated carbides, elimination of lath boundary carbides (Figs. 6.18) , and , the attainment of a fine grain size (Figs.6.1a and 6.2a) has primarily contributed to the attainment of USE in excess of 250J. To a lesser extent, use of vacuum melting and casting techniques and the low sulphur and phosphorus contents of the alloys has also contributed to an improvement in the USE. A lower ITT attained in alloy R2, in comparison to alloy R1 (Figs. 6.5 and 6.6) is attributed to a finer grain size in the former (Figs. 6.2a and 6.1a). This difference in grain size has also resulted in the alloy R2 being more ductile than R1 (Table 6.3).

On raising the carbon content to 0.055%, the structural changes that occur, which in turn would affect strength and toughness, primarily depend upon whether or not Nb is present. In alloy R3, which is Nb free, the structural changes would comprise of (a) appearance of the lath-boundary carbides (Fig. 6.17), and, (b) a slight increase in the amount of precipitated carbides. The former would adversely affect the USE as well as ITT whereas the latter may, at best, result in a very slight increase in strength. Thus one of the factors contributing to an appreciable lowering in the USE in alloy R3 (Table 6.6) is the appearance of lath-boundary carbides in the microstructure(206,207). However,

if the USE of the alloys R1 and R3 are compared (Table 6.4 and 6.6), it appears improbable that the appearance of lath-boundary carbides alone could account for this large decrease in the USE from ~270J (attained in alloy R1) to ~189J (attained in R3). The utilization of a reheating temperature of 1090°C employed during the control-rolling of R3, although far from satisfactory but nevertheless employed to ensure that the alloys R3 and R4 were identically hot-rolled, would result in the former attaining a relatively coarser grain size. This in someway should also contribute to a lowering in the USE. The effect of grain size in controlling the USE has been dealt with in detail in the section 'B' of this chapter. It thus appears that the attainment of a coarser grain size and the appearance of lath boundary carbides together can satisfactorily account for the comparatively lower USE attained in alloy R3.

In alloy R4, the structural changes to occur would mainly comprise of the precipitation of NbC during rolling. This would lead to grain refinement and may prevent the formation of lath-boundary carbides (Fig. 6.19), which were obtained in alloy R3. These factors would greatly assist in the alloy R4 attaining reasonable values of USE and ITT. Remembering that that the strength of alloy R4 is higher than that of

alloy R2, the overall toughness of the former, although appreciably lower than that of the latter, can be considered as satisfactory. Comparing the alloys R3 and R4, grain-refinement brought about by niobium has resulted in the latter attaining a better overall toughness (Table 6.6). Before proceeding further, it is necessary to comment upon the USE and ITT values attained in the alloys R3 and R4. As stated earlier, employing a reheating temperature, of $\sim$1090^{o}C prior to rolling alloy R3 is far from satisfactory. Thus it is certain that better overall toughness could have been attained if a reheating temperature, similar to that employed for alloys R1 and R2, had been employed. However, the advantage of using an appropriate reheating temperature would be offset by the presence of lath-boundary carbides i.e. the benefits expected from employing an appropriate soaking temperature would not be fully realized. As far as the alloy R4 is concerned, the reheating temperature employed prior to rolling is appropriate. However, a grain size finer than the one currently obtained could have been attained had it been feasible to impart a larger amount of (i) net deformation and, (ii) deformation per pass. The role of deformation in controlling grain refinement has been considered in a greater detail in the section (B) of this chapter.

Hardness, strength and ductility values obtained in the as-rolled condition are comparable with similar values reported for lath structures in Fe-Mn (187,208), Fe-Ni (151,172,209)* and, Fe-Ni-Co-Mo-Ti (210) systems. A note-worthy observation is the attainment of percentage elongation values $\geq$ 20%. As has been discussed in Chapter-V, strengthening would primarily result from a combination of solid solution and substructural hardening except perhaps in alloys R3 and R4 in which precipitated carbides may additionally contribute to strength.

Fracture appearances of the alloys R1 and R2 at room temperature, which are ductile (Figs. 6.20, 6.22) are consistent with the high USE values. However, at -70°C, the fracture instead of being fully brittle showed a small proportion of tear-dimples (Figs. 6.21 and 6.23). This observation suggests that even the alloy R1 is not wholly brittle at the test temperature. The occurrence of intergrannular facets, in addition to the features mentioned above, in the impact tested specimens of alloy R2 at -70°C may be attributed to the presence of NbC particles along grain boundaries.

(B) INVESTIGATIONS IN THE AS-FORGED CONDITION

B.6.1 Introduction

Studies on steels based on extra low-carbon lath structure in the as-rolled condition had established

* Typographical error: Hardness & strength values of Fe-Ni martensites are infact relatively lower.

beyond doubt the usefulness of the alloy system Fe-Mn-Si in general and of the base composition Fe-3.7 Mn-1.0 Si, with or without 0.042 Nb in particular, in attaining proof strength in excess of 770 MN/m^2, UTS $>$ 900 MN/m^2, percentage elongation $\sim$20% and excellent ambient temperature and subzero temperature toughness. Little information is, however, available on the structure-mechanical property correlation of the aforesaid steels in the forged condition. It was therefore decided to investigate this aspect of an air-hardening steel based on 'lath structure'. The composition currently investigated Fe-0.03C - 4 Mn-0.4 Si-0.4 Mo-0.074 Nb (Table 6.1), although a modification of the alloy R2, differed from the latter in its silicon, molybdenum and niobium contents. Molybdenum was incorporated in the composition for two specific reasons. Firstly, like silicon, it also reduces the volume changes associated with the $\alpha \rightarrow \gamma$ and reverse transformations (22, 164). Therefore, a partial replacement of silicon by molybdenum was feasible. Secondly, it is useful in eliminating the harmful effects of grain boundary precipitation and segregation on toughness (191). Therefore,it would suitably counteract the likely adverse effect on toughness if the carbon content were to exceed the critical concentration i.e. $\sim$ 0.06%. A higher niobium content was introduced to assess whether or not it is effective as a grain refiner when present

in excess of 0.06% (211,212).

B.6.2 Experimental

Steel of the specified composition was air-induction melted and cast into 115 mm round ingots. It was then homogenized at 1150°C for about 4 hours and forged with intermediate reheating to about 31.5 mm square section. The final processing consisted of hot forging from 31.5 mm square to ~15 mm square section. While forging in a controlled manner, no intermediate reheating was employed and a finishing temperature of 850-900°C attained. Soaking temperatures were based on considerations similar to those for the rolled alloys.

B.6.3 Results

B.6.3.1 Microstructure

Effect of austenitizing temperature and cooling rate on the microstructure and hardness was investigated and the results are summarized in Table 6.7. From the table, it can be inferred that lath structure formed over a wide range of cooling rates with a minimum attainable hardness of ~250 HV. Representative microstructure in the heat-treated condition is shown in Fig. 6.24.

The microstructure in the forged condition was 'lath like' in nature (Figs. 6.25- 6.27). As in the rolled alloys, the shear nature of the microstructure

was revealed only at a higher magnification (Figs.6.25a b). An examination of the longitudinal section revealed near-absence of directionality.

B.6.3.2 Mechanical Properties

Room temperature toughness in the forged condition was a function of the forging schedule. It was found, (i) to be too low (~30J) if intermediate reheating to the soaking temperature was employed during forging, (ii) a minimum of ~85J if forging was performed in a controlled manner, and, (iii) further, the toughness of the stock, forged with intermediate reheating improved on normalizing from 850°C to a value comparable with that obtained on control forging (Table 6.8). A variation in the forging schedule had little effect on the tensile properties, the percentage elongation and the UTS being ~20% and~930 MN/m^2 respectively (Table 6.8).

B.6.3.3 Fracture

Fractography tests were carried out on impact specimens tested at room temperature which were machined from the steel stock forged under two different conditions viz. (i) control-forged and, (ii) forged with intermediate reheating.

It was observed that in case of the former the fracture appearance was ductile showing tear dimples (Figs. 6.28

and 6.29) whereas in the latter, it was brittle in character (Fig 6.30 and 6.31).

B.6.4 Discussion

In the near-absence of carbon, manganese which is an austenite-stabilizer is most useful in promoting the formation of lath structure at moderate cooling rates over a range of section sizes. To a much lesser extent, silicon, molybdenum and Nb additions are useful in delaying the $\gamma \rightarrow \alpha$ transformation (sections 3.3.2.1 and 3.4). The combined beneficial effect of these elements has ensured that the composition being investigated is an air-hardening one with a minimum attainable hardness of $\sim$250 HV (Table 6.7).

Considering the toughness values, a minimum ambient temperature toughness (ATT) of 85J, obtained on control-forging, is because of the attainment of a fine grain size. This is attributed to the grain refining action of niobium and has been confirmed by metallographic observations (Fig. 6.26). The low ATT value obtained while forging with intermediate reheating is because of the attainment of a coarser grain size. (Fig. 6.27).

Occurrence of continued recrystallization in austenite is an essential condition for obtaining grain refinement during hot working (175). This is achieved by

regulating the thermal and deformation components of a hot working schedule i.e. by carrying out hot working in a controlled manner. In the present instance, considerable grain coarsening occurs during reheating to the soaking temperature. Since the deformation imparted to the austenite after the reheating stage is insufficient, the essential condition for obtaining grain refinement is not fulfilled. Thus, in a way, the effectiveness of Nb as a grain refiner is greatly reduced. Therefore, a microstructure with a coarse grain size is attained. Observation at (i) (section B.6.3.2) is thus explained. The observation at (iii) can be similarly explained, based upon grain-refining brought about by normalizing.

A minimum ATT value of 85J, obtained on control-forging, compares favourably with the maximum ATT attained in the forging quality low alloy high strength steels only after normalizing, normalizing and tempering (N and T) and quenching and tempering (Q and T) heat-treatments (213-215). Thus it may be possible to do away at least with the normalizing heat-treatment given to the forgings to improve their toughness provided the process parameters permit forging to be carried out in a controlled manner.

Hardness, strength and ductility values in the forged condition (Table 6.8) are comparable with those reported for similar steels in the as-rolled condition (Tables 6.3 and 6.5) and are in good agreement with the similar values reported for lath structures in the extra low carbon Fe-Mn (189; 208), Fe-Ni (156,172,209)* and multi-component (210) systems. The observation that ductility is independent of the forging schedule employed is of considerable significance. A similar result has been reported in Chapter-V and can primarily be attributed to a very-nearly carbon-free microstructure. It is noteworthy that an elongation value 20% is easily attainable in steels such as the present ones even after subjecting them to widely varying thermal and mechanical treatments (Table 6.8). The observation that the hardness and strength are nearly independent of (i) the sectiona size and (ii) the forging schedule, is logical since strengthening primarily results from a high dislocation density introduced during the shear transformation occurring during cooling.

The most significant observation of the present investigation has been the strong dependence of the ATT on grain size. Although grain size strongly influences ITT, instances where it has affected the ΔTT are few (46,175). A critical appraisal is therefore necessary, as to whether or not the grain size should

*. Pl. see foot-note on p. 132.

affect the ΔTT, to fully comprehend (a) this aspect of the structure-property correlation in the steel currently being investigated, and, (b) its implications.

It is known that an increase in strength generally results in a decrease in toughness. Empirically, an increase in hardness by 10HV raises the transition temperature by about 15°C (115). Considering for instance, a mild steel (hardness 125-150HV, ΔTT 100-135J) as a reference base, the empirical formula would reveal that at the strength (hardness) level currently attained (Tables 6.8), the ΔTT should be very low provided there is a continuous decrease in toughness with strength. But normally, this is not the case, since if it were so then the attainment of a high ΔTT and low ITT would not have been feasible in high strength alloy steels. Fundamentally, the basic principle involved in getting a desired combination of ATT and ITT at a given strength level is by improving the net available deformation, both at the ambient and more specifically at sub-zero temperatures. In practice this is achieved through a combination of alloying and heat-treatment. For example in the quenched and tempered (Q and T) steels, for getting the right combination of strength, ATT and ITT, it is necessary to make adjustments in the composition for (i) toughening the ferrite matrix, (ii) for eliminating temper-embrittlement (214). In addition, it

is essential to employ an overaged microstructure. Inspite of providing the best in terms of alloying and and heat treatment, conventional steels do undergo premature failure ~~due to unavoidable factor~~ because of factors beyond control eg (i) cracking of lamellar carbides (98) and formation of voids at the pearlite colonies in ferrite-pearlite steels (216), (ii) occurrence of elongated carbides surrounding bainitic ferrite regions and formation of austenite-martensite constitutent in the air-cooled bainitic steels (119), (iii) possibility of a variation in carbide zize, shape and distribution and also of precipitation occuring in unfavourable location in Q and T steels, and, (iv) the presence of boundary carbides in lath martensites (105). They (unintended microconstituents) generally have their origin in the carbon content and are difficult to investigate. Presence of unintended microconstituents affects both ATT and ITT adversely. Considering the alloy currently under investigation, unlike the Q and T steels, no pre-requisites regarding composition control and heat-treatment are necessary for obtaining the stipulated properties. Secondly, the alloy is designed in a way so as to provide a base microstructure free of unintended microconstituents. This has been primarily achieved by keeping the carbon content very low i.e. about 0.03 pct. (section 4.1). Presence of low sulphur and phosphorous contents (0.008 to 0.01 pct.) merely enhances

the benefits accruing from keeping the carbon content at a minimum .

However, providing a suitable microstructural base in itself is not a sufficient condition to ensure attainment of a high ATT value. Just as in the Q and T steels, both alloying and heat treatment play an equally significant role in controlling the strength and toughness, similarly, there must be some parameters controlling the properties of the type of steel under investigation, thereby facilitating the attainment of end requirements. This stipulation is valid barring one important difference. Whereas in the Q and T steels, the improvement in ATT is at the cost of strength, this is not so in the present steel since the attainable strength is nearly constant and independent of the section size. The microstructure of interest (lath structure) is neither soft nor tough in the sense the ferrite martix is in the Q and T steels. Under these conditions, the only way toughness can be improved is by improving the net available deformation. This is achieved by refining the prior austenite grain size. It is vital to emphasize here that the microstructure of interest (i.e. the lath structure), although, containing a high dislocation density, has been made amenable to a toughening treatments by grain refinement primarily because it is free from unintended microstructural features and

also because the dislocation sub-structure is mobile.

The room temperature fracture appearance is consistent with ATT attained on (i) control-forging (Figs. 6.28 and 6.29) and,(ii) forging with intermediate reheating (Figs. 6.30 and 6.31). This reinforces the reasoning put forward to explain the strong dependence of ATT on the forging schedule and hence the grain size.

SUMMARY

Air-hardening steels, based on lath structure i.e. MAR' steels, on being control-rolled and control-forged attain proof strength in excess of 770 MN/m^2, UTS in excess of 900 MN/m^2, percentage elongation $\sim$20%, and excellent overall toughness. Attainment of these properties and particularly the toughness has been attributed to (i) features constituting the lath structure, (ii) a very low carbon content of the matrix, (iii) fine grain size, and, (iv) melting and casting techniques employed.

Although it has been deduced that strengthening is most likely resulting from a combination of solid solution and sub-structural hardening, this aspect needs a more detailed investigation. The next chapter is therefore, devoted to a critical analysis of the strengthening mechanisms.

C H A P T E R - VII

STRENGTHENING-MECHANISMS

7.1 INTRODUCTION

It is now well accepted that the following factors, in general, contribute to the strength of martensites:

i) Interstitial solid solution hardening by carbon/ nitrogen.

ii) Precipitation during the transformation.

iii) Presence of substitutional elements.

iv) Existence of transformation induced dislocation or twinned sub-structure, and,

v) Lath size

When considered in the context of MAR steels, it is evident that their contribution to the strength would depend upon composition. In order to make the discussion more broad-based, examples of extra low-carbon lath martensites formed in other low, medium and high alloy steels have also been considered. Such a step was likely to prove useful since it would provide,(i) for a comparison between the strength levels obtained in the present investigation with those reported in the literature, and, (ii) the likely clues to the factors other than those listed above, which may contribute to strengthening in the

alloys currently investigated.

7.2 RESULTS

Relevant data pertaining to the alloys, investigated thus far, is summarized in Table 7.1. On the basis of the effect of Mn, Si, Nb and Mo on hardenability, the alloys presently investigated can be classified as under-alloyed, correctly-alloyed or balanced and over-alloyed (Table 7.2). Mechanical properties of steels based on lath structure, other than those currently investigated, are given in Table 7.3. A comparison of the data summarized in Tables 7.1 and 7.3, reveals that :

i) Most steels based on lath structure exhibit strength and hardness in the range of 800-900 MN/m^2 and 250-300 HV_{30} respectively, except the binary Fe-Ni martensites and those compositions in which the microstructure obtained is sensitive to a variation in the cooling rate e.g. Fe-4 Mn.

ii) Hardness of lath martensites in Fe-Mn and Fe-Ni systems is independent of the total alloy content and the M_s temperature in the range of Mn/Ni contents within which the microstructure formed is lath-like with a dislocated sub-structure.

iii) Hardness of carbon-free lath martensites formed in the medium and high alloyed multi-component systems

is similar to that of the binary Fe-Mn martensites.

iv) Hardness of lath martensites obtained in the,
(a) underalloyed and balanced (correctly-alloyed) compositions of the present investigation, and,
(b) the Fe-Mn binary system is comparable.

v) Raising the silicon content of Fe~4 Mn-1 Si by about 1 pct. results in an increase in hardness from 250-300 to ~360 HV_{30}.

vi) Hardness of the alloys H3 (5 Mn-1.5 Si), H4 (~4.0 Mn-2.6 Si) and H6 (4.7 Mn-2.3 Si) is similar.

vii) Hardness of alloy R1 (~4 Mn-1.0Si-0.022 C)and alloy R2 (~4 Mn-1.0 Si-0.022 C-0.042 Nb), in the control-rolled condition, is identical although the latter has a finer grain size compared to the former.

7.3 DISCUSSION

A feature common to all the alloys under consideration is that they contain ~0.02-0.03 pct. carbon and not exceeding 0.05 pct. in any case. At such low carbon levels, the contribution of the interstitial solid solution hardening component is negligible. Further, although the tendency for carbide precipitation is enhanced at low carbon contents, the volume fraction formed is very small. As such, the contribution of carbide precipitation during the austenite to martensite transformation, to the overall

strength can be considered to be small. Therefore, the net effect of interstitial solid-solution hardening and carbide precipitation on strength is of little consequence.

Substitutional alloying elements are mainly added to, (a) enhance hardenability so as to facilitate martensite transformation, (b) bring about any other desired effect such as grain-refinement or intermetallic precipitation etc., and, (c) by virtue of being in the dissolved state, affect solution hardening. It is now necessary to analyse the data summarized in Tables 7.1 and 7.3 in order to establish the relative contribution of the above parameters related to the presence of substitutional elements. Considering the data shown in Table 7.4(a), it is seen that raising the Mn content of the Fe-1.8 Mn-1.2 Si alloy by 1, 2 and 3 pct. has resulted in an increase in the minimum attainable hardness from 118 HV_{30} to 160 HV_{30}, 245 HV_{30} and 317 HV_{30} respectively. If the hardness of the Fe-1.8 Mn-1.2 Si Alloy is taken as the base and if it is assumed that the role of increasing manganese content is to affect solution hardening alone, then it is seen that the observed increase in the hardness is much larger than can be attributed to solution hardening brought about by Mn alone [Table 7.4(b)]. Effect (b), stated above, has not been utilized in any of the alloys under consideration. This being so, the data analysis given above leads to the inference that of the two effects brought about by the

addition of substitutional elements, namely (a) and (c), the former predominates. Thus, substitutional elements and particularly those which are austenite stablisers e.g. Mn basically promote sub-structural strengthening rather than solution-hardening. This reasoning is further confirmed by the near constancy of hardness values in alloys with widely different alloy contents, namely Fe-5 Mn and Fe-10 Mn alloys, Fe-10 Ni and Fe-25 Ni alloys and the marageing composition in the as-transformed condition (Table 7.3).

It would also be of interest to examine the role of substitutional atoms from a different view-point. Considering all the above alloys, the quantitative results summarized in Table 7.4(b) suggest that the contribution of dislocation density to the strength is a variable one. This however, needs a closer examination. Retention of a dislocation sub-structure in the final microstructure signifies that the transformation temperatures on cooling are below those at which thermally activated softening processes occur. Once this is so, in view of the similarity between dislocation substructure produced in heavily cold-worked metals and that induced during martensitic transformation, it can be deduced that the dislocation density within laths would be more or less constant over a range of transformation temperatures (Fig. 7.1). Therefore, the contribution of dislocation

density to the strength is invariant over the temperature range T_o to T. When this is considered along with the deductions stated in the preceeding paragraph, the important inferences are:

a) The main effect of substitutional elements and particularly the austenite-stabilisers is to enhance hardenability and thus strengthen predominantly by sub-structural hardening.

b) Increasing the alloy content, primarily the austenite-stabilisers, beyond that required to produce an air-hardening composition upto a stage below which no austenite is retained and no change in the transformation induced sub-structure occurs, only results in a lowering of the transformation temperature and has little effect on hardness and strength. This is because the basic mechanism involving solution-hardening is based on lattice distortion. A change in the mode of transformation from nucleation and growth (N and G) to shear is also accompanied by a distortion in the parent lattice to form a highly stressed product lattice. The magnitude of distortion which accompanies austenite to martensite transformations is appreciably larger than that produced from the presence of substitutional solute atoms.

c) Dislocation density is likely to be nearly constant over a range of temperature T to T_o and would be independent of the alloy content, provided transformation to martensite occurs over a wide range of cooling rates.

d) Estimation of the solution hardening component in the alloys under consideration, based on the results summarized in Table 7.4(b), would be incorrect since the calculated values of $\Delta\sigma_{ss}$ are valid only for that particular alloy system and would vary depending upon the system under consideration. This is because the interaction parameters in any alloy system are a function of the number and type of components and the estimation of additional strengthening from such interactions is difficult to assess.

In view of (c) and (d), it is difficult to isolate solution-hardening effect from sub-structural contribution. It is, therefore, postulated that the solid-solution hardening component contributes effectively to strengthening only to a limit upto which there is no change in the nature of transformation and hence the microstructure. The relatively lower hardness values attained in binary Fe-Ni martensites are due to a smaller $\Delta\sigma_{ss}$ value which can be explained on the basis of Hume-Rothery laws.

Qualitatively, it can however be concluded that the substructural and solution-hardening together constitute a single factor primarily responsible for strengthening with the major contribution coming from the former. The order of magnitude of dislocation density within laths has been estimated to be 10^{13}-$10^{16}/cm^2$ (173). The above interpretation explains the hardness values reported in Tables 7.1 and 7.3 except for those of alloys H3, H4 and H6 (Table 7.1).

The discussion so far has been limited only to the existence of a high dislocation density contained within laths. However, lath (martensite) structure, besides a high dislocation density, also has other substructural features which are likely to have an important bearing on the strength and toughness. They include:

i) Packet/Block size, and,

ii) Lath width

As has been described earlier (Section 3.2), packets are small blocks present within a prior austenite grain which are mis-oriented from one another or may be twin related (153). They contain an array of nearly parallel laths which are separated from one another by low angle boundaries (153). Packets can be considered as equivalent to subgrains except that unlike the latter, they are not separated by low-angle boundaries. Factors

controlling packet size are not clearly understood. It is postulated that the following factors would be of relevance :

a) Prior austenite grain-size,

b) Cooling rate from roll finishing temperature, and,

c) Transformation temperature.

Thus, composition and process parameters controlling grain size are expected to influence packet-size. A reduction in packet-size might be expected to improve proof strength and toughness in accordance with the Hall-Petch type relation (67,68). Establishing such a correlation is, however, likely to lead to incorrect results because packets further contain sub-structure in the form of laths which in turn contain a high dislocation density/dislocation cell structure whose effect on strength has already been deduced to be a major one. Therefore, the effective contribution of packet-size to the strength is in terms of the sub-structure contained in it.

It has already been suggested that factors affecting grain size would affect packet size. Therefore, if grain-size is reduced, the packet-size is automatically refined. Another theoretical possibility is that for a given grain-size, packet size may vary. Such an occurrence would improve toughness provided the packet-size decreases. Therefore, factors controlling the packet-size other than

those related to grain-size need further examination. possible parameter in this regard would be the cooling rate from the roll finishing/forge finishing temperature. This possibility can be considered provided different cooling rates employed from the finishing temperature do not affect the final microstructure. Practical considerations, however, preclude utilization of such an approach which is more of a theoretical possibility. It would, therefore, not be of interest to control the packet-size beyond what is normally achieved by grain refinement. Existence of packets/blocks , however, has a distinct advantage as it is highly unlikely that orientation of laths within two adjacent packets would be the same. This would automatically bring about a change in the direction of crack propagation thereby improving toughness.

There are conflicting views on the effect of lath size on strength. Whereas some workers have considered laths as equivalent to grains and advocated correlating lath width with yield strength (219), others have shown that their effect on flow stress is of some significance only at very small lath widths (103,159). A clear picture would emerge if fine structure of laths is considered. The term lath signifies a configuration in which one dimension is much larger compared to the other. Laths

are separated by low angle boundaries (52,153). A reduction in lath size would bring the lath boundaries closer to one another. Since the dislocation content within laths is very high, lath boundaries coming closer would have little effect on the strength. The effect of lath width would assume some significance only at very small widths when low angle boundaries would have come so close to each other as to bring about an effective increase in the dislocation density. This explains why strengthening is marked only at very small values of lath width. It is further clear that laths are not equivalent to grains and therefore establishing any relationship between lath size and flow stress, as suggested earlier(219), would not be correct. The factor primarily controlling lath size is the transformation temperature. It is possible that factors affecting packet size may also influence the lath size. In view of the near constancy of lath-widths normally attained (52,103,145,172), factors controlling lath size have only theoretical relevance. It is, therefore, only the dislocation content within laths which has a major effect on strength.

Summarising, it can be stated that the net effect of fine-structure of the lath micro-constituent on strength is primarily controlled by dislocation density. Although refining packet-size might be expected to improve toughness, packet-size is related to the grain-size and,

in practice, is not an independent variable. Therefore, correlating packet size to the impact transition temperature, as attempted by some investigators (220-222) is somewhat out of place. It has, however, to be accepted that the existence of blocks containing nearly parallel lath arrays of different orientations is certainly beneficial from the point of view of toughness. Hence there is not sufficient justification for considering the effect of lath size and packet size in isolation. This implies that the earlier inference, which envisages dislocation density to be the major parameter controlling strength, is materially unaltered.

Grain size is generally considered an important parameter in controlling strength and toughness. In the alloys presently investigated, grain-refinement has been primarily employed for improving toughness and its contribution in this regard has been discussed in detail in Chapter-6. Considering the role of grain size on strengthening, the data reported in Tables 5.11, 5.12, 5.14 and 6.8, which indicate that, (i) for a given cooling rate, austenitizing temperature has little effect on hardness and strength and, (ii) forging schedule has little effect on strength in alloy F, suggest that the strength is nearly independent of the grain size. This reasoning agrees well with the inference that dislocation density is the primary factor controlling strength. Referring more

specifically to alloys R1 and R2, their mechanical properties (Table 6.3) indicate that although R2 has a finer grain size compared to R1, their strengths are nearly the same suggesting it to be independent of the grain size. However, the same result can be looked at differently by stating that strengthening in R1 consists of contributions from dislocation density and grain refinement and a further refinement in the grain-size over that attained in R1, does not contribute additionally to the strength. Considering this interpretation to be more plausible, the contribution of grain refinement to the strength can be assessed by comparing the proof strength values obtained on air-cooling R1 from 990°C with that obtained after control rolling R1 from the same temperature. This way, the contribution of grain refinement works out to be about 10-12 pct. of the total strength. Thus, from all accounts, the major source of strengthening is the high dislocation density and, therefore, it would not be incorrect to infer that strength as a whole (PS and UTS) is nearly independent of the grain size.

A very significant observation of the current investigation is that hardness and strength values attained in alloys H3, H4 and H6 (350-370 HV_{30}) were much higher than those obtained in alloys H5, R1, R2 and F (250-300 HV_{30}). It is, therefore, necessary to identify factors

which induce additional strengthening in the alloys H3, H4 and H6. This aspect has been investigated by X-ray diffraction and the results obtained form the basis of the next chapter.

7.4 CONCLUSIONS

Based on the above discussion, the following important inferences can be drawn regarding strengthening in steels based on extra low lath structure:

1) Primary strengthening mechanisms are dislocation sub-structure and solution hardening with the major contribution originating from the former.

2) Estimation of solution hardening component could at best be carried out in carbon free binary systems but not in ternary or multi-component systems, because of the interference from complex interactions.

3) Influence of packet size on the strength and toughness is only through its relation with the grain size. In view of the near-constancy of lath-widths, its contribution to strengthening, when considered in isolation, is of little consequence.

4) Contribution of grain refinement to strengthening is at best a minor one i.e. not exceedings 10-12 pct. of the total strength.

5) Existance of laths of different orientations in adjoining packets improves toughness by altering the direction of crack propagation.

C H A P T E R - VIII

STRUCTURAL INVESTIGATIONS BY X-RAY DIFFRACTION

8.1 INTRODUCTION

A critical analysis of the results reported in chapter-VII revealed that alloys H3, H4 and H6 attained hardness and strength values much higher than those obtained in the other alloys. It was therefore inferred that structural features, other than solid solution and sub-structural components were possibly responsible for the additional strengthening. These may include:

a) Occurrence of ordering

b) Existence of an additional micro-constituent

c) Change in the nature of transformation induced deformation sub-structure

d) Possibility of a change in the crystal structure.

Since the M_s and M_f temperatures of the alloys are well above room temperature, the possibility of (c) can be ruled out.

In order to identify the microstructural features contributing to additional strengthening, alloys H3, H4, H5, H6, R1, R2 and F were subjected to structural investigations by X-ray diffraction technique.

8.2 EXPERIMENTAL

Powder samples of the different alloys were heat-treated by adopting a procedure described in the section 4.8. In most cases, this consisted of soaking at 900° and 1000°C for nearly 30 minutes followed by water-quenching. In some instances, soaking periods upto 2 hours were employed.

Powder photographs were obtained with the help of 114.6 mm and 90 mm diameter Debye-Scherrer cameras employing filtered iron-Kα radiation. The X-ray diffraction patterns, thus obtained, were analysed in the usual manner.

8.3 RESULTS

The results obtained can be classified as follows:

1) Instances where a single phase structure α' (bcc) was obtained (Tables 8.1 to 8.9). This occured in the majority of cases (Fig. 8.1).

2) Instances where the structure attained was a combination of α' (b.c.c.) + retained austenite (fcc) (Tables 8.10 to 8.12).

3) Instances where the structure in the heat-treated condition was a combination of α', retained austenite and a carbide of the type $M_{23}C_6$ (Table 8.13).

4) Instances where the structure attained was a combination of α' + a complex carbide of the type $M_{23}C_6$ (Tables 8.14 to 8.18).

5) Instances where unconventional structure e.g. diamond cubic structure has been attained in the heat-treated condition (Table 8.19) - Fig. 8.1.

8.4 DISCUSSION

Carbon free ferrous martensites based on substitutional alloying elements generally have a bcc structure(60). Therefore, the results reported in the Tables 8.1 to 8.9, establishing the crytal structure of α' formed in all the alloys to be bcc, are consistent with the above observation. Splitting of the $\{110\}$ reflection was observed in some of the diffraction patterns obtained in the present investigation. This did not necessarily imply that tetragonality was present, since if it were so, splitting should have been observed not only in the $\{110\}$ reflection but also in all the subsequent high angle reflections. Therefore, it was concluded that the presence of a faint additional line close to the $\{110\}$ reflection could be attributed to the presence of an additional phase.

Referring to the observations (2), (3) and (4) in section 8.3, the initial reaction to the presence of extra lines in the diffraction patterns was of the possibility of the formation of an ordered phase.

Formation of ordered phases has been reported in the Fe-Si and Fe-Mn systems (223,224). However, a critical examination of the concerned alloy diagrams reveals that ordered phases are formed at Si/Mn contents much larger than those contained in the alloys presently investigated. Further indexing of diffraction patterns on the premise that ordering was occurring, did not appear possible. This thought was, therefore, discarded.

The other possibility considered was the retention of austenite. Although such an occurrence appears improvable since the M_s and M_f temperatures are well above room temperature, yet it was given due consideration. Based o this assumption, the diffraction patterns of alloy R1 Tables 8.10 and 8.11 could be fully indexed and that of the alloy R2 only partly (Table 8.12). However, not all the diffraction patterns could be indexed based on the premise that austenite was retained. This evidently led to the inference that a second phase was formed during soaking for heat treatment. After considering the different possibilities, it emerged that all the remaining patterns (observations 3 and 4 of section 8.3) could be indexed based on the formation of a carbide of the type $M_{23}C_6$ with a simple cubic structure (Tables 8.13 to 8.18). The probable reasons which might have led to the formation of a carbide of this type will be discussed later. Thus it was possible to index all the diffraction patterns

of alloys H3, H5, H6 and R1 and R2 i.e. other than those already indexed (Tables 8.13 to 8.18).

Attainment of a diamond cubic structure in the alloy H3, in the heat-treated condition, is an unexpected results (Table 8.19). Inspite of several attempts, it has not been possible to reproduce this structure. However, the result is being reported to emphasize that unintended and unexpected microconstitutents may form in heat-treated steels. This observation assumes a wider significance in the present context since one of the primary objectives of the present investigation was to arrive at steel compositions in which the probability of unintended microconstituents forming is reduced to a minimum. However, it is important to reiterate that the alloys presently under investigation are better placed in comparison to the conventional steels to overcome the problems arising from the presence of unintended microconstituents. Wider implications of the formation of a diamond cubic structure in heat treated extra low carbon MAR steels would be assessed only after the structure has been reproduced in powder samples and probability of its formation in bulk samples assessed. This would however, require extensive experimentation.

The most significant observation needing a careful analysis and consideration is the retention of austenite. This result is all the more surprising since the M_s and M_f temperatures and well above room temp. Retention of austenite

in heat-treated steels is not a new observation. Infact 9 pct. Ni cryogenic steel is one of the earliest reported steels in which austenite retention in the Q and T condition led to a considerable improvement in the sub-zero temperature toughness (225). In recent years, there has been an ever increasing evidence of the presence of inter-lath retained austenite in conventional steels (66,226,227). Infact there are positive indications that the presence and quantity of inter-lath austenite primarily controls the toughness of as-quenched martensitic low carbon to medium C steels alloyed with Mo and/or Cr(66). Similarly, in some of the recent investigations it has been reported that austenite retention in conventionally employed low alloy steels, through modified heat treatment cycles, can lead to an improvement in the toughness (226). It has been further reported that low additions of austenite stabilizers Ni, Mn or Co may facilitate inter-lath austenite retention in low carbon (0.2 pct.) alloy steels(66). These are some of the observations which provide a basis for evaluating whether or not austenite can be retained in steels presently under investigation.

It has been reported that very small additions of Mn to carbon-free iron is very useful in producing ultra fine grain sizes by using alternate cycles of cold deformation and annealing (228). This has been attributed to the tendency of Mn atoms to segregate to the grain

boundaries (228). In another study involving the transformation behaviour of carbon-free binary Fe-Mn alloys containing upto 10 pct. Mn, it has been reported that the inherently low toughness exhibited by them is perhaps due to a classical temper-embrittlement type phenomenon attributed to the solute/impurity atom segregation to grain boundaries (208). Occurrence of solute-segregation in the alloys under investigation cannot be ruled out. This being so, it is easy to visualize that this phenomenon has a direct bearing on austenite retention. A solute concentration build-up in the regions adjoining the grain-boundaries may enrich parent austenite to an extent that austenite is retained in the final microstructure. Since the major alloying species is manganese, there is a strong possibility that the austenite retention would be localized to areas adjoining the grain boundaries. Therefore, retention of austenite in alloys R1 and R2 can be justified.

In the light of the above observation the microstructures of alloys R1 and R2, in the as-rolled condition, were re-examined under polarized light after successively etching with nital and acid-ferric chloride until an over-etched surface was obtained. On doing so, it was observed that the dark jagged regions, representing lath structure, were bounded by bright etching thin net work representing retained austenite (Figs. 8.2a and 8.2b). Its presence has been further confirmed by X-ray

diffractometry. The location of austenite retention is extremely beneficial from the point of view of both ambient as well as sub-zero temperature toughness particularly if it were to be stable.

Having thus explained austenite retention in alloys R1 and R2, it is now necessary to comment upon (a) the formation of complex carbide of the type $M_{23}C_6$ in combination with retained austenite in alloy R2, and, (b) absence of retained austenite and the formation of $M_{23}C_6$ carbide in alloys H3, H5, H6 and R1. It has already been stated that the solute atom build-up most likely occurs along and in the regions adjoining the grain-boundaries. This can be described as clustering. In an assembly of Mn, Si, Fe and C atoms, the Mn-C and Fe-C interactions would be stronger than Mn-Si or Fe-Si interactions (229). In such a situation, three distinct possibilities arise: (a) austenite is retained, (b) austenite is rendered unstable and $M_{23}C_6$ precipitates and, (c) partial retention of austenite with some formation of $M_{23}C_6$. Clustering of atoms leading to austenite-retention is favoured by the following conditions :

i) a large Mn/ferrite stabilizing element ratio,
ii) a high Mn content, and,
iii) faster cooling rate.

Whereas conditions opposite to these i.e. (i) an imbalance

in the Mn/ferrite stabilizing element ratio or a low Mn/ferrite stabilizing element ratio, (ii) a lower Mn content, and (iii) a slower cooling rate, would lead to its decomposition and subsequent formation of $M_{23}C_6$. Any combination of these opposing tendencies/conditions could lead to the partial retention of austenite with formation of some $M_{23}C_6$. This reasoning satisfactorily explains the formation of $M_{23}C_6$ in alloys H3, H5, H6, R1 and R2 (Tables 8.13 to 8.18). A more detailed discussion of the effect of soaking time and heat-treating temperature on the extent of the formation of $M_{23}C_6$ has not been pursued since the effect of soaking time at a given austenitizing temperature on the formation of $M_{23}C_6$ has not been investigated in all the alloys. However, on the basis of the limited information derived from the investigations carried out on alloy H3, it can be safely deduced that the formation of $M_{23}C_6$, which essentially forms by clustering, can be reduced to a minimum by (i) employing heat-treating temperature 1000 °C or more, (ii) avoiding holding in the 850 to 1000°C temp. range for prolonged periods during any thermal and/or mechanical working schedule, and, (iii) by employing faster cooling rate. Infact it can be inferred that quenching extra low carbon MAR steels would be beneficial as a whole since, (a) it can lead to the formation of a micro-constituent such as austenite at the desired location, and,

(b) would lead to the elimination of unintended micro-constituents, such as $M_{23}C_6$, without the danger of developing any quench/transformation cracking.

The basic reason for carrying out the x-ray studies was to investigate why the alloys H3, H4 and H6 attained higher hardness and strength levels than normally expected. Surprisingly, structural investigations carried out do not provide any positive clues to the likely reasons. However, it is postulated that a stronger Mn-Si interaction (230) may be responsible for the additional strengthening in alloy H3, H4 and H6. This being so, a question most likely to arise is why a stronger Mn-Si interaction is not manifested in the alloys H5, R1, R2 and F. This can be explained by further postulating that the stronger Mn-Si interaction would be manifested only if the alloy content (i.e. either Mn or Si or both) is increased beyond the threshold composition i.e. beyond the composition at which austenite changes to α' in preference to α.* In the present investigation, the threshold composition has been demonstrated to be the base composition R1 (Fe 4Mn-1.0Si or an equivalent Fe-Mn-Si-Mo composition). This reasoning can most satisfactorily explain the attainment of higher strength in alloys H3, H4 and H6.

8.5 CONCLUDING REMARKS

It is reaffirmed that the α/α' microstructures in

* (In a way that the final microstructure is α'.)

the extra low carbon alloys presently investigated have a bcc crystal structure. A strong possibility of austenite retention in the microstructure, in the heat treated condition, is indicated. This would lead to an improvement in toughness, provided austenite is retained along and in the regions adjoining prior-austenite grain boundaries. Formation of $M_{23}C_6$ is primarily a consequence of clustering of atoms. In view of the compatibility of the crystal structure, the presence of $M_{23}C_6$ may not adversely affect toughness unless it forms at unfavourable locations. The possibility of the formation of $M_{23}C_6$ may be reduced to a minimum by a proper selection of thermal and or hot working schedules.

In the absence of direct evidence, it is postulated that additional strengthening in alloys H3, H4 and H6 can be attributed to the stonger Mn-Si interactions and hence to a relatively higher bond strength. The possibility of the formation of the metastable dc structure appears to be an extension of this tendency.

C H A P T E R - IX

CONCLUSIONS

The usefulness of the alternative approach of developing new high strength steels, based on the utilization of extra low-carbon lath structure, is amply demonstrated. Although enough has already been said about the adverse effects associated with twinned martensite as a constituent, a yet another factor which is receiving considerable attention and goes against its utilization, is the occurrence of microcracks accompanying the formation of twinned-martensite. This not only goes against using low to medium carbon contents for developing steels but also highlights the problems that can develop in steels in which twinned-martensite may form indirectly.

Another factor which is of utmost importance while developing steels is the occurrence of temper-embrittlement. This factor has not been discussed since in the present context Q and T heat-treatment is eliminated, 'C' content of the base matrix is very low and also because the carbide forming tendency of the major alloying element (Mn) is moderate.

With this brief introduction, the important conclusions arrived at in this study can be summarized

as follows:

1) Manganese and silicon can be used advantageously in much larger proportions than hitherto employed in developing new high strength steels.

2) From the point of view of attaining lath structure, it is essential to maintain a proper balance — approx 3:1 ratio of austenite/ferrite stabilizing elements. This is also useful in ensuring that toughness is not adversely affected.

3) Silicon contents upto 1% can be safely employed. At this silicon content, the manganese content required to produce an air-hardening composition is approximately 4 percent.

4) Silicon reduces volume changes associated with the γ to α and reverse transformations. The higher the amount of silicon, the greater is the reduction in volume changes. If steels containing high ($\sim$2%) silicon contents are to be employed, then the minimum manganse content required to produce an air-hardening composition would have to be stepped up, at least to ensure that possibility of the formation of polygonal ferrite is eliminated.

5) The base composition Fe-3.7Mn-1.0Si (Composition R1) represents the limiting composition for

producing lath structure over a range of section sizes. In combination with 0.022%C and $\sim$ 0.04%Nb, the composition (i.e. R2) can be adjudged to be the best, in terms of the overall mechanical properties amongst all the alloys investigated. With this composition, PS = 790 MN/m^2, UTS = 950 MN/m^2, % elongation 27%, USE in excess of 270J and a transition temperature of $-90^{o}C$ can be obtained in the control-rolled condition at least in 17 mm round section

6) The attainment of high USE and a low ITT in alloys R1 and R2 in the control-rolled condition has been attributed to the presence of (i) very low carbon content and therefore a nearly carbide-free matrix (ii) fine grain size, (iii) retention of austenite (iv) relatively low sulpher and phosphorus contents, and, (v) to the utilization of vacuum melting and casting techniques.

7) Raising the carbon content of the base composition from 0.022 to 0.055% resulted in an increase in strength without any substantial decrease in ductility. The overall toughness was also reduced. The USE and ITT values were found to be a function of (i) working schedule and (ii) presence or absence of a grain-refiner. The former influenced the grain-size and the latter the tendency to lath boundary carbide precipitation in addition to the grain size.

8) In a given air-hardening steel composition, grain size is the single most important factor controlling the overall toughness of steels based on lath structure. This has been clearly brought out while studying the effect of forging schedule on the mechanical properties of an air-hardening composition Fe-4 Mn-0.4 Mo-0.Si-0.074 Nb-0.03C which is basically an extension of the base composition R1 and its modified counterpart R2.

9) The hardness and strength levels attained in the different alloys are nearly the same except for alloys H3, H4 and H6. The mechanisms responsible for strengthening are dislocation substructure contained within laths and solid solution hardening, with the major contribution coming from the former. In the alloys H3, H4 and H6, the additional strengthening primarily results from the stronger manganese silicon interactions.

10) The contribution of the sub-structure to the strength is nearly constant and independent of the alloy content and Ms temperature within a composition range over which there is no change in the nature of the transformation product and transformation induced sub-structure.

11) Lath and packet size do not have a direct bearing on the strength since the former is a function

of the transformation temperature and has been found to be nearly constant in different alloy systems and the latter is not an independent variable.

12) In view of the above, it can be inferred that the overall strength would be nearly independent of the grain-size, In the alloys in which grain refinement has been done, the contribution of fine grains to the strength is at best 10%. The useful strength of steels such as the present ones lies between 800 to 1200 MN/m^2.

13) In view of (12) above, grain size has the most dominant effect on the overall toughness from amongst the three parameters - grain-size, packet-size and lath width.

14) Possibility of formation of unintended micro-constituent $M_{23}C_6$ is indicated. However, from the limited evidence available, it appears that its formation is most likely to occurs, predominantly in the temperature range 850 to 1000°C, on prolonged holding. This has been attributed to the clustering of atoms. Raising the temperature has been shown to be effective in restricting the formation of $M_{23}C_6$. Hence its formation can be avoided provided appropriate thermal/mechanical working schedules are employed.

15) There is limited evidence to suggest that in alloys containing Mn as the major alloying element, austenite retention is most likely to occur at/or in the regions adjoining grain boundaries. This would lead to an improvement in overall toughness. Therefore, it is recommended that Mn content of the air-hardening composition may be increased deliberately with the sole purpose of introducing austenite into the microstructure at the right location.

16) A remote possibility is indicated of the formation of unconventional structural features e.g. occurence of a diamond cubic structure (d.c.) in an instance in alloy H3, in heat-treated MAR steels. This aspect needs further investigation before any further deductions could be made regarding its likely impact on properties.

FUTURE WORK

1) Assessment of fracture toughness.

2) A more detailed investigation to ascertain the nature of the unintended microconstituents, if any, that may form.

3) Detailed evaluation of the rolling/forging response.

REFERENCES

1. W.E.DUCKWORTH and J.BAIRD;
JISI Centenary Issue, 105 (1969).

2. K.J.IRVINE,
'Strong and Tough Structural Steels',
ISI Sp. Rep. 104, 11 (1967)

3. K.J.IRVINE, F.B.PICKERING
JISI, 201, 518 (1963).

4. K.J.IRVINE, F.B.PICKERING, T.GLADMAN;
JISI, 205, 161 (1967).

5. L.MEYER and H.DE BOER;
Journal of Metals, 29(1), 17 (1977).

6. T.BURGAN and M.G.STANUISTREET,
Ref. 2, p. 79

7. W.E.DUCKWORTH et al.,
'High Strength Steels', ISI Sp. Rep 76 ,1 (1962).

8. A.S.KENNEFORD;
'LOW ALLOY STEELS', ISI Sp. Report 114,65 (1968).

9. J.WOOLMAN,R.A.MOTTRAM;
'Mechanical and Physical Properties of British Standard EN Steels', Vol 2, (1966).

10. R.BROOK, J E RUSSEL,
'High Alloy Steels', ISI Sp. Report 86, 19 (1964).

11. M.J.MAY; Ref. 2, p 11.

12. A.K.PATWARDHAN and P.TEWARI;
'Eastern Metals Review Annual No.,(1966).

13. W.E.DUCKWORTH;
Ref. 2, p.60 and Discussion on p. 231.

14. C.L.M.COTTRELL - Ref. 7, p.1.

15. G.M.BOYD; Ref. 2, p.23.

16. R.W.K. HONEYCOMBE;
'Low Alloy Steels';ISI Sp. Rep. 114, 65 (1968).

17. H.J.ADAMS and A.J.JOHNSON; Ref. 2, p.27.

18. H.C.COTTOM; Ref. 2, p. 31.

19. P.G.WINCHELL and M.COHEN;
'Electron Microscopy and Strength of Crystals',
Ed. G.Thomas and J.Washburn, 995 (1963).

20. A.S.KENNEFORD; Ref. 7, p. 74.

21. A.S.KENNEFORD and T.WILLIAMS;
JISI, 185, 467 (1957).

22. A.S.KENNEFORD; Ibid 189, 135 (1958).

23. A.S.KENNEFORD; Ibid 192, 215 (1959).

24. A.S.KENNEFORD; Ibid 188, 16 (1958).

25. W.E.DUCKWORTH et al; Ref. 7, p.22.

26. A.S.KENNEFORD et al.; Ref.16,p.91.

27. Mechanical Properties of Nickel Alloy Steels -
International Nickel Co., London.

28. R.W.K.HONEY-COMBE; Ref. 10, p.1.

29. J.NUTTING; Rep. 1, p.123.

30. G.G.BROWN; Ph.D.Thesis, University of Sheffield

31. E.N.Bower; Ph.D.Thesis, University of Sheffield

32. R.Papaleo; Ph.D.Thesis, University of Sheffield

33. R.Blower; R.K.Greenwood, G.P.Miller; Ref. 8, p.119.

34. F.B.Pickering; Ref. 8, p.131.

35. J.A.Whiteman; Ref. 8, p.233.

36. F.B.Pickering; Ref. 8, p.234.

37. R.F.Decker et al; Trans. ASM Quart; 55,58 (1962).

38. J.J.IRANI, D.DULIEU, G.TITHER; Ref. 8, p.75.

39. U.S.Patent 3, 132, 025: May 5, 1964.

40. British Patent No.688, 617.

41. A.S.KENNEFORD, C.H.OXLEE; JISI, 205, 38 (1967).

42. M.R.KRISHNADEV, I.LE MAY; JISI, 208, 458 (1970).

43. R.W.K.HONEYCOMBE Private Communication to F.B.PICKERING - Ref. 34.

44. K.J.IRVINE et al.; JISI, 186, 54 (1957).

45. K.J.IRVINE and F.B.PICKERING; Ibid, 187, 292.(1958).

46. F.B.PICKERING;
'Climax Molybdenum on Transformation and Hardenability in Steels', 109 (1967).

47. K.J.IRVINE and F.B.PICKERING;
'Physical Properties of Martensite and Bainite'
ISI Sp. Rep. 93, 110 (1965).

48. D.N.SHACKLETON and P.M.KELLEY; Ref. 47, p. 126

49. J.W.CHRISTIAN; Ref. 47, p.1.

50. J.W.CHRISTIAN;
'Mechanism of Phase Transformation in Crystalline Solids', Institute of Metals Monograph No. 33, 129 (1969).

51. P.M.KELLY and J.NUTTING; Ref. 47, p.166.

52. A.R.MARDER and G.KRAUSS;
Trans. ASM Quart, 60, 651 (1967).

53. A.R.TROIANO and A.B.GRENINGER;
Metal Progress, 50, 303 (1946).

54. M.Cohen, E.S.MACHLIN and V.G. PARANJPE;
'Thermodynamics in Physical Metallurgy', ASM, Ohio; 242 (1949).

55. T.G.DIGGES; Trans. ASM Quart; 575 (1940).

56. L.KAUFMAN and M.COHEN;
'Progress in Metal Physics', 7, 165 (1958).

57. M.G.BIBBY and J.G.PARR; JISI, 202, 100 (1964).

58. T.BELL and W.S.OWEN; JISI, 205, 428 (1967).

59. T.BELL; ibid, 206, 1017 (1968).

60. P.M.KELLY; Ref. 10, p. 146.

61. P.M.KELLY and J.NUTTING; Ref. 7, p.7.

62. J.J.IRANI et al.; JISI, 204, 702 (1966).

63. G.THOMAS; Met. Trans., 2, 2373 (1971).
Also see references 109 and 146.

64. G.THOMAS and S.K.DAS; JISI, 209, 801 (1971).

65. D.H.HUANG and G.THOMAS;
Met. Trans. 2, 1587 (1971).

66. G.THOMAS; Iron and Steel International,451 (Oct.1973).

67. N.J.PETCH; JISI; 174, 25 (1953).

68. N.J.PETCH; 'Fracture', Wiley, New York; 54 (1959).

69. I.CODD and N.J.PETCH; Phil. Mag. 5, 30 (1960).

70. J.J.JONAS, C.M.SELLARS and W.J.McG-TEGART; Met Review 130;
'Metals and Materials', 1 (1969).

71. R.A.GRANGE; Trans. ASM Quart; 59, 26 (1966).

72. M.HILLERT; Act a Met.; 13, 227 (1965).

73. T.GLADMAN; Proc. Roy Soc., A 294, 298 (1966).

74. T.GLADMAN and F.B.PICKERING; JISI, 205,653 (1967).

76. D.HALL and G.H.J.BENNET; Ibid, 205, 309 (1967).

76. S.F.DARKEN et al; Trans. AIME, 191, 1174 (1951).

77. D.McLEAN, 'GRAIN BOUNDARIES IN METALS', Oxford
University Press; 241, (1957).

78. W.B.MORRISON; JISI, 201, 317 (1963).

79. H.NORDBERG and B.ARONSSON; JISI, 206, 1263 (1968).

80. K.J.IRVINE; Ref. 2, p.201-203.

81. G.P.AIREY; Ph.D.Thesis, Sheffield University, 1964.

82. G.P.COTNER; Ph.D.Thesis Sheffield University, 1966.

83. D.H.KEANE, C.M.SELLARS and W.J.McG.TEGART; Deformation under Hot Working Contitions', ISI Sp. Rep. 108, 21 (1968).

84. G.A.REDFERN and C.M.SELLARS; Ref. 83, p.29.

85. S.F.EXELL; Ph.D.Thesis, University of Sheffield etc.'70.

86. M.FUENTES; Ph.D.Thesis, Sheffield University, 1971.

87. T.L.UVIRA and J.J.JONAS; Trans. AIME;

88. M.M.FARAG, C.M.SELLARS and W.J.McG.TEGART; Ref.83,p.60.

89. W.A.WONG, H.J.McQUEEN and J.J.JONAS; JIM, 95, 129 (1967).

90. E.OROWAN; 'Sympo. On Internal Stresses in Metals and Alloys', 451 (1948).

91. W.D.BENNET; JISI, 171, 232 (1952).

92. V.ZACKAY and E.S.PARKER; 'High Strength Materials', Wiley, New York, 130 (1964).

93. M.J.MAY and E.F.WALER; Ref. 8, p.149.

94. G.W.GREENWOOD; 'Fracture Toughness', ISI Pub. 121, 1 (1968).

95. KOVESI and LEAVERLAND; Ref. 7, p. 63.

96. C.L.M.COTTRELL; Ref. 7, p.52.

97. W.ATKINSON; JISI, 195, 64 (1960).

98. T.GLADMAN, B.HOLMES and I.McIVOR. Proceedings of the Joint ISI/BISRA Conference on 'Effect of Second Phase Particle on the Mechanical Properties of Steel', 53, (1971).

99. W.B.MORRORION; Metals Technology, 2(1), 33 (1975).

100. R.M.GOLDHOFF; JISI, 195, 298 (1960).

101. P.S.SCHAFFERS et al; Modern Castings, 38(4), 95(1960).

102. P.E.RUFF and R.W.STEUR; Metals Progress, 80, 79 (1961).

103. G.R.SPEICH snd H.WARLIMONT; JISI, 206, 385 (1968).

104. R.H.ABORN; Trans. ASM; 48, 51 (1959).

105. K.J.IRVINE, F.B.PICKERING and J.GARSTONE; JISI, 196, 60 (1960).

106. A.J.BAKER, P.M.KELLY and J.NUTTING; 'Electron Microscopy and Strength of Crystals', Interscience, 899 (1963).

107. C.C.BUSBY et al; Trans ASM 47, 135 (1955).

108. W.H.McFARLAND; Trans.AIME, 233, 2028 (1965).

109. P.M.KELLY and J.NUTTING; JISI, 197, 199 (1 61).

110. R.H.VYHNALL and J.RADCLIFFE, Acta Met,(1968).

111. V.ZACKAY and W.M.JUSTUSSON; Ref. 7, p.14.

112. T.BONISZEWSKI ; Ref. 10, p.71.

113. T.BONISZEWSKI ; Ref.2 , p.201.

114. A.R.ROSENFIELD; Conference on 'Yield and Fracture', Oxford, Sep. 1966.

115. F.B.PICKERING and T.GLADMAN; 'Metallurgical Developments in Carbon Steels', ISI Sp.Rep. 81, 10 (1963).

116. J.J.IRANI and P.R.TAYLOR; Ref. 83, p.83.

117. J.J.IRANI; JISI, 206, 363 (1968).

118. J.J.IRANI and D.J.LATHAM; Ref. 8, p.55.

119. A,P.COLDREN et al; 'Climax Molybdenum Symposium on Strengthening Mechanism in Steels', 17 (1969).

120. G.T.HAHN, B.L.AVERBACH, W.S.OWEN and M.COHEN; 'Fracture', Wiley, New York; 91 (1959).

121. C.J.McMAHON and M.COHEN; Acta Met; 13, 591 (1965).

122 A.J.BIRKLE et al; Trans. ASM Quart; 58,285 (1965).

123. L.J.HARBRAKEN et al; Ref. 46, p. 69.
Ref. 2, p 110.

124. J.J.IRANI, D.BURTON, J.D.JONES and A,B.ROTHWELL; Ref. 2, p.110.

125. W.E.DUCKWORTH, R.A.PHILLIPS and J.A.CHAPMAN; JISI, 203, 1108 (1965).

126. R.PHILLIPS and J.A.CHAPMAN; ibid, 204, 615 (1966).

127. J.D.JONES and A.B.ROTHWELL; Ref. 83, p.78.

128. T.GEORGE; Ref. 2, p.123.

129. W.E.DUCKWORTH, D.A.LEAK and R.PHILLIPS; Ref.7,p.22.

130. J.J.IRANI; Ref. 47, p.193.

131. A.J.McEVILEY et al; Trans ASM Quart; 56, 753 (1963).

132. O.JOHARI and G.THOMAS; ibid; 58, 563 (1965).

133. R.PHILLIPS and W.E.DUCKWORTH;
'Proceedings of International Conference on High Strength Materials', 307 (1964).

134. G.THOMAS et al; ibid, p.251.

135. LEMENT; Trans. ASM Quart; 46, 851 (1954).

136. D.V.WILSON; Acta Met., 5, 293 (1957).

137. STEPHENSON and M.COHEN; Trans. ASM Quart; 54, 72 (1961).

138. M.COHEN; JISI; 201, 833(1963).

139. A.R.ENTWISTLE; Met. Trans. 2,

140. .B.GRENINGER and A.R.TR.IANO; ASM Trans 28, 537 (1940).

141. C.S.ROBERTS; Trans. AIME, 197, 203 (1953).

142. W.S.OWEN, T.BELL and E.A.WILSON;
'High Strength Materials', Ed. V.Zackay, John Wiley, New York; 157. (1965).

143. W.S.OWEN and E.A.WILSON; Ref. 47, p.53.

144. R.H.GOODNEW, S.J.MATAS and R.F.HEHEMAN;
Trans AIME 227, 651 (1963).

145. R.G.BRYANS, T.BELL and V.M.THOMAS; Ref. 50, p.181

146. P.M.KELLY and J.NUTTING;
Proc. Roy. Soc., A259, 45 (1960).

147. G.KRAUSS and A.R.MARDER; Met. Trans. 2, 2345(1971).

148. A.J.McEVILEY, R.G.DAVIS, C.L.MAGEE and T.L.JOHNSTON
Ref. 46, p.179.

149. J.A.KLOSTERMANN and W.G.BURGERS;
Acta. Met. 12, 355 (1964).

150. J.HONMA; J.Japan Instt. of Metals; 22, 122 (1957).

151. G.R.SPEICH and P.R.SWANN; JISI, 203, 450 (1965).

152. J.A.LUND, A.M.LAWSON; Trans. AIME; 236, 581 (1968).

153. J.M.MARDER and A.R.MARDER; Trans. ASM Quart; 62,
1 (1969).

154. J.S.BOWLES; Acta Cryst.; 4, 162 (1951).

155. P.McDOUGAL; Ref. 47, p.164.

156. A.R.ENTWISTLE;Institute of Metals, Monograph No.18,
315(1955).

157. J.M.CHILTON, C.J.BARTON, G.R.SPEICH; JISI; 208,
184 (1970).

158. D.S.SARMA; J.A.WHITEMAN, J.H.WOODHEAD; Metal Science,
391 (Nov. 1976).

159. J.D.EMBURY, A.S.KEH and R.M.FISCHER; Trans. AIME,
236, 1252 (1966).

160. S.K.DAS and G.THOMAS; Met.Trans., 1, 325 (1970).

161. S.K.DAS and G.THOMAS; Trans. ASM Quart; 62,
659 (1969).

162. S.R.KEOWN; M.Met. Thesis, Univ. of Sheffield, 1971.

163. M.COHEN Trans. AIME; 224, 638 (1962).

164. P.G.WINCHELL and M.COHEN;
'Electron Microscopy and Strength of Crystals',
Ed.G.THOMAS and J.WASHBURN, 995 (1963).

165. P.G.WINCHELL and M.COHEN; Trans. ASM Quart, 55, 347 (1962).

166. W.S.OWEN et al;
'The Structure and Properties of Quenched Iron Alloys' - Proc. of the 2nd International Symposium on Materials, University of California, June 1964.

167. M.J.ROBERTS and W.S.OWEN; Ref. 47, p 171.

168. M.J.ROBERTS and W.S.OWEN; JISI, 206, 375 (1968).

169. J.M.CHILTON and P.M.KELLEY; Acta.Met, 16, 637 (1968).

170. Y.A.BAGARYATSKI, Docald. Akad. Nauk S.S.R., 73, 1161 (1950).

171. W.PITSCH and A.SHRADER; Arch. Eisen; 29, 715 (1958).

172. M.J.ROBERTS and W.S.OWEN;
Trans. ASM Quart, 60, 679 (1967).

173. M.KEHOE and P.M.KELLEY;
Scripta Met. 4(6), 473 (1970).

174. G.R.SPEICH; Trans. AIME; 245, 2553 (1969).

175. A.J.McEVILEY and C.L.MAGEE, Ref. 8, p 111.

176. E.C.BAIN and H.W.PAXTON;
'Alloying Elements in Steels', ASM, Metals Park, Ohio; (1962).

177. ASM Metals Handbook, (1948).

178. ASM Metals Handbook, Vol. 1, (1961).

179. ASM Metals Handbook, Vol. 2, (1964).

180. U.S.Steel Cprporation; 'Making Shaping and Treating of Steel', Pittsburgh, Ohio (1964).

181. FISCHER and GEILS; Trans. AIME, 245, 2405 (1969).

182. W.HUME ROTHERY; 'The Structure of Alloys of Iron' Pergamon (1966).

183. C.H.WHITE; Ph.D.Thesis University of Sheffield.

184. C.H.WHITE, R.W.K.HONEYCOMBE; JISI, 200, 457 (1962).

185. C.L.MAGEE and R.G.DAVIES; Cross Reference 10 of Ref. 175.

186. J.D.BOLTON, E.R.PETTY and G.B.ALLEN; JISI, 209, 1314 (1969).

187. A.HOLDEN, J.D.BOLTON and E.R.PETTY; JISI, 211, 721 (1971).

188. W.JOLLEY; JISI, 206, 170 (1968).

189. R.A.WULLAERT; 'The Effect of Microstructure on the Fracture Behaviour of Low Carbon Ferritic Steel' AIME Fall Meeting, Chicago, 1966. (Cross-ref. of Ref. 186).

190. W.JOLLEY; Trans. AIME, 242, 306 (1968).

191. S.FLOREEN and G.R.SPEICH; Trans ASM Quart; 57, 714 (1964).

192. R.E.SMALLMAN; 'Modern Physical Metallurgy', Butterworths London (1972).

193. B.W.R.A. BULLETIN; 7, 149-178 (June 1966).

194. T.BONISZEWSKI, F.WATKINSON; Metals and Materials; 7(2), 90 (1973).

195. T.BONISZEWSKI and F.WATKINSON; ibid, 7(3),145 (1973).

196. A.G.HAYNES; Ref. 8, p. 189.

197. R.Sharma, M.Met.Thesis, University of Sheffield,1969.

198. F.Erdman et al; Arch.Eisen, 28, 345 (1957).

199. F.B.PICKERING; Ref. 7, p 53.

200. V.G.PARANJPE; Personal Communication.

201. Polaron Manual of Instruction.

202. T.B.MASALSKI - To be published in Acta Met.

203. C.J.McMAHON and M.COHEN;
"Proceedings of the First International Conference on Fracture" Sendai, Japan, Vol. 2, 779 (1965).

204. S.R.KEOWN and F.B.PICKERING: Personal Communication.

205. P.C.PHILLIPS; Personal Communication.

206. C.J.NOVAK and L.M.DIRAN; Journal of Metals; 15(3), 200 (1963).

207. G.DELISLE and A.GALIBOIS; JISI, Dec. 1969, p.1628.

208. J.D.BOLTEN, E.R.PETTY and G.B.ALLEN; Met. Trans. 2(10), 2915 (1971).

209. C.L.MAGEE and R.G.DAVIS; Publication Preprint, Ford Motor Company, Jan. 27, 1970.

210. G.P.CONTRACTOR; Journals of Metals, 22, 938 (1966).

211. BISRA Rep. MG/C/189/66

212. R.A.GRANGE, U.S. Steel Res. Rep., 1051.

213. S.S.LAKKUNDI; Personal Communication

214. Metals Handbook Vol. I. ASM, Ohio (1961).

215. C.A.PARSONS LTD., Specifications for Rotor Forgings (1970).

216. A.ROSENFIELD, Metallurgical Reviews 13, 29 (1968).

217. E.N.BOWER, R.PAPALEO and J.A.WHITEMAN; Ref. 98, p. 143.

218. K.J.IRVINE and F.B.PICKERING; JISI, 201, 944 (1963).

219. J.H.WOODHEAD, Ref. 8, p. 222 (discussion).

220. M.J.ROBERTS; Met. Trans. Vol. I, 3287 (1970).

221. J.P.NAYLOR and P.KRAHE; Met Trans. 5 (7), 1699 (1974).

222. J.P.NAYLOR and R.BLONDEAU, ibid 7(7), 891 (1976).

223. M.HANSEN; 'Constitution of Binary Alloys', McGraw Hill, New York (1958).

224. H.J.GOLDSCHMIDT; Interstitial Alloys; Butterworths London, (1967).

225. D.HARDWICK; Ref. 10, p. 49.

226. G.Y.LAI, W.E.WOOD, R.A.CLARK, V.F.ZACKAY and E.R.PARKER; Met. Trans. 5(7), 1663 (1974).

227. G.THOMAS; Met. Trans. 9A(3), 439 (1978).

228. V.RAMACHANDRAN; Personal Communication

229. M.L.KAPOOR; Personal Communication.

230. M.L.MEHTA, Personal Communication.

TABLE - 4.1

CHEMICAL ANALYSIS OF THE BASE MATERIALS

Element	Low Carbon Iron (ppm)	Electrolytic Sponge Iron (ppm)
C	400	20.0
Ni	600	32.0
Mn	400	80.0
Si	500	42.0
Al	500	-
As	-	3.2
Sb	-	0.9
Sn	120	5.1
S	-	48.0
P	200	7.0
Cu	500	14.0
Co	200	80.0
Cr	400	9.0
Mo	200	2.6
W	200	3.6
V	200	0.7
Ti	-	4.0

TABLE - 5.1

CHEMICAL ANALYSIS OF PRELIMINARY ALLOYS

Element	Alloy H1 (wt%)	Alloy H2 (wt %)
C	0.011	0.01
Ni	0.02	2.64
Mn	1.85	0.02
Mo	<0.02	<0.02
B	<0.001	<0.001
Si	1.12	1.23
W	<0.02	<0.02
V	<0.02	<0.02
Cr	<0.02	<0.02
Nb	<0.02	<0.02
Ti	<0.02	<0.02
Co	<0.02	<0.02
Al	<0.005	<0.005
Cu	<0.02	<0.02

TABLE - 5.2

EFFECT OF HEAT-TREATMENT ON THE HARDNESS AND MICROSTRUCTURE IN ALLOY H 1

S. No.	Heat Treatment	Approx. Specimen Thickness (mm)	Hardness (HV_{10})	Microstructure
1.	1100°C - FC	5.0	118	Polygonal Ferrite
2.	900°C - WQ	5.0	125	Polygonal Ferrite
3.	1000°C - WQ	5.0	135	Polygonal Ferrite
4.	1100°C - WQ	5.0	156	Polygonal Ferrite with some semblence of shear
5.	1100°C - WQ	2.5	160	Massive Ferrite
6.	1100°C - WQ	1.25	168(HV_5)	Massive Ferrite
7.	1100°C - WQ	0.90	171(HV_5)	Massive Martensite
8.	1100°C - WQ	0.50	-	Massive Martensite

TABLE - 5.3

EFFECT OF HEAT-TREATMENT ON THE HARDNESS AND MICROSTRUCTURE IN ALLOY H-2

S. No.	Heat Treatment	Approx. Specimen Thickness (mm)	Hardness (HV_{10})	Microstructure
1.	1100°C - FC	5.0	130	Polygonal Ferrite
2.	900°C - WQ	5.0	144	Polygonal Ferrite
3.	1000°C - WQ	5.0	160	Massive Ferrite
4.	1100°C - WQ	5.0	172	Massive Ferrite
5.	1100°C - WQ	2.5	178	Massive Ferrite
6.	1100°C - WQ	1.25	185(HV_5)	Massive Ferrite tending to Massive Martensite
7.	1100°C - WQ	0.90	192(HV_5)	Massive Martensite
8.	1100°C - WQ	0.50		Massive Martensite

TABLE - 5.4

MECHANICAL PROPERTIES OF ALLOYS (TREATMENT-1100°C WQ)

Alloy Designation	YS (MN/m^2)	UTS (MN/m^2)	El. (%)	RA (%)	REMARKS
H 1.	294.5	457.0	55	80	Shear lips observed
H 2.	304.0	457.0	40	75	Shear lips observed

TABLE - 5.5

CHEMICAL ANALYSIS OF 0.03 C ALLOYS

Element	Alloy H3 (wt %)	Alloy H4 (wt %)	Alloy H5 (wt %)	Alloy H6 (wt %)
C	0.033	0.033	0.03	0.031
Mn	5.06	3.9	2.61	4.7
Si	1.5	2.6	0.96	2.47
Mo	<0.02	<0.02	<0.02	<0.02
Ni	0.10	0.09	0.12	0.09
B	<0.001	<0.001	<0.001	<0.001
W	<0.02	<0.02	<0.02	<0.02
V	<0.02	<0.02	<0.02	<0.02
Cr	0.12	0.09	0.11	0.08
Nb	<0.02	<0.02	<0.02	<0.02
Ti	<0.02	<0.02	<0.02	<0.02
Co	<0.02	<0.02	<0.02	<0.02
Al	<0.09	<0.080	<0.07	<0.062
Cu	<0.09	<0.70	<0.09	<0.08
S	<0.02	<0.02	<0.02	<0.02
P	<0.02	<0.02	<0.02	<0.02

TABLE - 5.6

DILATOMETRIC-ANALYSIS

Alloy Designation	Mn/Si Ratio	AC_1 °C	AC_3 °C	Ar_3/M_s °C	Ar_1/M_f °C	Volume Change on Cooling (%)	REMARKS
H 3	5.0 : 1.5	650	780	404	345	0.287	Volume changes on heating and cooling discernable
H 4	3.9 : 2.6	690-732	770-800	438	390	0.080	Volume change on heating very small
H 5	2.6 : 0.96	722-842	880	690	635	0.325	Volume changes on heating and cooling discernable
H 6	4.7 : 2.47	680	770	415	350	0.100	Volume change on heating very small

(Temperature range indicates effect of thermal - hysteresis)

TABLE - 5.7

EFFECT OF HEAT TREATMENT ON THE HARDNESS AND MICROSTRUCTURE IN ALLOY H-3

S. No.	Heat Treatment	Hardness (HV_{30})	Microstructure
1.	1100°C - FC	317	Lath-like
2.	1100°C - CC	338	--do--
3.	1000°C - FC	325	--do--
4.	1100°C - WQ	352	--do--
5.	1000°C - WQ	360	--do--
6.	900°C - WQ	366	--do--
7.	800°C - WQ	366	--do--
8.	1100°C - AC	354	--do--
9.	1000°C - AC	363	--do--
10.	900°C - AC	362	--do--
11.	800°C - AC	364	--do--
12.	Hot swaged from 1100°C and air-cooled	358	--do--

TABLE - 5.8

EFFECT OF HEAT TREATNENT ON THE HARDNESS AND MICROSTRUCTURE IN ALLOY H-4

S. No.	Heat Treatment	Hardness (HV_{30})	Microstructure
1.	1100°C - FC	305	Lath-like and Polygonal Ferrite
2.	1100°C - CC	334	Lath-like
3.	1000°C - FC	-	-
4.	1100°C - WQ	362	Lath-like
5.	1000°C - WQ	370	--do--
6.	900°C - WQ	360	--do--
7.	800°C - WQ	310	--do--
8.	1100°C - AC	357	--do--
9.	1000°C - AC	360	--do--
10.	900°C - AC	358	--do--
11.	800°C - AC	305	--do--
12.	Hot swaged from 1100°C and air-cooled	358	--do--

TABLE - 5.9

EFFECT OF HEAT-TREATMENT ON THE HARDNESS AND MICROSTRUCTURS IN ALLOY H-5

S. No.	Heat Treatment	Hardness (HV_{30})	Microstructure
1.	1100°C - FC	158	Mostly Polygonal Ferrite + some Lath structure
2.	1100°C - CC	175	--do--
4.	1000°C - FC	165	--do--
4.	1100°C - WQ	318	Lath-like
5.	1000°C - WQ	320	--do--
6.	900°C - WQ	300	--do--
7.	1100°C - AC	220	Massive Ferrite tending to be Lath-like
8.	1000°C - AC	218	Massive Ferrite
9.	900°C - AC	206	--do--
10.	Hot-swaged from 1100°C, air cooled and partially cold-swaged	307	--do--

TABLE - 5.10

EFFECT OF HEAT-TREATMENT ON THE HARDNESS AND MICROSTRUCTURE IN ALLOY H-6

S. No.	Heat Treatment	Hardness (HV_{30})	Microstructure
1.	1100°C - FC	318	Lath-like
2.	1100°C - CC	340	--do--
3.	1000°C - FC	325	--do--
4.	1100°C - WQ	363	--do--
5.	1000°C - WQ	362	--do--
6.	900°C - WQ	367	--do--
7.	800°C - WQ	328	--do--
8.	1100°C - AC	360	--do--
9.	1000°C - AC	363	--do--
10.	900°C - AC	367	--do--
11.	800°C - AC	328	--do--
12.	Hot swaged from 1100°C and air-cooled	367	--do--

TABLE - 5.11

MECHANICAL PROPERTIES OF ALLOY H-3

S. No.	Heat Treatment	Hardness (HV_{30})	Microstructure	PS (MN/m^2)	UTS (MN/m^2)	El. (%)	RA (%)	PS/UTS Ratio
1.	1100°C - FC	317	Lath-like	-	976.5*	-	-	-
2.	1100°C - CC	338	-do-	-	1038.5*	-	-	-
3.	1100°C - WQ	352	-do-	-	1085.0*	-	-	-
4.	1100°C - AC	354	-do-	-	1085.0*	-	-	-
5.	1000°C - WQ	360	-do-	1054.0	1131.5	22	66	0.93
6.	1000°C - AC	363	-do-	1054.0	1131.5	24	65-66	0.93
7.	1000°C - FC	325	-do-	-	1007.5	25	65	-
8.	900°C - WQ	366	-do-	1077.2	1147.0	25	65-66	0.94
9.	900°C - AC	362	-do-	1069.5	1147.0	23	68-70	0.93
10.	800°C - AC	366	-do--	-	1131.5*	-	-	-
11.	800°C - WQ	364	-do-	-	1131.5*	-	-	-
12.	Hot swaged from 1100°C and air-cooled	358	-do-	1023.0	1100.5	24	65-66	0.93

* Probable UTS as estimated on 5 $HV_{30} \equiv 15.5$ MN/m^2

TABLE - 5.12

MECHANICAL PROPERTIES OF ALLOY H-4

S. No.	Heat Treatment	Hardness (HV_{30})	Microstructure	PS (MN/m^2)	UTS (MN/m^2)	El. (%)	RA (%)	PS/UTS Ratio
1.	1100°C - FC	305	Lath-like+PF*	-	945.4**	-	-	-
2.	1100°C - CC	334	Lath-like	-	1023.0**	-	-	-
3.	1100°C - WQ	362	--do--	-	1116.0**	-	-	-
4.	1100°C - AC	357	--do--		1100.5**	-	-	-
5.	1000°C - FC							
6.	1000°C - WQ	370	--do--	1085.0	1162.5	21	65	0.93
7.	1000°C - AC	360	--do--	1038.5	1140.8	27	68	0.91
8.	900°C - WQ	360	--do--	1054.0	1106.7	26	65-66	0.95
9.	900°C - AC	358	--do--	1023.0	1160.0	25	66-68	0.92
10.	800°C - WQ	310	--do--	-	961.0**	-	-	-
11.	800°C - WQ	308	--do--	-	961.0**	-	-	-
12.	Hot swaged from 1100°C and air cooled	358	--do--	1023.0	1147.0	24	66-68	0.89

* Polyonal Ferrite ; ** Probable UTS as estimated on 5 $HV_{30} \equiv 15.5$ MN/M^2

TABLE - 5.13

MECHANICAL PROPERTIES OF ALLOY H-5

S. No.	Heat Treatment	Hardness (HV_{30})	Microstructure	PS (MN/m^2)	UTS (MN/m^2)	El. (%)	RA (%)	PS/UTS Ratio
1.	1100°C - FC	158	Mostly PF*Some Lath-Structure	-	496.0**	-	-	-
2.	1100°C - CC	175	--do--	-	542.5**	-	-	-
3.	1100°C - WQ	318	Lath-like	-	976.5**	-	-	-
4.	1100°C _ AC	225	Massive to Acicular Ferrite	-	728.5**	-	-	-
5.	1000°C - WQ	320	Lath-like	930.0	992.0	18	66-68	0.93
6.	1000°C - AC	218	Massive Ferrite	440.0	657.2	44	68	0.67
7.	1000°C - FC	165	Mostly PF*+some Lath Structure	325.5	595.7	42	-	0.59
8.	900°C - WQ	300	Lath-structure	806.0	899.0	26	70	0.90
9.	900°C - AC	206	Massive Ferrite	449.5	669.6	42	70	0.67

* Polygonal Ferrite , ** Probable UTS as estimated on 5 HV_{30} ≡ 15.5 MN/m^2

TABLE - 5.14

MECHANICAL PROPERTIES OF ALLOY H-6

S. No.	Heat Treatment	Hardness (HV_{30})	Microstructure	PS (MN/m^2)	UTS (MN/m^2)	El. (%)	RA (%)	PS/UTS Ratio
1.	1100°C - FC	318	Lath-like	-	992.0*	-	-	-
2.	1100°C - CC	340	--do--	-	1054.0*	-	-	-
3.	1100°C - WQ	363	--do--	-	1116.0*	-	-	-
4.	1100°C - AC	360	--do--	-	1116.0*	-	-	-
5.	1000°C - FC	350	--do--	930.0	1078.7	25	66	0.86
6.	1000°C WQ	362	--do--	1085.0	1140.8	22	66	0.95
7.	1000°C - AC	363	--do--	1069.5	1162.5	27	66	0.92
8.	900°C - WQ	367	--do--	1077.2	1162.5	25	65-66	0.92
9.	900°C - AC	367	--do--	992.0	1103.6	24	68	0.90
10.	800°C - WQ	328	--do--	-	1007.5*	-		-
11.	800°C - AC	328	--do--	-	1007.5*	-	-	-
12.	Hot swaged from 1100°C and air-cooled	367	--do--	1023.0	1147.0	22	66	0.88

* Probable UTS as estimated on 5 $HV_{30} \equiv 15.5\ MN/m^2$

TABLE - 5.15

VARIATION OF TOUGHNESS* WITH TEMPERATURE

(Treatment : 1000°C WQ.)

Alloy Designation	Temperature °C	Energy Absorbed		REMARKS
		ft-lbs.	Joules. J	
H_3	150	13.5	18.2	Unbroken
	100	14.8	20.0	Unbroken
	Room Temp.	13.25	17.9	Unbroken
	0	9.5	12.8	Unbroken
	- 25	4.90	5.4	Broken
	- 50	3.0	4.00	Broken
	- 70	-	-	-
H_4	150	11.0	14.85	Unbroken
	100	11.4	15.40	Unbroken
	Room Temp.	3.0	4.05	Broken
	0	2.8	3.78	Broken
	- 25	2.5	2.7	Broken
	- 50	1.25	1.7	Broken
	- 70	-	-	-

* Sub-standard Charpy.

Table 5.15 Contd.

Table 5.15 Contd.

H_5	150	-	-	-
	100	-	-	-
	Room Temp.	13.0	17.6	Unbroken
	- 0	13.0	17.6	Unbroken
	- 25	11.0	14.85	Unbroken
	- 50	10.3	13.9	Unbroken
	- 70	9.5	12.8	Broken
	150	13.8	18.65	Unbroken
	100	15.0	20.3	Unbroken
H_6	Room Temp.	8.25	11.15	Broken
	0	3.25	4.4	Broken
	- 25	2.5	3.4	Broken
	- 50	2	2.7	Broken
	- 70	-	-	-

TABLE - 5.16

IMPACT-TRANSITION DATA

(Treatment : 1000°C WQ.)

Alloy Designation	Energy Absorbed at Dif. Temp. (ft-lbs., Substandard Charpy)								Transition Temperature* (°C)
	150°C	100°C	Room Temp.	0°C	-25°C	-50°C	-70°C	-100°C	
H_3	13.5	14.8	13.25	9.5	4.0	3.0	-	-	- 18
H 4	11.0	11.4	3.0	2.8	2.0	1.25	-	-	+ 48
H 5	-	-	13.0	13.0	11.0	10.3	9.5	-	< - 70
H 6	13.8	15.0	8.25	3.25	2.5	2.0	-	-	+ 19

* Based on an Arbitrary Energy value of 5.8 ft-lbs.

TABLE - 6.1

CHEMICAL ANALYSIS OF THE ROLLED AND FORGED ALLOYS

Alloy	C	Mn	Si	Nb	Mo	S	P
R1	0.022	3.60	0.94	-	-	< 0.02	< 0.020
R2	0.022	3.70	0.96	0.042	-	< 0.02	< 0.020
R3	0.055	3.80	1.04	-	-	< 0.02	< 0.020
R4	0.055	3.70	1.10	0.045	-	< 0.02	< 0.020
R	0.030	4.08	0.42	0.074	0.4	0.01	0.008

All values are in weight - percent.

TABLE - 6.2

EFFECT OF COOLING RATE ON HARDNESS AND MICROSTRUCTURE

Alloy Designation	Treatment	Hardness (HV_{30})	Microstructure
R1	1200°C - WQ	278	Lath-like
	1200°C - AC	240	-do-
	1200°C - FC	190	Massive Ferrite
	840°C - WQ	328	Lath-like
	840°C - AC	240	-do-
	840°C - FC	236	-do-
	990°C - AC	245	-do-
R2	1200°C - WQ	305	Lath-like
	1200°C - AC	242	Lath-like
	1200°C - FC	237	-do-
	1000°C - WQ	293	-do-
	1000°C - AC	250	-do-
	1000°C - FC	240	-do-
	840°C - WQ	305	-do-
	840°C - AC	238	-do-
	840°C - FC	240	-do-

TABLE - 6.3

MECHANICAL PROPERTIES OF STEELS IN THE AS-ROLLED CONDITION

Steel Designation	HARDNES HV_{30}			MECHANICAL PROPERTIES - 17mm Round			
	As Cast	Rolled From 1150°C to 20.5 mm round	60 mts.at 990°C+Rolled in 3 passes to 17 mm round	PS ( ) (MN/m^2)	UTS ( ) (MN/m^2)	El. ( ) (%)	RA ( ) (%)
R 1	240	250	285	793	916.3	22.5	66-68
R 2	250	265	295	780	900.5	27.5	68-70

TABLE - 6.4

VARIATION OF IMPACT STRENGTH WITH TEMPERATURE

Alloy Designation	Specimen No.	Temperature °C	Energy Absorbed Standard Charpy ft-lbs.	Joules	REMARKS
R 1	1	R.T.	201	271	Specimen Unbroken
	2	-25	181	243	-do-
	3	-50	163	220	-do-
	4	-70	34	46	Broken
	5	-100	15	19.3	-do-
R 2	1	R.T.	206	278	Specimen Unbroken
	2	-25	204	275	-do-
	3	-50	191	258	-do-
	4	-70	167	225	-do-
	5	-100	28	38	Broken
	6	-195	3	4	-do-

TABLE - 6.5

MECHANICAL PROPERTIES OF STEELS IN THE AS-ROLLED CONDITION

Steel Designation	HARDNESS (HV_{30})			MECHANICAL PROPERTIES (~17 mm round)			
	As Cast ~50 mm round	Rolled from 1150°C to ~20.5 mm round	60 mts. at 1090°C + air cooled to 990°C + rolled in 3 passes to ~17 mm round	PS PS (MN/m^2)	UTS (MN/m^2)	El (%)	RA (%)
R 3	285	326	320	862.4	1010.2	21	66
R 4	318	348	364	939.4	1096.5	22	68-70

TABLE - 6.6

VARIATION OF IMPACT STRENGTH WITH TEMPERATURE

(As rolled ~ 17 mm Round)

Alloy Desit-nation	Specimen No.	Tempera-ture ^{o}C	Energy Absorbed Standard Charpy ft-lbs.	Joules	REMARKS
R 3	1	R.T.	140	189	Specimen Unbroken
	2	-10	120	162	-do-
	3	-20	42	56	Specimen Broken
	4	-30	47	63	-do-
R 4	1	R.T.	125	169	Specimen Unbroken
	2	-10	90	121	-do-
	3	-20	50	67	Specimen Broken
	4	-30	52	70	-do-
	5	-40	17	23	-do-
	6	-60	6	8	-do-

TABLE - 6.7

EFFECT OF HEAT TREATMENT ON HARDNESS AND MICROSTRUCTURE OF ALLOY F

Ac_1 (A_s) - 730 °C
Ac_3 (A_f) - 830 °C
M_s - 450°C
M_f - 300 °C

Heat Treatment	Hardness (HV_{30})	Microstructure
1200°C - WQ	305	Lath-like
1200°C - AC	265	-do-
1200°C - FC	250	-do-
950°C - WQ	310	-do-
950°C - AC	270	-do-
950°C - FC	250	
850°C - WQ	315	-do-
850°C - AC	-	
850°C - FC	-	
1150°C - Hot Forged*	285	-do-

* From 115 mm square to about 31 mm Round with intermediate reheating

TABLE - 6.8

MECHANICAL PROPERTIES OF ALLOY F

(As Forged ~15 mm Square)

S. No.	Schedule of Working	MECHANICAL PROPERTIES					REMARKS
		Hardness (HV_{30})	PS (MN/m^2)	UTS (MN/m^2)	El. (%)	Minimum USE	
1.	1/2 hr. at 1200°C+ forged to about 15 mm square with intermediate re-heating when cross-section ~19 mm square	290	-	915	22	34	Nature of Impact Fracture Brittle
2.	Same as above but forged with no intermediate reheating	297	-	935	24	85	Fracture Appearance Ductile
3.	Schedule 1. + Normalize from 850°C	295	-	930	23	85	-do-
4.	Steel ESR melted + Schedule 1.	285	-	939	26	90	-do-

TABLE-7.1

MECHANICAL PROPERTIES OF ALLOYS INVESTIGATED

Designation	Composition	MECHANICAL PROPERTIES 0.2% PS MN/m^2	UTS MN/m^2	%Elongation	Thermal/ Mechanical Treatment
H3	Fe-5Mn-1.5Si	-	976.5	-	1100°C FC
		1077.2	1147.0	25	900°C WQ
		1069.5	1147.0	23	800°C AC
H4	Fe-3.9Mn-2.6Si	-	1023.0	-	1100°C,CC
		1085	1162.5	21	1000°C WQ
		1023	1160.0	25	900°C AC
H5	Fe-2.6Mn-1.0Si	806	899.0	26	900°C WQ
		930	990.0	18	1000°C WQ
		-	496.0	-	1100°C FC
H6	Fe-4.7Mn-2.3Si	-	992.0	-	11100°C FC
		1069.5	1162.5	27	1000°C AC
			1007.5	-	800°C AC
R1	Fe-3.7Mn-1.0Si	793.0	916.3	$22\frac{1}{2}$	Control Rolled
R2	Fe-3.7Mn-1.0Si -0.042 Nb	780.0	900.5	$27\frac{1}{2}$	Control Rolled
F	Fe-4Mn-0.4Si-4 Mo-0.03C-0.074Nb	790.0	900.5	20	Control Forged

TABLE-7.2

CLASSIFICATION OF THE ALLOYS CURRENTLY INVESTIGATED

Alloy	Designation	TRANSFORMATION TEMP. $A\gamma_3/Ms$ ^oC	TRANSFORMATION TEMP. $A\gamma_1/M_f$ ^oC	Min Hardness HV_{30}
H 3	Over-Alloyed	404	345	317
H 4	Over-Alloyed	438	390	305
H 5	Under-Alloyed	690	635	158
H 6	Over -Alloyed	415	350	318
R1	Correctly Alloyed	475	380	~240
R2	Correctly Alloyed	470	372	~240
F	Correctly Alloyed	460	350	~250

TABLE - 7.3

DATA ON EXTRA LOW-CARBON LATH (MARTENSITE) STRUCTURE FORMED IN DIFFERENT ALLOY SYSTEMS

Alloy System	Composition	Ar_3/M_s °C	Ar_1/M_f °C	Thermal/ Mech. Treatment	Structure	Mechanical Properties: Hardness HV_{30}	P S MN/m^2	UTS MN/m^2	% El / % RI	Reference
1	2	3		4	5	6	7	8	9	10
	Fe-4Mn	550	-	SC	MF	235	430	600	30(El)	
	-do-	-do-	-	1000°C BQ	LS	-	784.8	794.6	68 (RA)	
	-do-	-do-	-	800°C BQ	LS	-	895.2	902.0	65(RA)	
	Fe-5 Mn	-	-	SC	LS	-	-	-	-	
	Fe-6Mn	380	300	SC	LS	-	800	880	20(El)	
Fe-Mn	-do-	-do-	-do-	1000°BQ	LS	-	746	765	69(RA)	J.D.Bolton et al (208)
	-do-	-do-	-do-	800° BQ	LS	-	815	865	66(RA)	
	Fe-8Mn	300	180	1000°BQ	LS	270	853.5	893	63(RA)	
	-do-	-do-	-do-	800° BQ	LS	-	890.0	-	-	
	Fe-10Mn	180	100	1000°BQ	LS	290	814	878	65(RA)	
	-do-	-do-	-do-	800°BQ	LS	-	840	910	65(RA)	

contd.....

1	2	3	4	5	6	7	8	9	10
Fe-Ni	Fe-10Ni	-	-	WQ	LS	-	457.8	--	-	Speich and Swann (151) and Roberts and Owen (172)
	Fe-15Ni	-	-	WQ	LS	-	492.9	-	-	
	Fe-20Ni	-	-	WQ	LS	-	514.3	-	-	
	Fe-25Ni	-	-	WQ	LS	-	528.4	-	-	
Fe-Mn-Si Cr-Ti	Fe-8.7Mn -5Cr-2.5Si -0.8 Ti	-	-	1050°C WQ	LS	-	900	970	15.1(E) 73(RA)	E.N. Bower et al (217)
Fe-Ni-Si -V-Ti	Fe-12Ni-2.5Si -2.5V-0.5Ti		-	800°C WQ	LS	-	940	990	14(E) 76 (RA)	
Fe-Ni-Co -Mo-Ti	200 Grade Marageing	-155°C	-100°C	815°C	LS	-280	824.3	1024	17(E) 79 RA	Contractor (210)
	250 Grade Marageing	-do-	-do-	-do-	LS	-300	817.6	1028.0	19(E) 72(RA)	

MF = Massive Ferrite; LS = Lath structure

Unless otherwise stated, all the temperatures referred to in the above table are in centrigrade.

TABLE-7.4 (A)

EFFECT OF INCREASING MANGANESE CONTENT ON THE MINIMUM HARDNESS OF Fe-1% Si ALLOYS*

Designation	Alloy Composition**	Minimum Hardness HV_{30}	Thermal/ Mechanical Treatment
H1	Fe-1.8 Mn - 1.2Si	118	1100°C FC
H5	Fe-2.6 Mn - 1.0Si	158	1100°C FC
R1	Fe-3.7 Mn - 1.0Si	240	1100°C FC
H3	Fe-5 Mn - 1.5Si	317	1100°C FC

* Present Investigation

** In Weight Percent.

TABLE-7.4 (B)

SOLID SOLUTION STRENGTHENING CONTRIBUTION OF DIFFERENT ELEMENTS

Element	Change in Y.S./P.S. For 1 Wt.% Addition MN/m^2
C, N.	+ 4340.0
P	+ 852.5
Sn	+ 133.3
Si	+ 83.7
Cu	+ 38.75
Mn	+ 32.55
Mo	+ 10.95
Ni	0
Cr	- 31.0

After Irvine and Pickering Ref. 218.

TABLE-8.1

X-RAY POWDER PHOTOGRAPH OF ALLOY H3

Treatment : 850°C WQ.
Radiation : Filtered Fe-Kα

Sl. No.	$Sin^2\theta_{obs.}$	$Sin^2\theta_{cal.}$	$I_{obs.}$	hkl	a(A°)
1.	0.2327	0.2282	s	(110)	2.839
2.	0.4599	0.4564	m	(200)	2.855
3.	0.6864	0.6846	s	(211)	2.863
4.	0.9135	0.9128	ms	(220)	2.865

Structure : α' (bcc)

Lattice Parameter: 2.867 A°

TABLE-8.2

X-RAY POWDER PHOTOGRAPH OF ALLOY H3

Treatment : 1000°C WQ.
Radiation : Filtered Fe-K_α

Sl. No.	$Sin^2\theta_{obs.}$	$Sin^2\theta_{cal.}$	$I_{obs.}$	hkl	a(A°)
1.	0.2352	0.2292	s	(110)	2.824
2.	0.4616	0.4583	ms	(200)	2.850
3.	0.6974	0.6875	s	(211)	2.841
4.	0.9179	0.9166	m	(220)	2.859

Structure : α' (bcc)

Lattice Parameter: 2.861 A°

TABLE-8.3

X-RAY POWDER PHOTOGRAPH OF ALLOY H4

Treatment : 900°C WQ.

Radiation : Filtered Fe-K_α

Sl. No.	$Sin^2\theta_{obs.}$	$Sin^2\theta_{cal.}$	$I_{obs.}$	hkl	a(A°)
1.	0.2338	0.2249	s	(110)	2.832
2.	0.4627	0.4498	m	(200)	2.847
3.	0.6832	0.6747	s	(211)	2.869
4.	0.9121	0.8996	ms	(220)	2.887

Structure : α' (bcc)

Lattice Parameter : 2.888 A°

TABLE-8.4

X-RAY POWDER PHOTOGRAPH OF ALLOY H4

Treatment : 1000°C WQ.

Radiation : Filtered Fe-K_α

Sl. No.	$Sin^2\theta_{obs.}$	$Sin^2\theta_{cal.}$	$I_{obs.}$	hkl	a(A°)
1.	0.2313	0.2290	s	(110)	2.848
2.	0.4619	0.4580	m	(200)	2.855
3.	0.6897	0.6870	s	(211)	2.857
4.	0.9156	0.9160	ms	(220)	2.862

Structure : α' (bcc)

Lattice Parameter: 2.862 A°

TABLE-8.5

X-RAY POWDER PHOTOGRAPH OF ALLOY H5

Treatment : 900°C WQ.

Radiation : Filtered Fe-K_α

Sl. No.	$Sin^2\theta_{obs.}$	$Sin^2\theta_{cal.}$	$I_{obs.}$	hkl	a(A°)
1.	0.2386	0.2280	s	(110)	2.804
2.	0.4608	0.4560	ms	(200)	2.853
3.	0.7042	0.6841	s	(211)	2.826
4.	0.9121	0.8920	s	(220)	2.868

Structure : α' (bcc)

Lattice Parameter: 2.868 A°

TABLE-8.6

X-RAY POWDER PHOTOGRAPH OF ALLOY H5

Treatment : 1000°C WQ.

Radiation : Filtered Fe-K_α

Sl. No.	$Sin^2\theta_{obs.}$	$Sin^2\theta_{cal.}$	$I_{obs.}$	hkl	a(A°)
1.	0.2350	0.2278	s	(110)	2.825
2.	0.4634	0.4557	ms	(200)	2.845
3.	0.6908	0.6836	s	(211)	2.854
4.	0.9121	0.9115	ms	(220)	2.868

Structure : α' (bcc)

Lattice Parameter : 2.869 A°

TABLE-8.7

X-RAY POWDER PHOTOGRAPH OF ALLOY H6

Treatment : 900°C WQ.

Radiation : Filtered Fe-K_α.

Sl. No.	$Sin^2\theta_{obs.}$	$Sin^2\theta_{cal}$	I_{obs}	hkl	a(A°)
1.	0.2307	0.2268	s	(110)	2.852
2.	0.4490	0.4536	m	(200)	2.890
3.	0.6743	0.6804	s	(211)	2.888
4.	0.9070	0.9072	m	(220)	2.875

Structure : α' (bcc)

Lattice Parameter : 2.876 A°

TABLE-8.8

X-RAY POWDER PHOTOGRAPH OF ALLOY F

Treatment : 900°C WQ.

Radiation : Filtered Fe-K_α

Sl. No.	$Sin^2\theta_{obs.}$	$Sin^2\theta_{cal.}$	$I_{obs.}$	hkl	a(A°)
1.	0.2343	0.2269	s	(110)	2.828
2.	0.4495	0.4538	ms	(200)	2.888
3.	0.6860	0.6807	s	(211)	2.864
4.	0.9096	0.9077	ms	(220)	2.872

Structure : α' (bcc)

Lattice Parameter : 2.875 A°

TABLE-8.9

X-RAY POWDER PHOTOGRAPH OF ALLOY F

Treatment : 1000°C W.Q.

Radiation : Filtered Fe-K_α

Sl. No.	$Sin^2\theta_{obs.}$	$Sin^2\theta_{cal.}$	$I_{obs.}$	hkl	a(A°)
1.	0.2321	0.2274	s	(110)	2.843
2.	0.4616	0.4548	m	(200)	2.851
3.	0.6864	0.6822	s	(211)	2.850
4.	0.9108	0.9096	ms	(220)	2.870

Structure : α' (bcc)

Lattice Parameter : 2.872 A°

TABLE-8.10

X-RAY POWDER PHOTOGRAPH OF ALLOY R1

Treatment : 900°C WQ.

Radiation : Filtered Fe-K_α

Sl. No.	$Sin^2\theta_{obs.}$	$Sin^2\theta_{cal.}$	$I_{obs.}$	hkl	a(A°)
1.	0.2153	0.2129	vw	$(111)_\gamma$	3.615
2.	0.2252	0.2239	s	$(110)_{\alpha'}$	2.886
3.	0.2853	0.2839	vvw	$(200)_\gamma$	3.626
4.	0.4439	0.4479	ms	$(200)_{\alpha'}$	2.906
5.	0.5668	0.5678	vvw	$(220)_\gamma$	3.639
6.	0.6718	0.6718	ms	$(211)_{\alpha'}$	2.893
7.	0.7853	0.7807	vw	$(311)_\gamma$	3.624
8.	0.8520	0.8517	vvw	$(222)_\gamma$	3.634
9.	0.8998	0.8958	s	$(220)_{\alpha'}$	2.889

Structure : α'(bcc) + γ(fcc)

Lattice Parameter : α' = 2.894 A°

γ = 3.635 A°

TABLE-8.11

X-RAY POWDER PHOTOGRAPH OF ALLOY R1

Treatment : 1000°C WQ.
Radiation : Filtered Fe-K_α

Sl. No.	$Sin^2\theta_{obs.}$	$Sin^2\theta_{cal.}$	$I_{obs.}$	(hKl)	a(A°)
1.	0.2136	0.2122	vvw	$(111)_\gamma$	3.629
2.	0.2236	0.2236	s	$(110)_{\alpha'}$	2.896
3.	0.2821	0.2830	vvw	$(200)_\gamma$	3.647
4.	0.4454	0.4472	m	$(200)_{\alpha'}$	2.901
5.	0.5565	0.5660	vvw	$(220)_\gamma$	3.642
6.	0.6710	0.6709	ms	$(211)_{\alpha'}$	2.896
7.	0.7899	0.7782	vvw	$(311)_\gamma$	3.614
8.	0.8568	0.8490	vw	$(222)_\gamma$	3.624
9.	0.8992	0.8946	ms	$(220)_{\alpha'}$	2.886

Structure : α' (bcc) + Retained Austenite(fcc)

Lattice Parameter : α', a = 2.896 A°

γ , a = 3.641 A°

TABLE-8.12

X-RAY POWDER PHOTOGRAPH OF ALLOY R2

Treatment : 900°C WQ.

Radiation : Filtered Fe-K_α

Sl. No.	$Sin^2\theta_{obs.}$	$Sin^2\theta_{cal.}$	$I_{obs.}$	hKl	a (A^o)
1.	0.2175	0.2155	w	$(111)_\gamma$	3.596
2.	0.2325	0.2272	s	$(110)_{\alpha'}$	2.841
3.	0.2887	0.2874	vw	$(200)_\gamma$	3.604
4.	0.4564	0.4544	ms	$(200)_{\alpha'}$	2.867
5.	0.5765	0.5748	vw	$(220)_\gamma$	3.607
6.	0.6832	0.6816	m	$(211)_{\alpha'}$	2.869
7.	0.7912	0.7903	vvw	$(311)_\gamma$	3.611
8.	-	-	-	-	-
9.	0.9096	0.9088	s	$(220)_{\alpha'}$	2.872

Structure : α' (bcc) + Retained Austenite(fcc)

Lattice Parameter : α' a = 2.873 A^o

γ' a = 3.613 A^o

TABLE-8.13

X-RAY POWDER PHOTOGRAPH OF ALLOY R2

Treatment : 1000°C WQ

Radiation : Filtered Fe-K_α

Sl. No.	$Sin^2\theta_{obs.}$	$Sin^2\theta_{cal.}$	$I_{obs.}$	(hKl)	a(A^o)
1.	0.1421	0.1418	vw	$(330)_M$	-
2.	0.1872	0.1891	vw	$(422)_M$	-
3.	0.2058	0.2049	vw	$(510)_M$	-
4.	0.2143	0.2128* 0.2147*	vw	$[(511),(333)]_M$ $(111)_\gamma$	
6.	0.2252	0.2244	s	$(110)_{\alpha'}$	2.886
6.	0.2872	0.2837* 0.2863**	vm	$[(600),(422)]_M$ $(200)_\gamma$	-
7.	0.4451	0.4488	s	$(200)_{\alpha'}$	2.902
8.	0.6672	0.6732	s	$(211)_{\alpha'}$	2.904
9.	0.9065	0.8976	s	$(220)_{\alpha'}$	2.887

*Based on $M_{23}C_6$

$M = M_{23}C_6$ **Based on Retained Austenite

Structure : α' (bcc) + γ (fcc)

+ $M_{23}C_6$ (sc)

Lattice Parameter : a, α' = 2.891 A^o

$M_{23}C_6$, a = 10.91 A^o

TABLE - 8.14

X-RAY POWDER PHOTOGRAPH OF ALLOY H3*

Treatment : 1 h 900°C WQ

Radiation : Filtered Fe - K_α

Sl. No.	$Sin^2\theta_{obs.}$	$Sin^2\theta_{cal.}$	$I_{obs.}$	hKl	a (A^o)
1.	0.1163	0.1162	vw	$(321)_M$	-
2.	0.1482	0.1494	vw	$(411)(330)_M$	-
3.	0.1993	0.1992	vw	$(422)_M$	-
4.	0.2227	0.2258	s	$(110)_{\alpha'}$	2.903
5.	0.2890	0.2905	vw	$(531)_M$	-
6.	0.3983	0.3984	vw	$(444)_M$	-
7.	0.4524	0.4516	ms	$(200)_{\alpha'}$	2.879
8.	0.6766	0.6834	s	$(211)_{\alpha'}$	2.883
9.	0.9045	0.9032	s	$(220)_{\alpha'}$	2.880

$M = M_{23}C_6$

Structure = α'(bcc) + $M_{23}C_6$ (sc)

Lattice Parameter = For α', a = 2.882 A^o

$M_{23}C_6$, a = 10.630 A^o

Similar pattern obtained by a heat-treatment comprising of 1/2 h at -50°C - WQ.

TABLE-3.15

X-RAY POWDER PHOTOGRAPH OF ALLOY H3

Treatment : 2 h 850°C WQ.

Radiation : Filtered Fe-K_α

Sl. No.	$Sin^2\theta_{obs}$	$Sin^2\theta_{cal.}$	$I_{obs.}$	hKl	a(A°)
1.	0.1345	0.1350		$(400)_M$	-
2.	0.1710	0.1688		$(420)_M$	-
3.	0.2205	0.2292		$(110)_{\alpha'}$	2.916
4.	0.2461	0.2448		$(520)_M$ $(432)_M$	-
5.	0.3125	0.3123		$(510)_M$	-
6.	0.4202	0.4220		$(710)_M$ $(550)_M$ $(543)_M$	-
7.	0.4725	0.4583		$(200)_{\alpha'}$	2.818
8.	0.5712	0.5739		$(820)_M$	-
9.	0.6197	0.6161		$(830)_M$	-
10.	0.6977	0.6875		$(211)_{\alpha'}$	2.839
11.	0.9176	0.9166		$(220)_{\alpha'}$	2.859

$M = M_{23}C_6$

Structure : $\alpha'(bcc) + M_{23}C_6(sc)$

Lattice Parameter : α', a = 2.861 A°

$M_{23}C_6$, a = 10.542 A°

TABLE-8.16

X-RAY POWDER PHOTOGRAPH OF ALLOY H5

Treatment : 2 h at 900°C WQ.

Radiation : Filtered Fe-K_α

Sl. No.	$Sin^2\theta_{obs.}$	$Sin^2\theta_{cal.}$	$I_{obs.}$	hKl	a(A°)
1.	0.1552	0.1534		$(411)_M$ $(330)_M$	-
2.	0.2059	0.2049		$(422)_M$	-
3.	0.2332	0.2288	s	$(110)_{\alpha'}$	2.836
4.	0.2993	0.2982		$(531)_M$	-
5.	0.4065	0.4089		$(444)_M$	-
6.	0.4608	0.4578	ms	$(200)_{\alpha'}$	2.853
7.	0.5569	0.5538		$(810)_M$	-
8.	0.6076	0.6134		$(822)_M$	-
9.	0.6892	0.6865	s	$(211)_{\alpha'}$	2.857
10.	0.9165	0.9154	s	$(220)_{\alpha'}$	2.860

M = $M_{23}C_6$

Structure : α'(bcc)+$M_{23}C_6$(sc)

Lattice Parameter : α', a= 2.863 A°

$M_{23}C_6$, a = 10.492 A°

TABLE-8.18

X-RAY POWDER PHOTOGRAPH OF ALLOY R1

Treatment : 2 h at 900°C WQ.

Radiation : Filtered Fe-K_α

Sl. No.	$Sin^2\theta_{obs.}$	$Sin^2\theta_{cal.}$	$I_{obs.}$	(hKl)	a (A^o)
1.	0.1506	0.1503		$(411),(330)_M$	-
2.	0.2066	0.2087		$(500)_M$	-
3.	0.2166	0.2171		$\begin{matrix}(510),(431)_M \\ (111)_\gamma\end{matrix}$	-
4.	0.2325	0.2280		$(110)_{\alpha'}$	2.838
5.	0.3232	0.3173		$(611),(532)_M$	-
6.	0.3756	0.3757		$(630),(542)_M$	-
7.	0.4287	0.4259		$(711),(551)_M$	-
8.	0.4616	0.4560		$(200)_{\alpha'}$	2.851
9.	0.6871	.6840		$(211)_{\alpha'}$	2.862
10.	0.9124	.9120		$(220)_{\alpha'}$	2.867

M = $M_{23}C_6$

Structure : α'(bcc)+$M_{23}C_6$ (sc)

Lattice Parameter : α', a = 2.868 A^o

$M_{23}C_6$, a = 10.598 A^o

TABLE-8.19

X-RAY POWDER PHOTOGRAPH OF ALLOY H3

Treatment : 900°C WQ.

Radiation : Filtered Fe-K_α

Sl. No.	$Sin^2\theta_{obs.}$	$Sin^2\theta_{cal.}$	$I_{obs.}$	(hKl)	a(A°)
1.	0.1076	0.09490	s	(111)	5.114
2.	0.2705	0.2530	ms	(220)	5.266
3.	0.3631	0.3479	ms	(311)	5.331
4.	0.5186	0.5061	w	(400)	5.379
5.	0.6125	0.6010	w	(331)	5.393
6.	0.7638	0.7591	m	(422)	5.429
7.	0.8576	0.8540	m	(333)	5.434

Structure : Diamond Cubic

Lattice Parameter : 5.445 A°

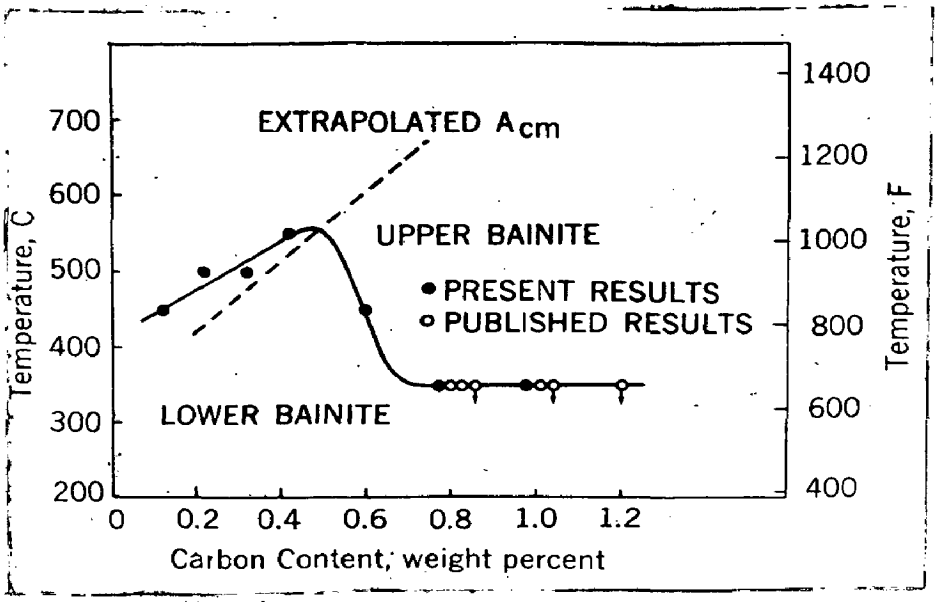
EXTRAPOLATED Acm
UPPER BAINITE
PRESENT RESULTS
PUBLISHED RESULTS
LOWER BAINITE
Temperature, C
Temperature, F
Carbon Content, weight percent

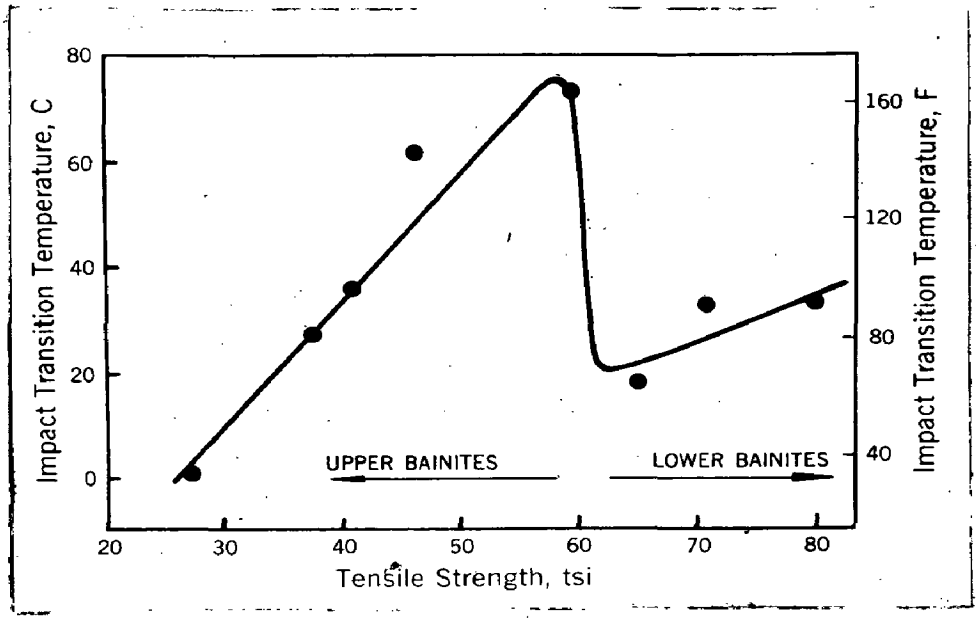
Impact Transition Temperature, C
Impact Transition Temperature, F
UPPER BAINITES
LOWER BAINITES
Tensile Strength, tsi

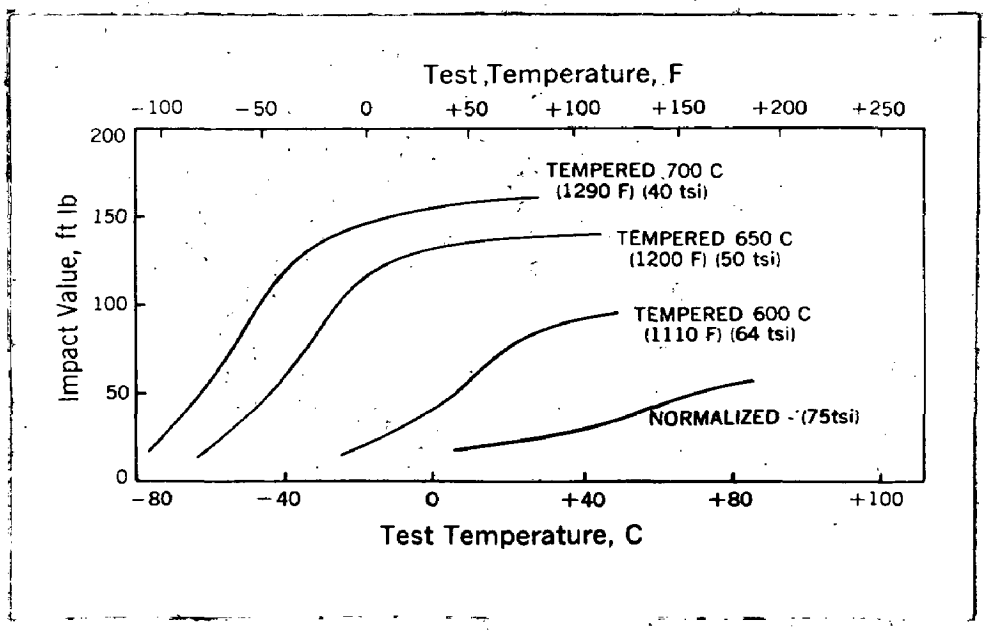
Test Temperature, F
TEMPERED 700 C (1290 F) (40 tsi)
TEMPERED 650 C (1200 F) (50 tsi)
TEMPERED 600 C (1110 F) (64 tsi)
NORMALIZED (75tsi)
Impact Value, ft lb
Test Temperature, C

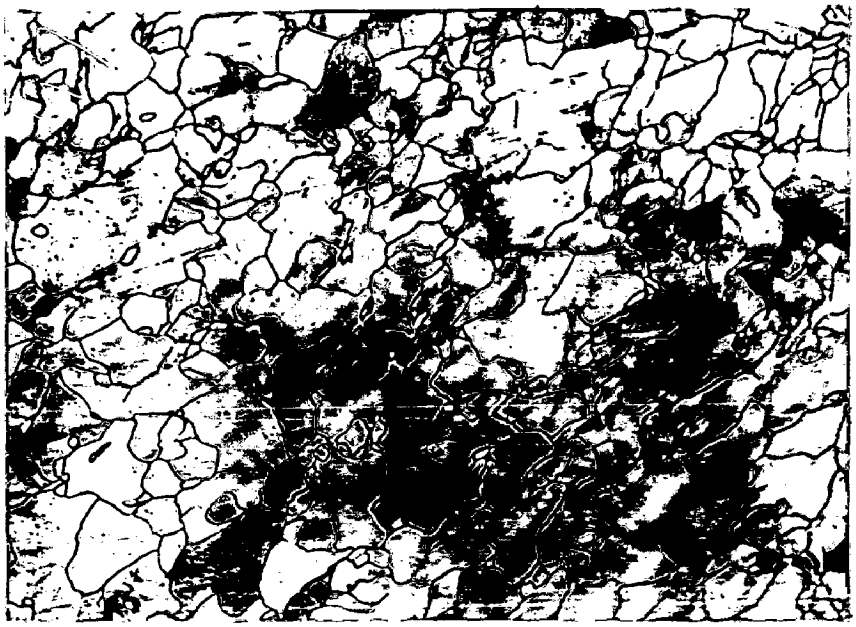

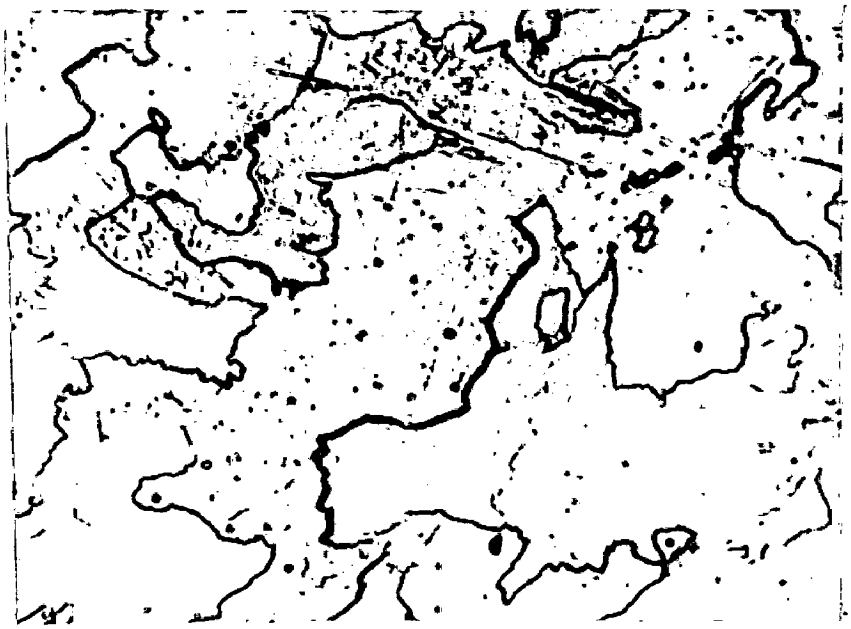

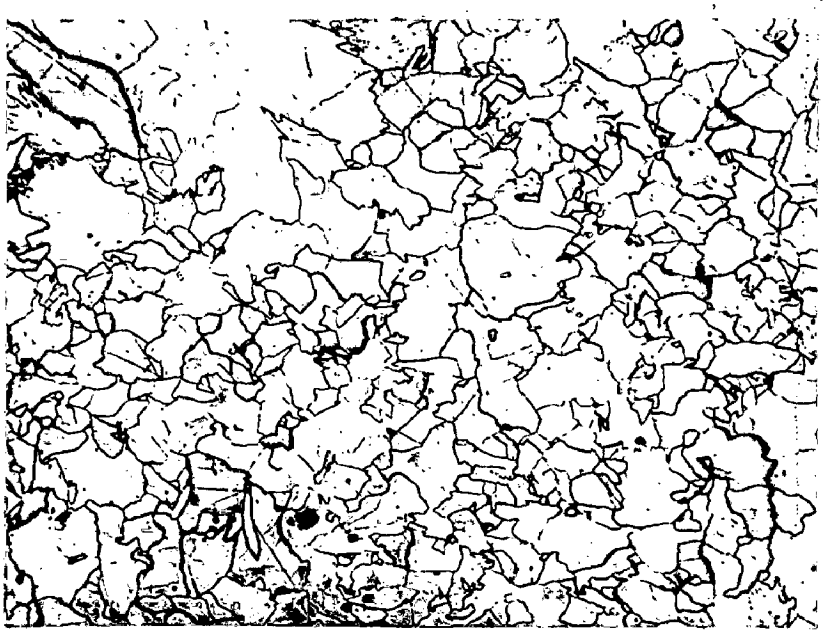

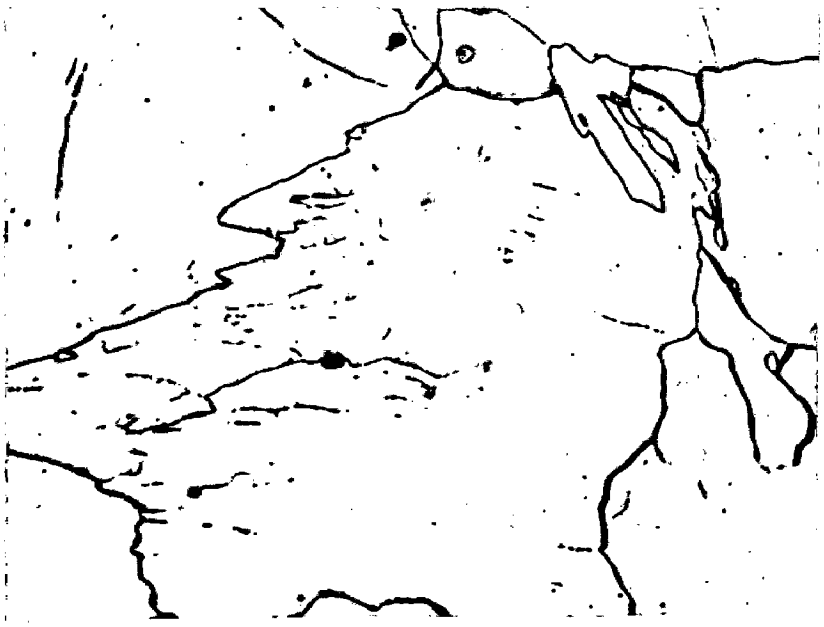

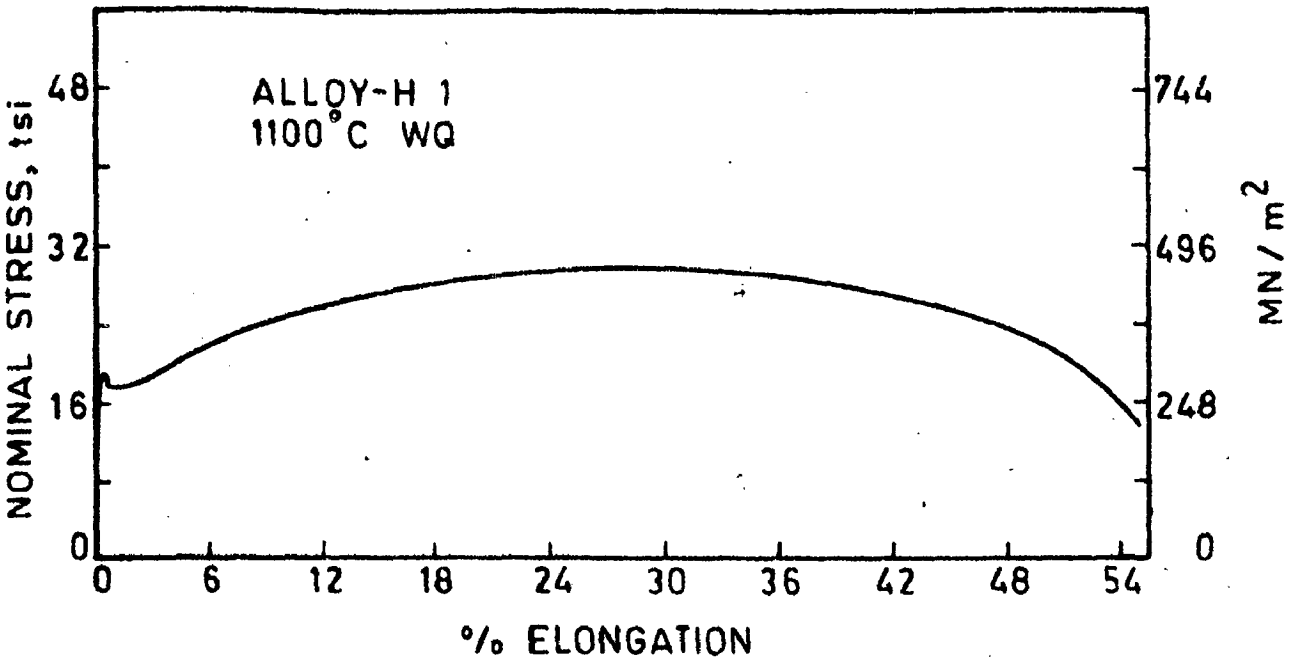

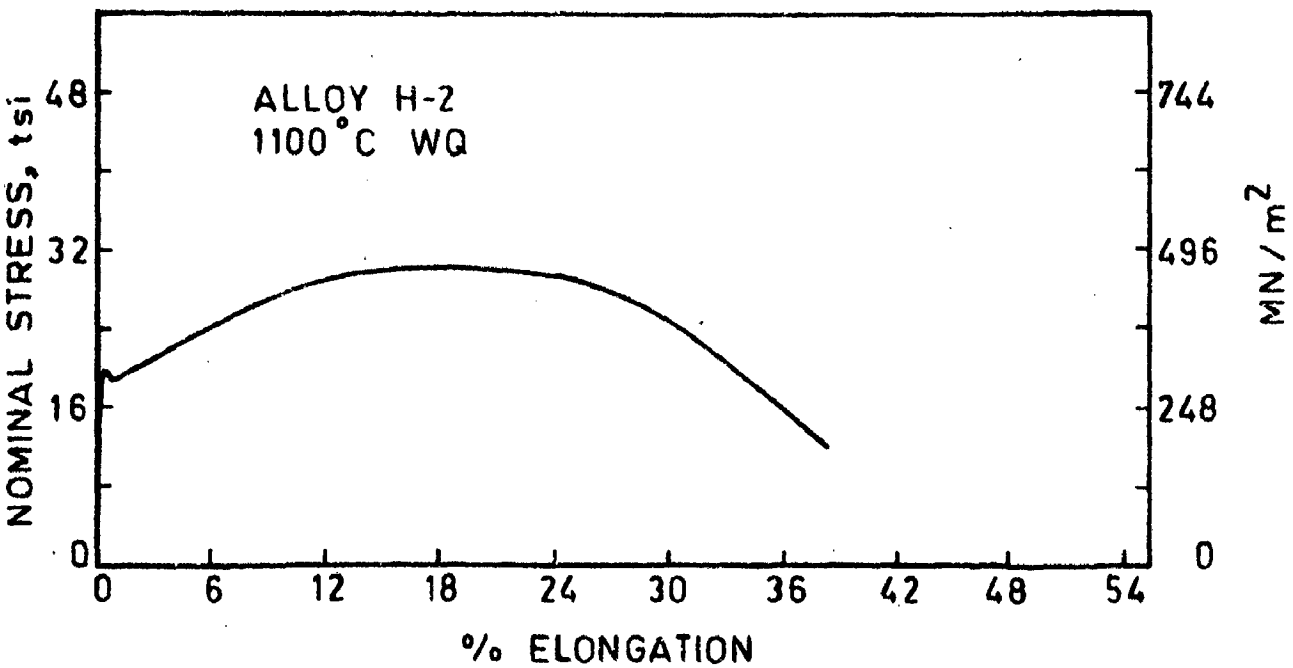

FIG.5.5 STRESS-STRAIN CURVES FOR ALLOYS H-1 AND H-2

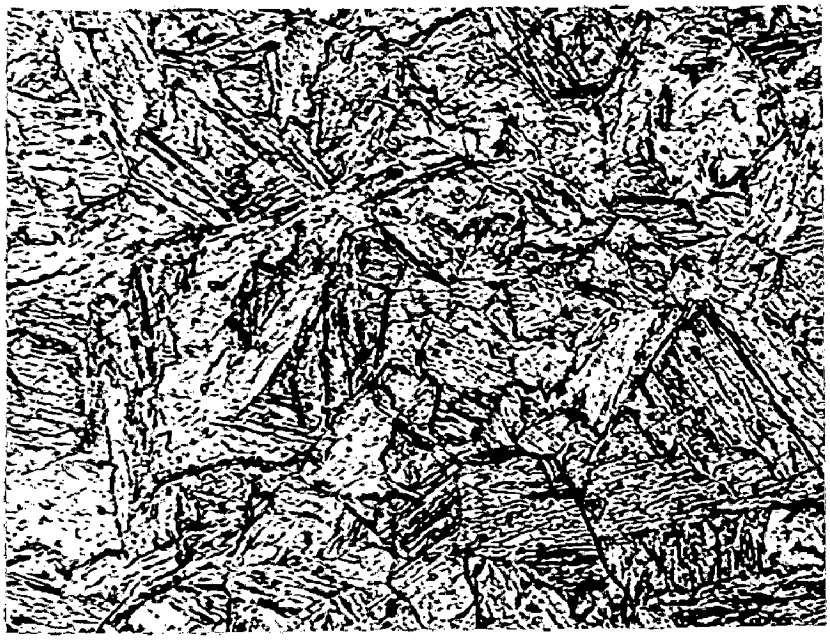

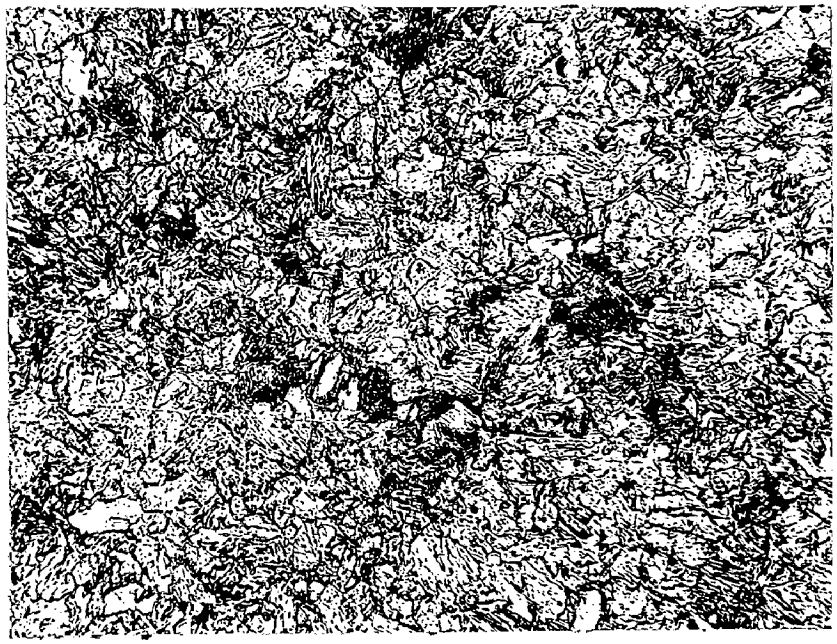

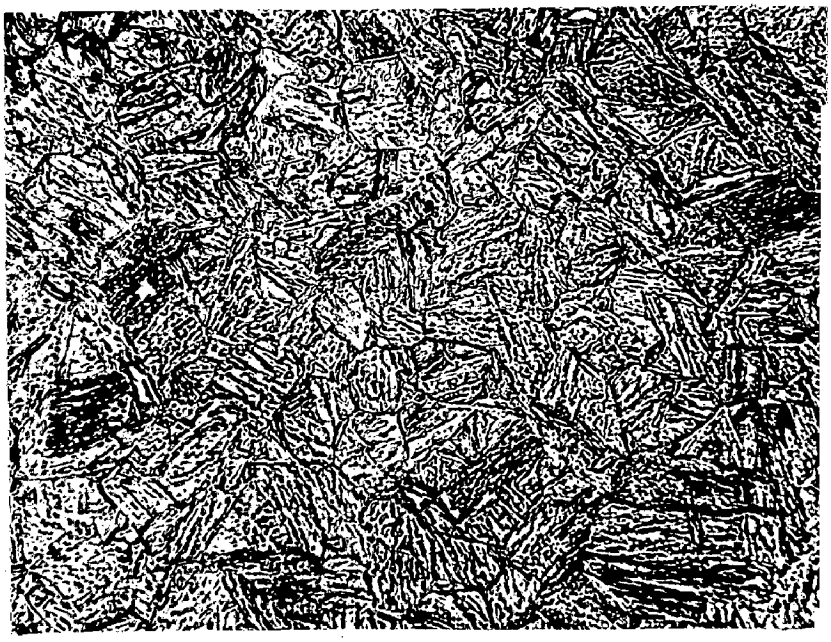

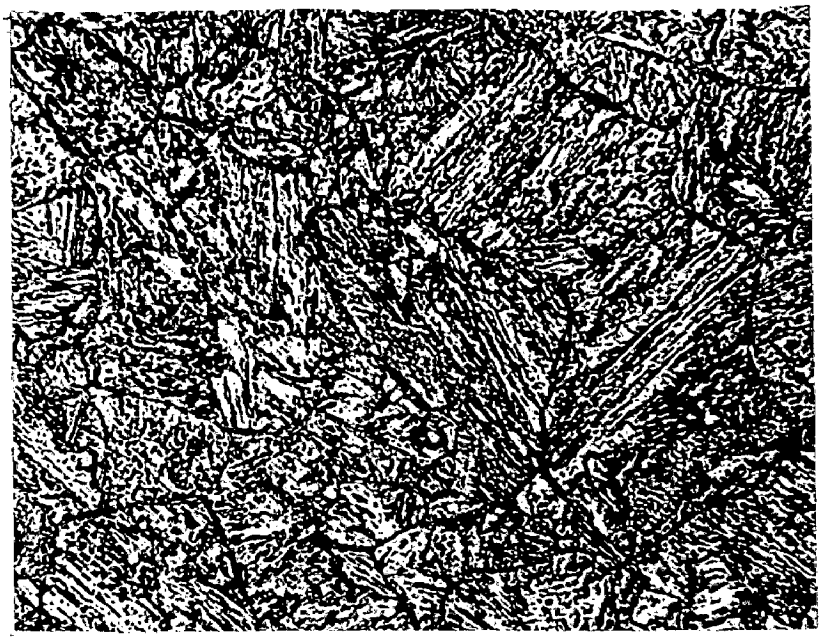

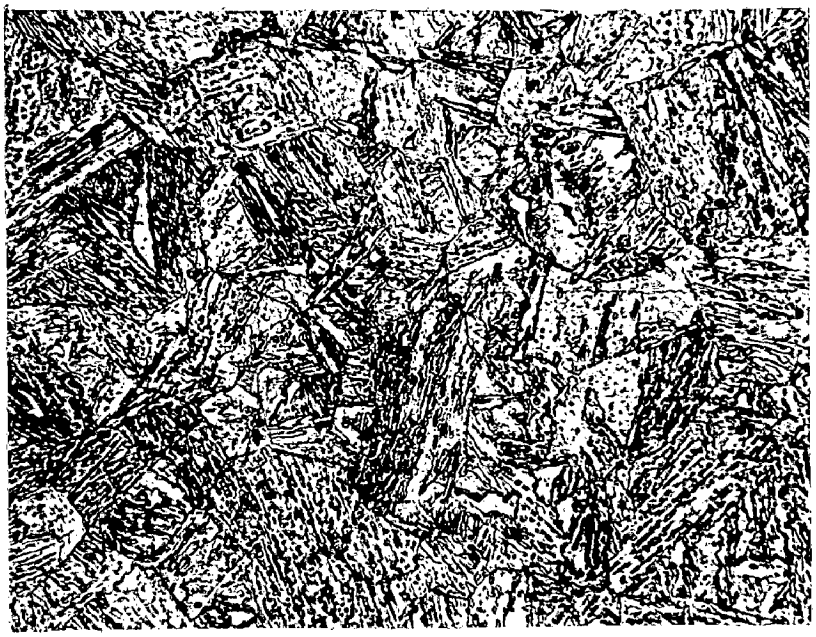

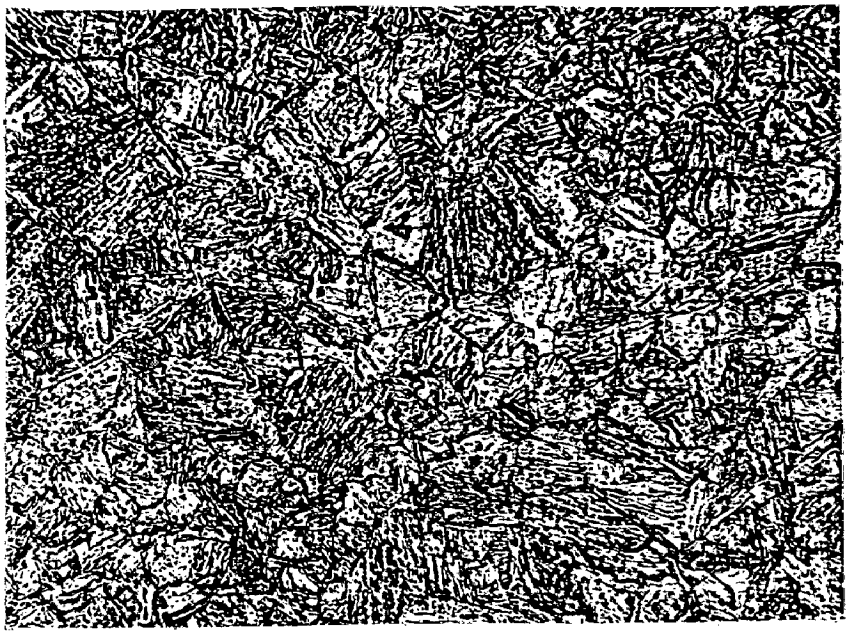

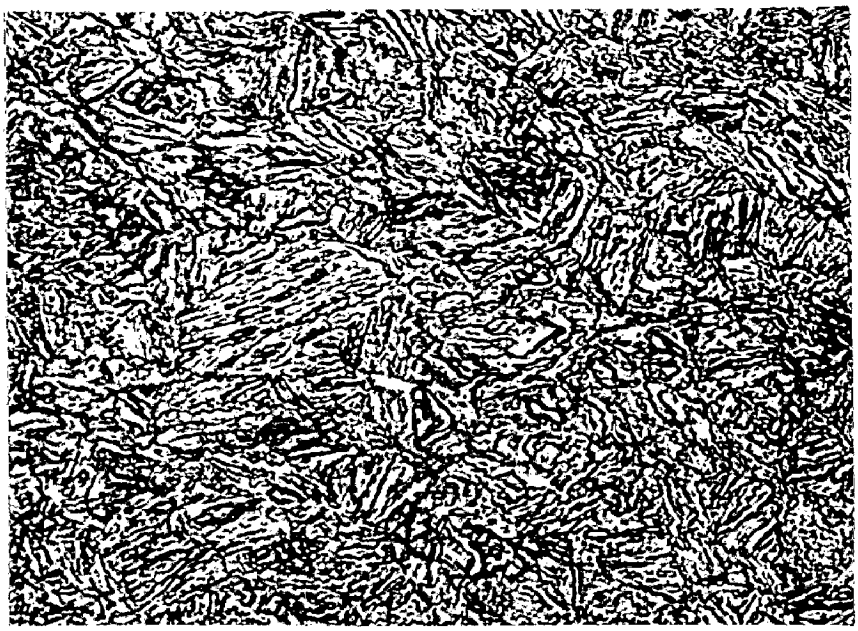

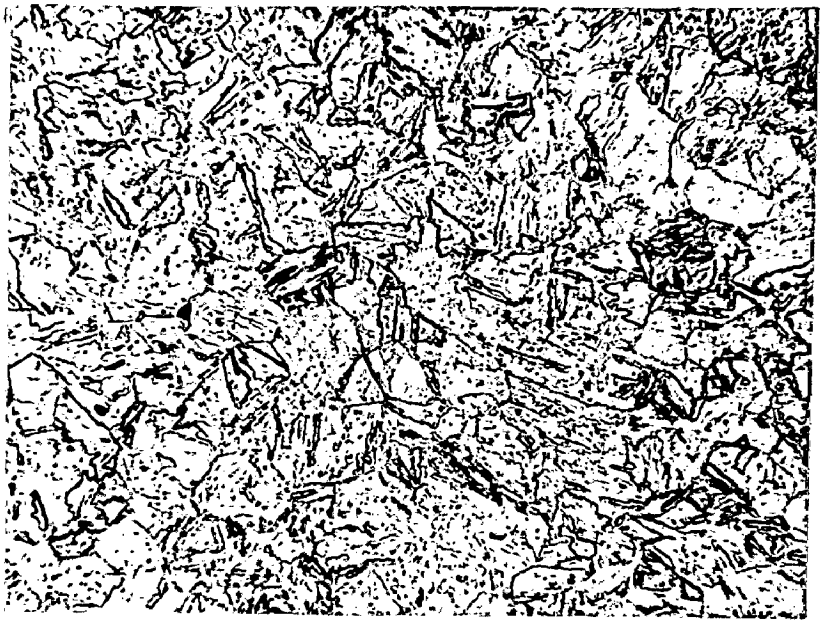

Fig. 5.15 (b)

Alloy H5; 900°C AC
Massive Ferrite 400 X

fig. 5.16

Alloy H5 ; 1100°C CC
Massive Ferrite + Lath structure 400 X

Fig. 5.17 (a)

Alloy H6 ; 1100°C WQ.
Lath structure 400 X

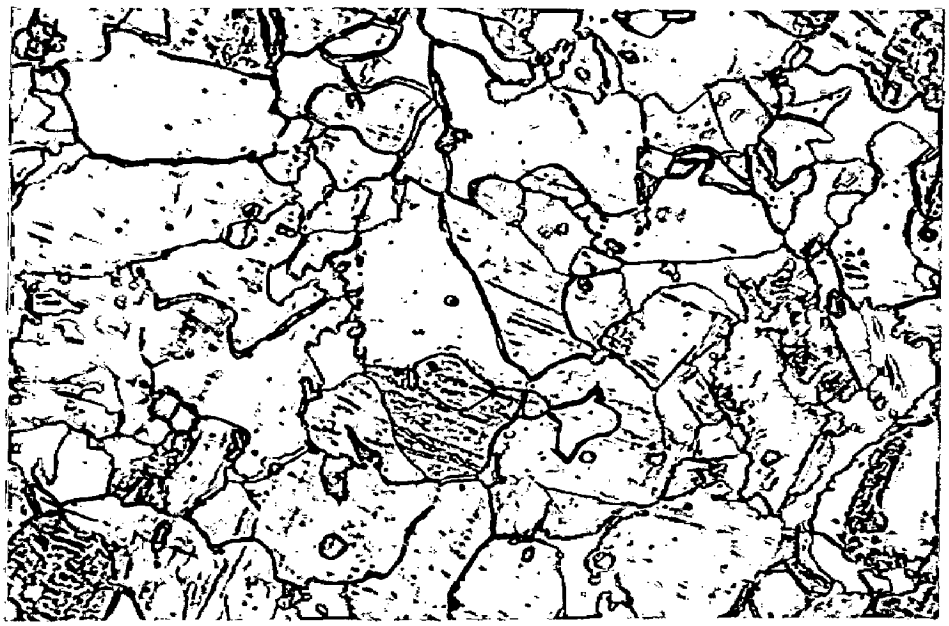

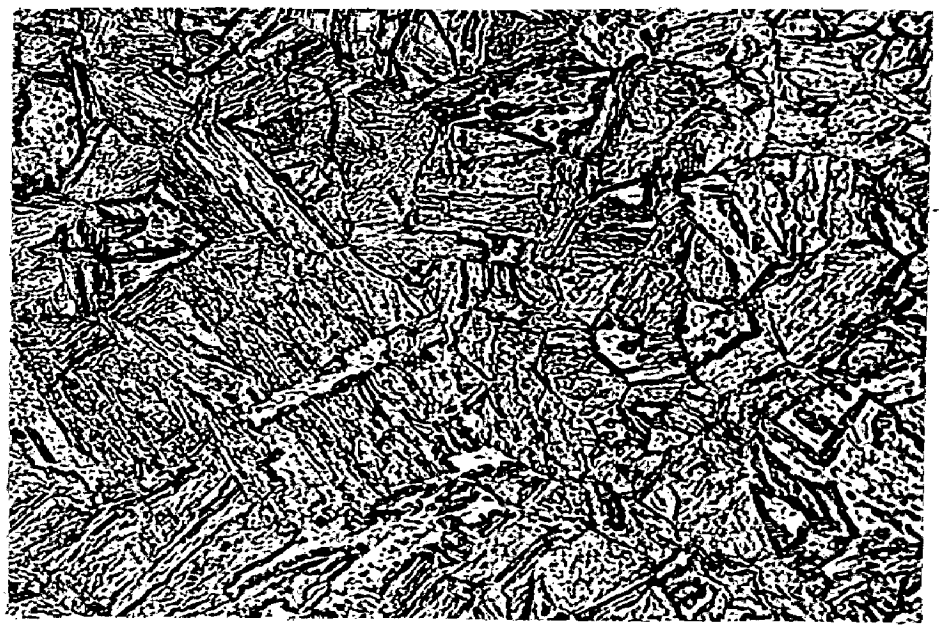

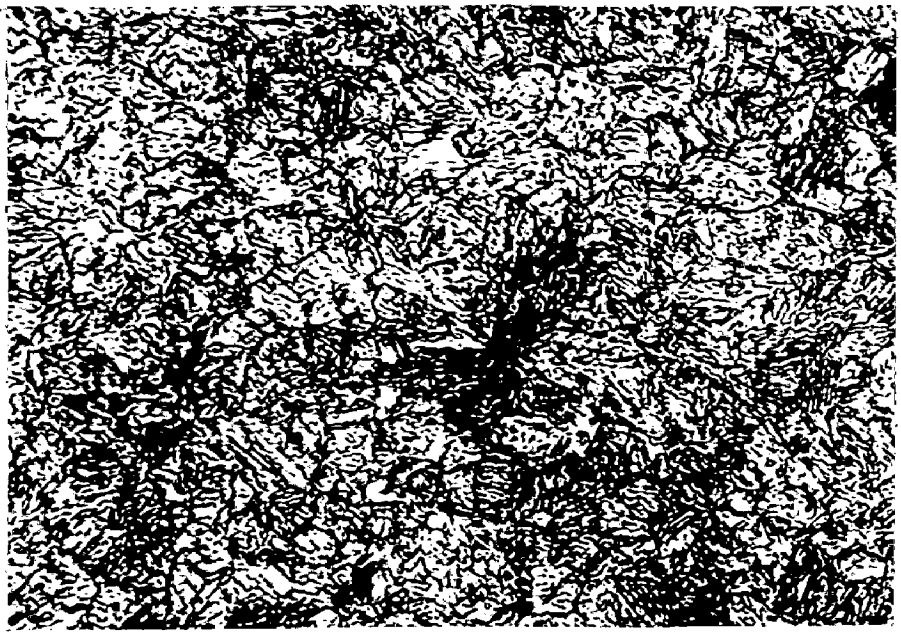

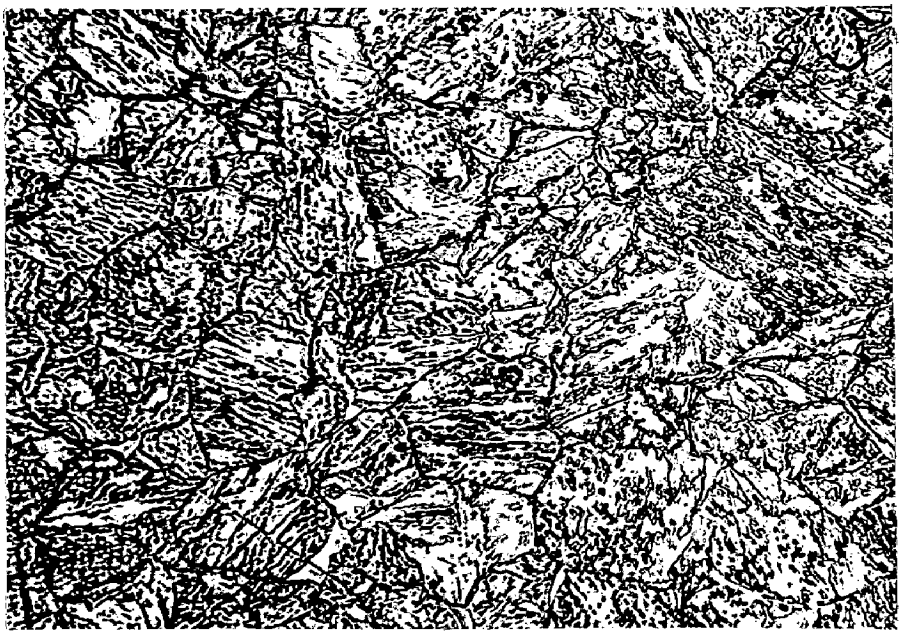

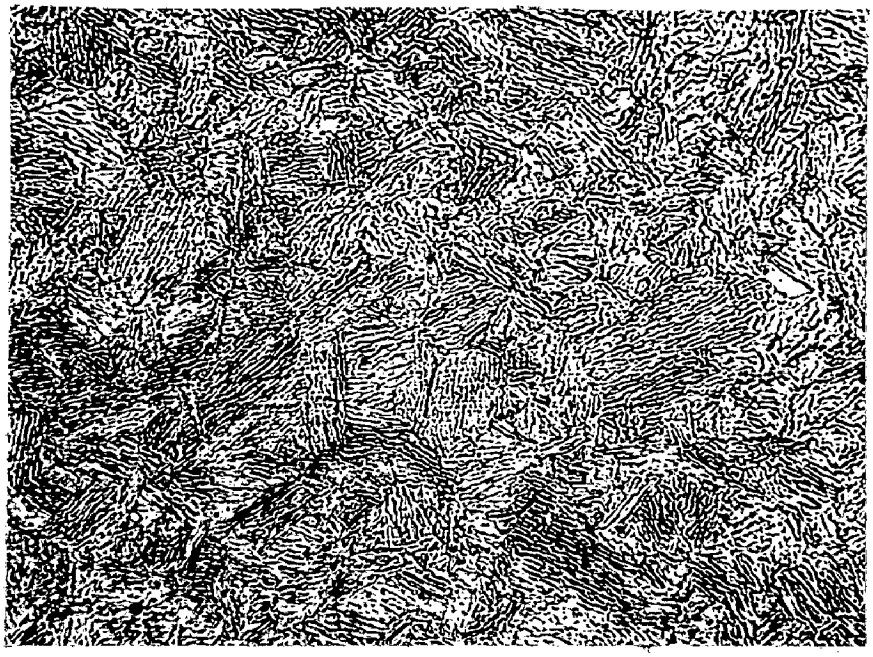

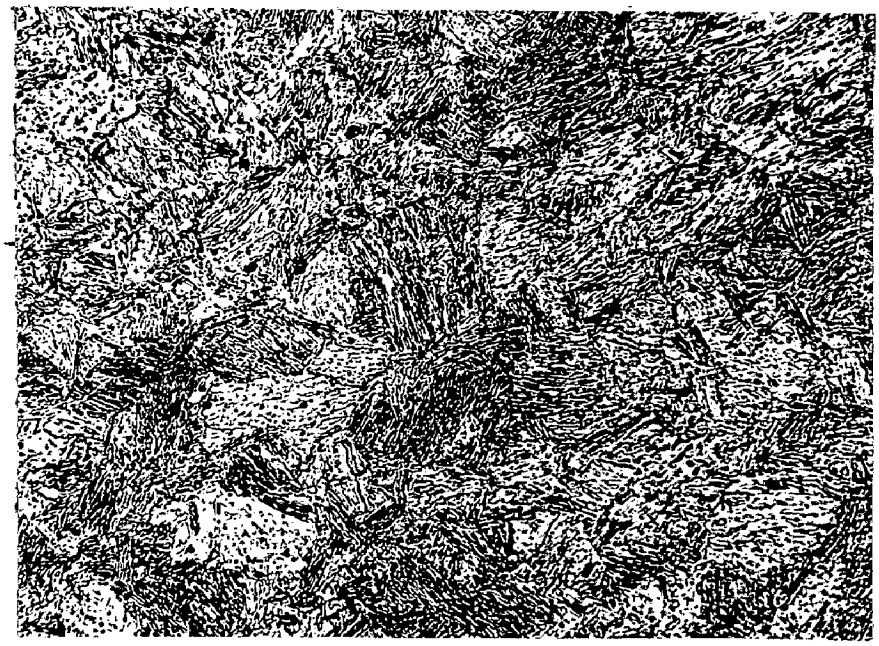

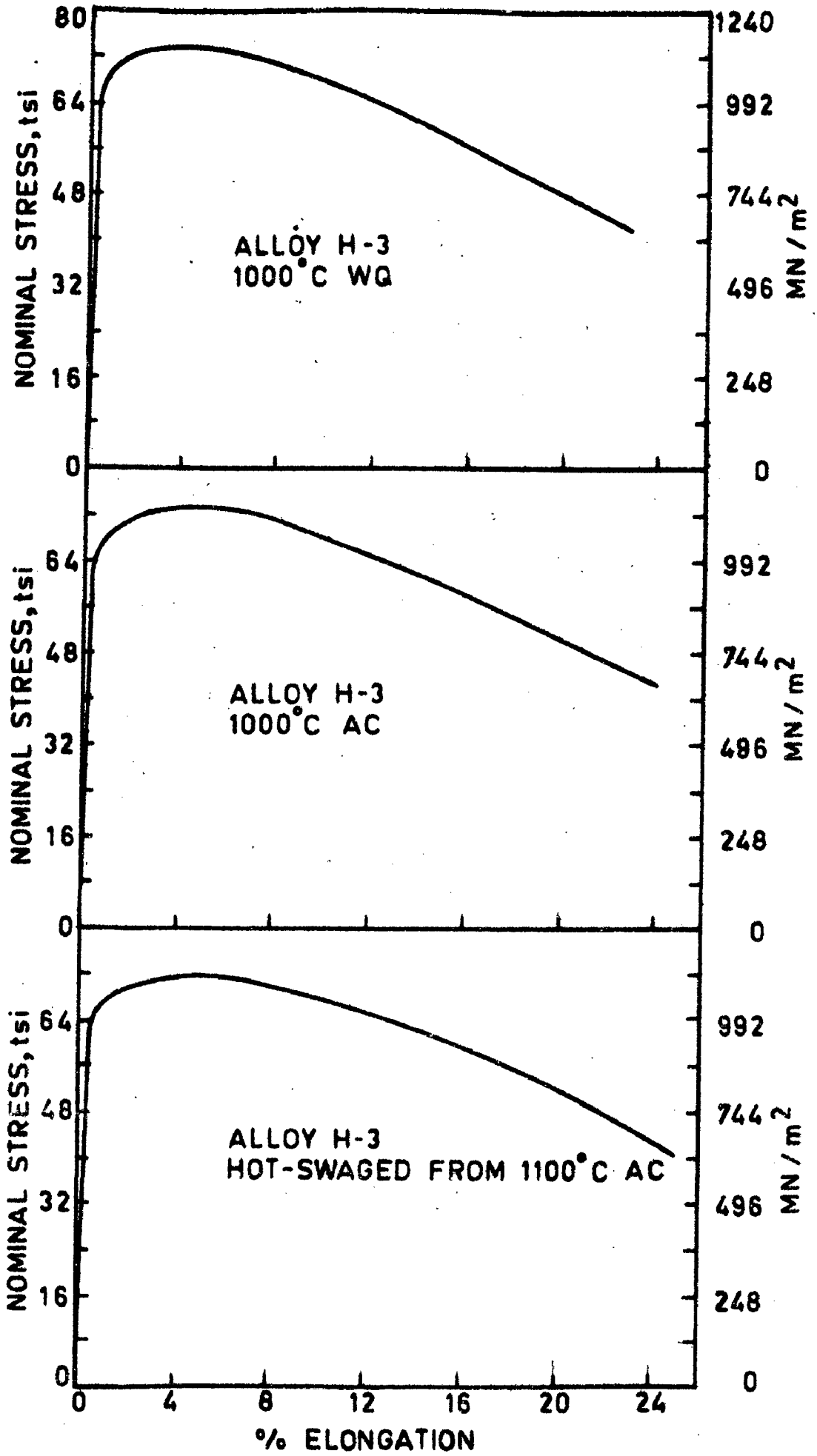

FIG.5.21 STRESS-STRAIN CURVES FOR ALLOY H-3

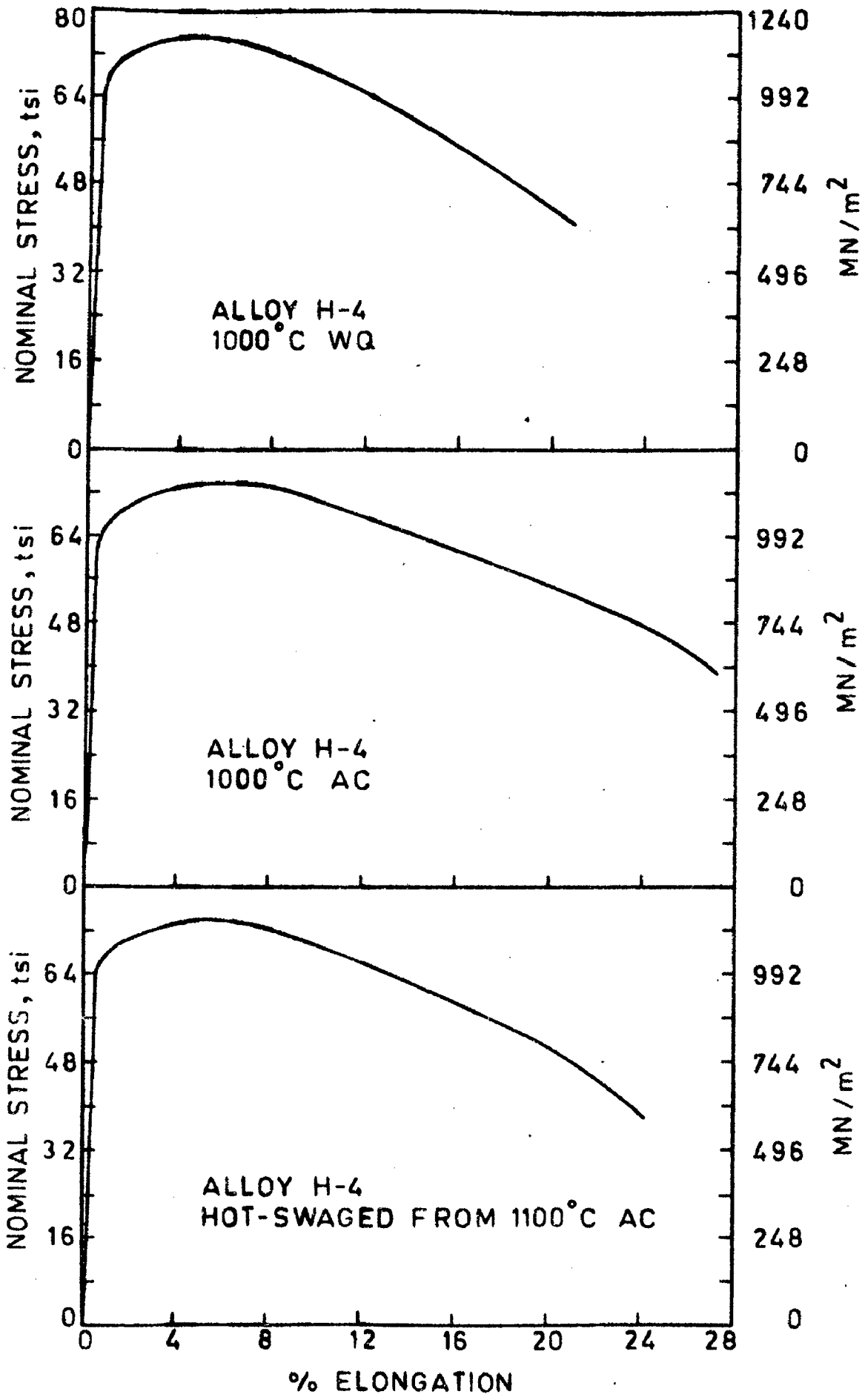

FIG. 5.22 STRESS-STRAIN CURVES FOR ALLOY H-4

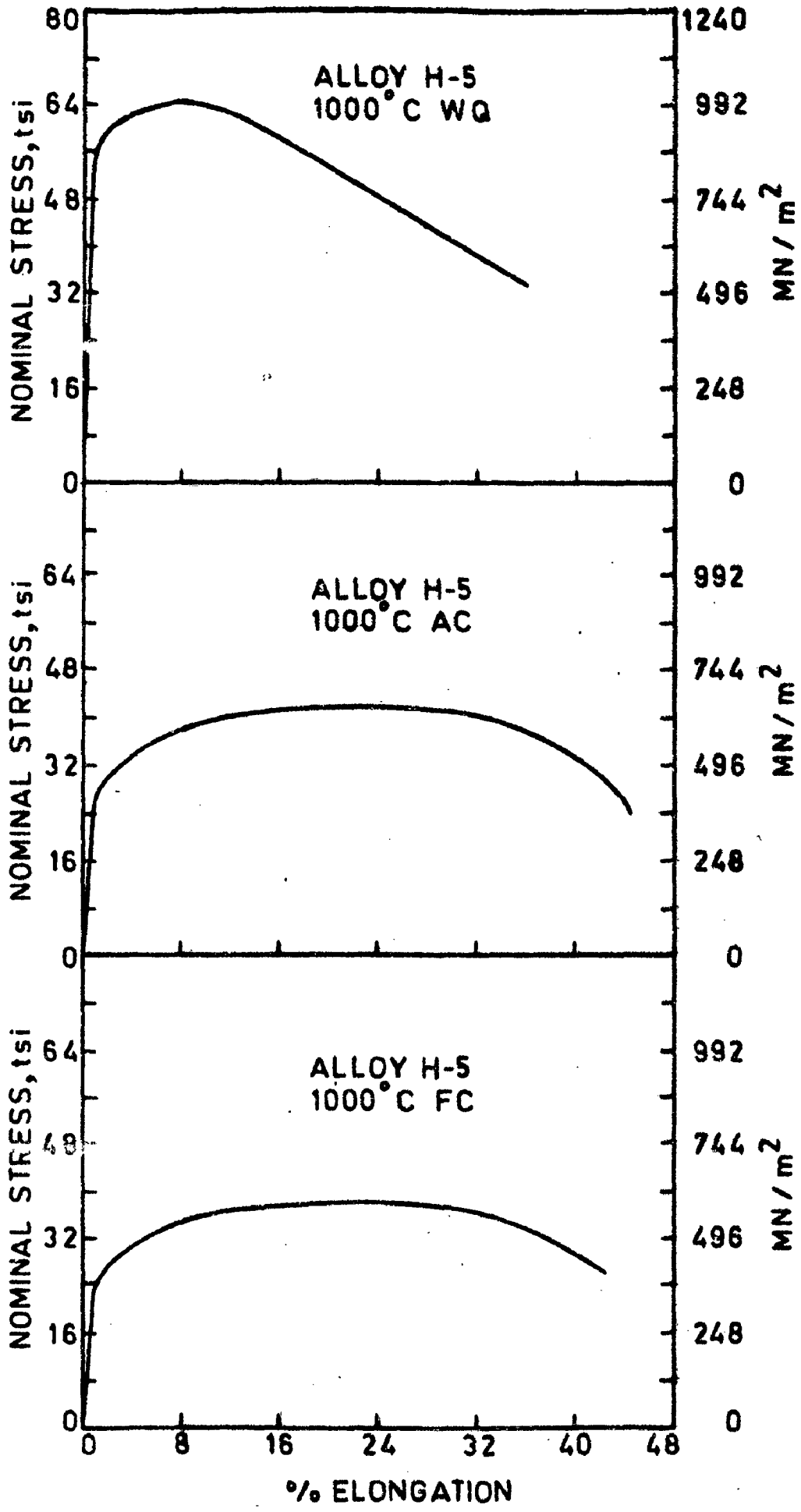

FIG.5.23 STRESS-STRAIN CURVES FOR ALLOY H-5

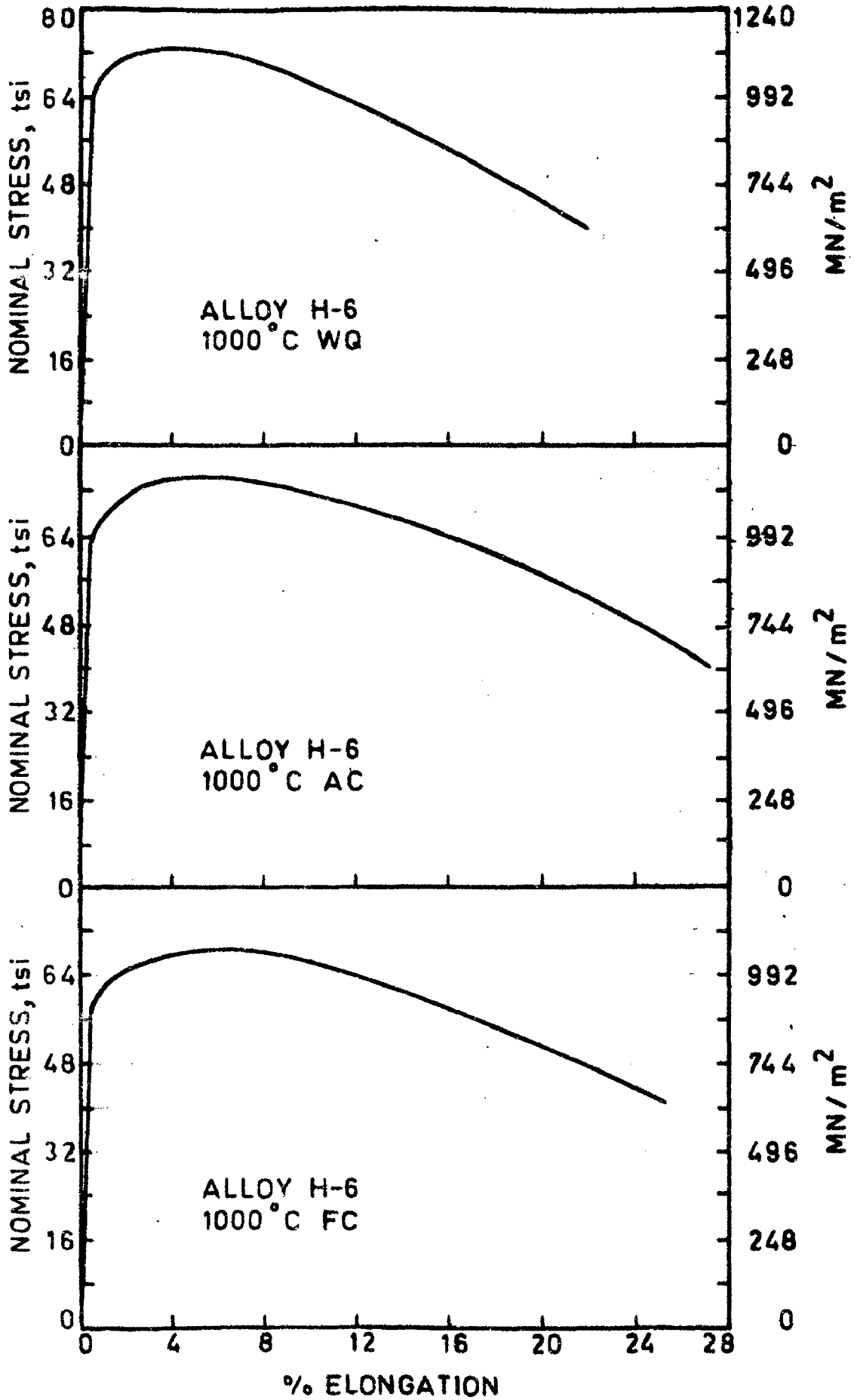

FIG. 5.24 STRESS-STRAIN CURVES FOR ALLOY H-6

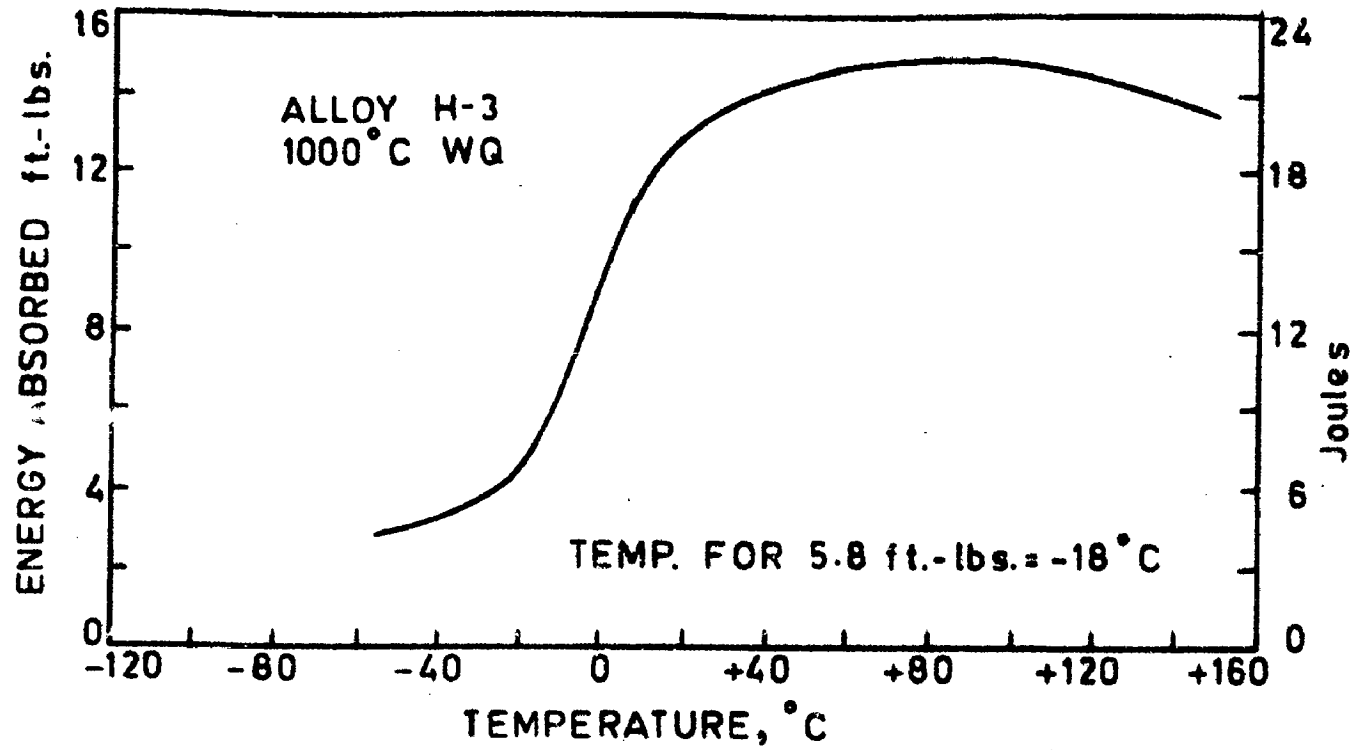

FIG.5.25 IMPACT TRANSITION CURVE FOR ALLOY H-3
(sub-standard charpy specimen)

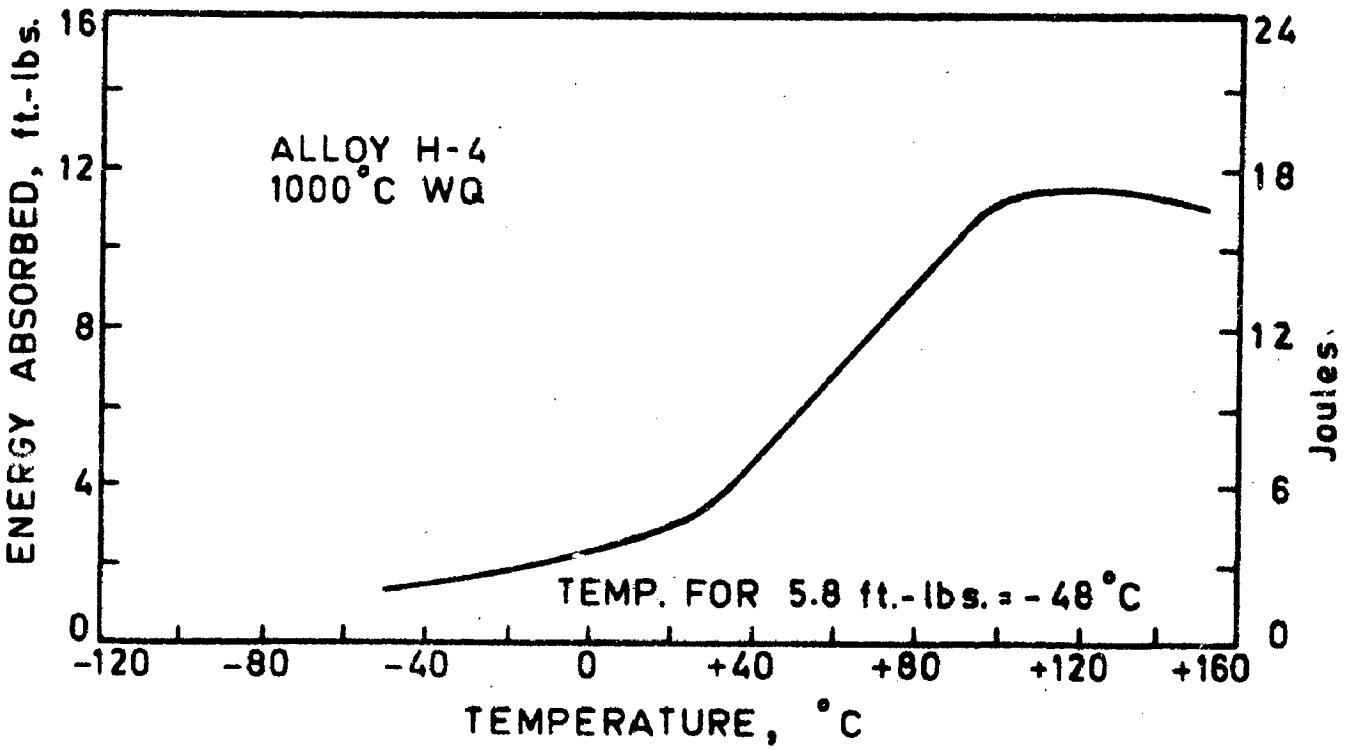

FIG. 5.26 IMPACT TRANSITION CURVE FOR ALLOY H-4
(sub-standard charpy specimen)

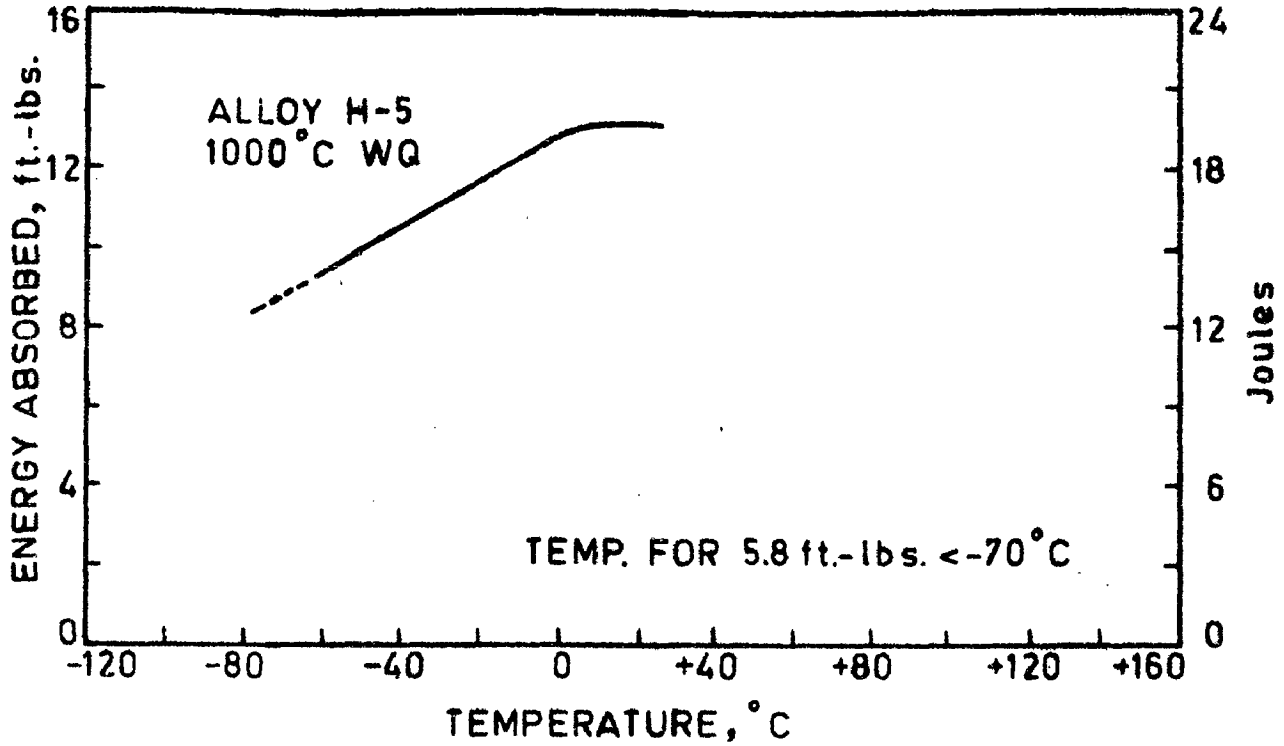

FIG.5.27 IMPACT TRANSITION CURVE FOR ALLOY H-5
(sub-standard charpy specimen)

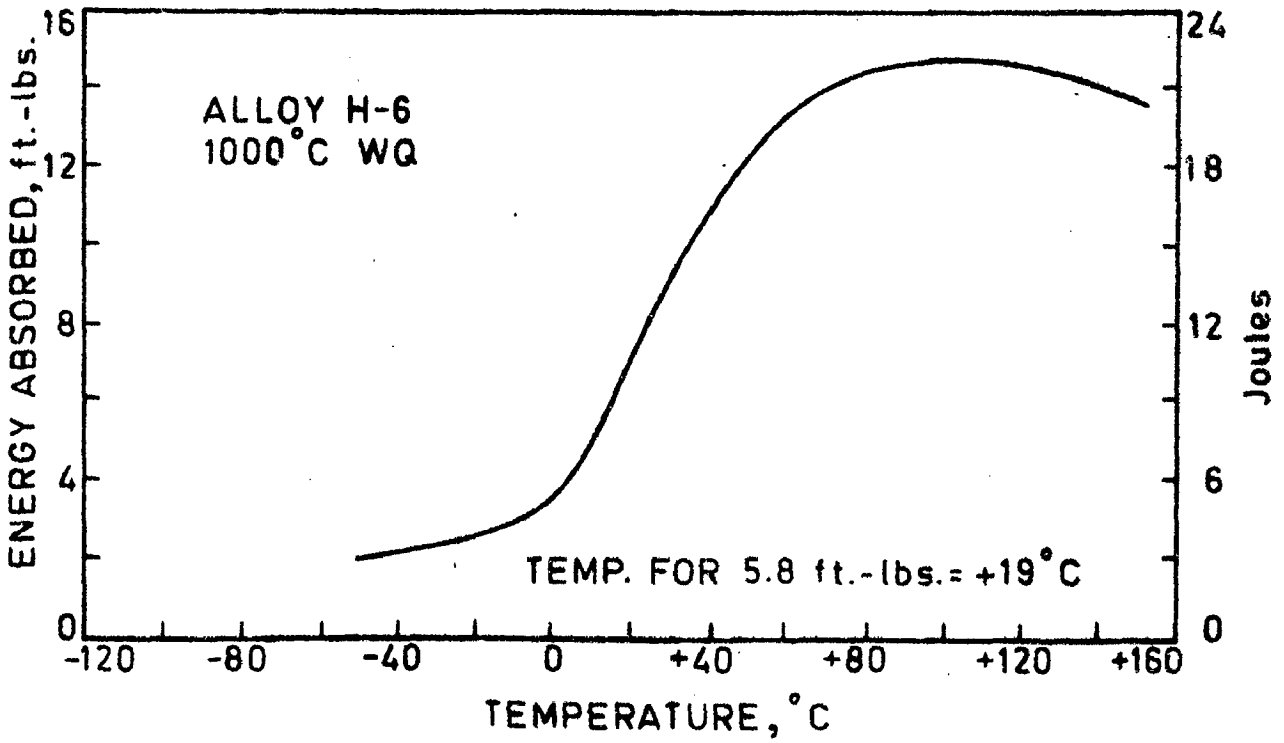

FIG. 5.28 IMPACT TRANSITION CURVE FOR ALLOY H-6
(sub-standard charpy specimen)

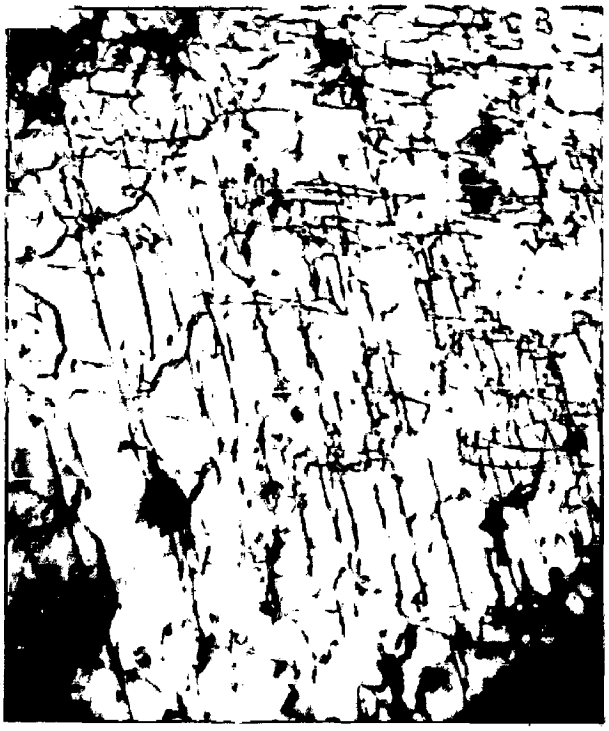

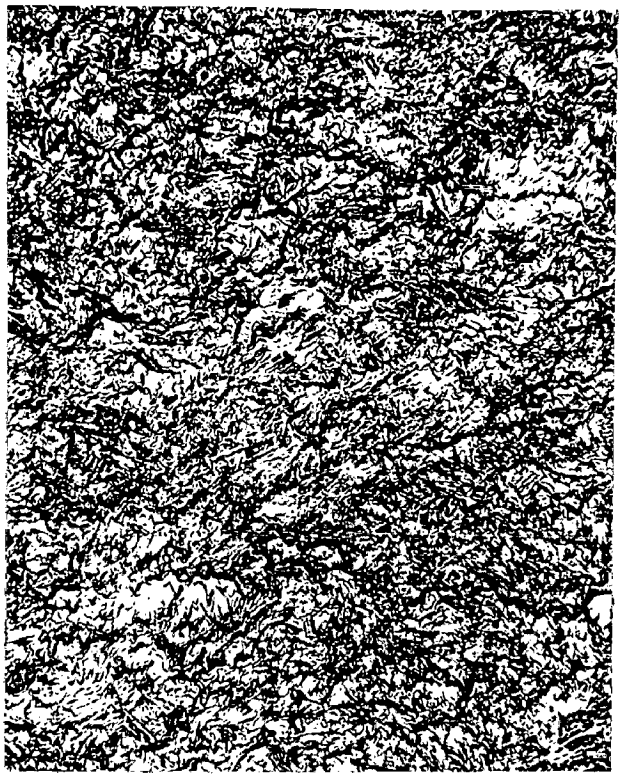

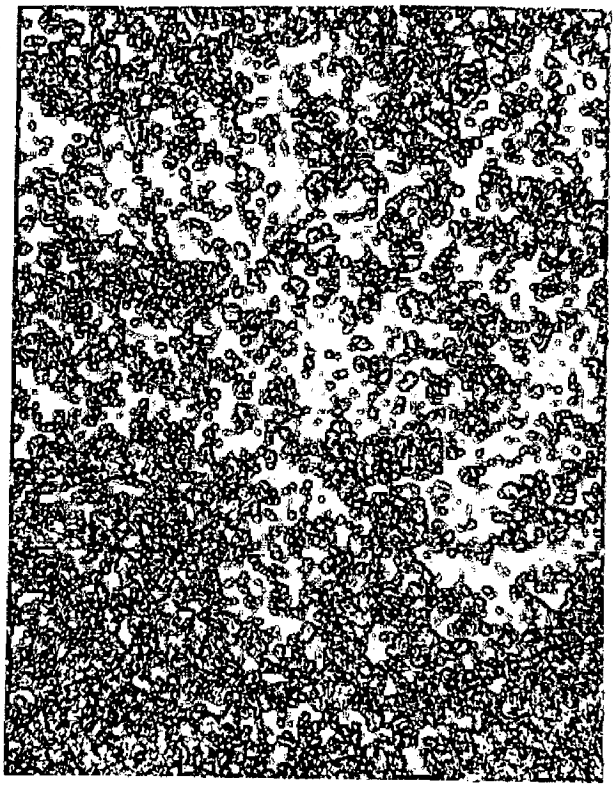

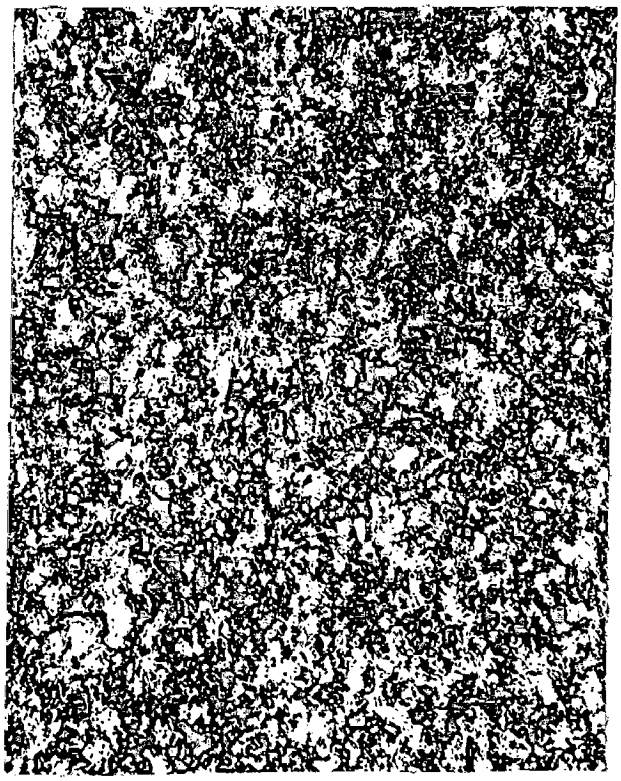

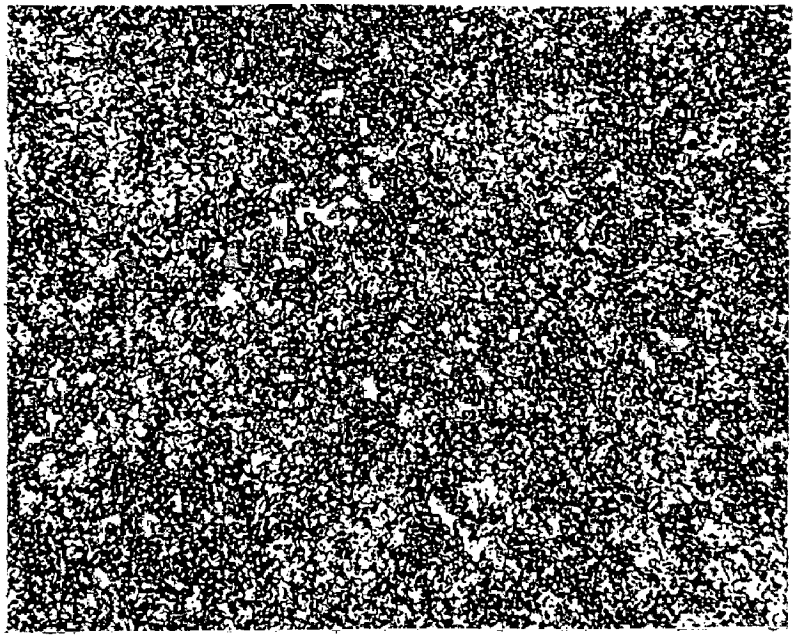

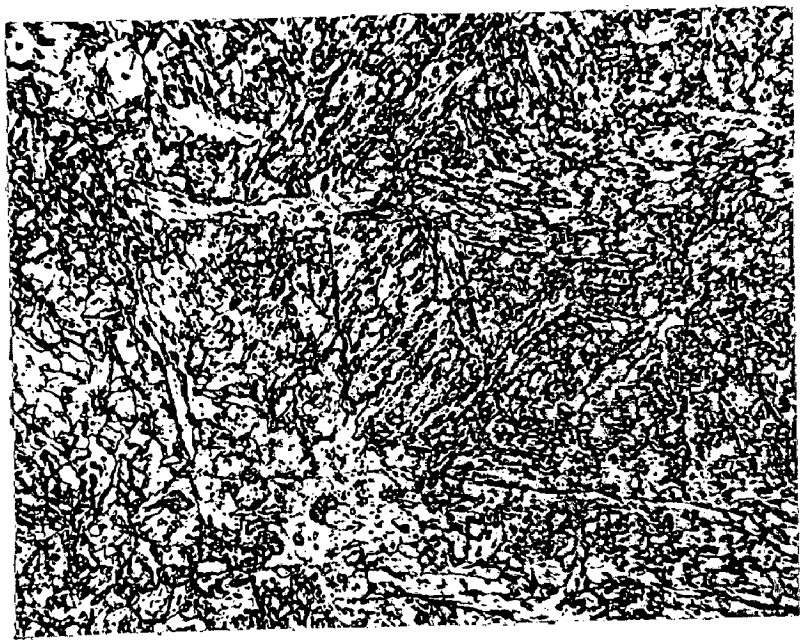

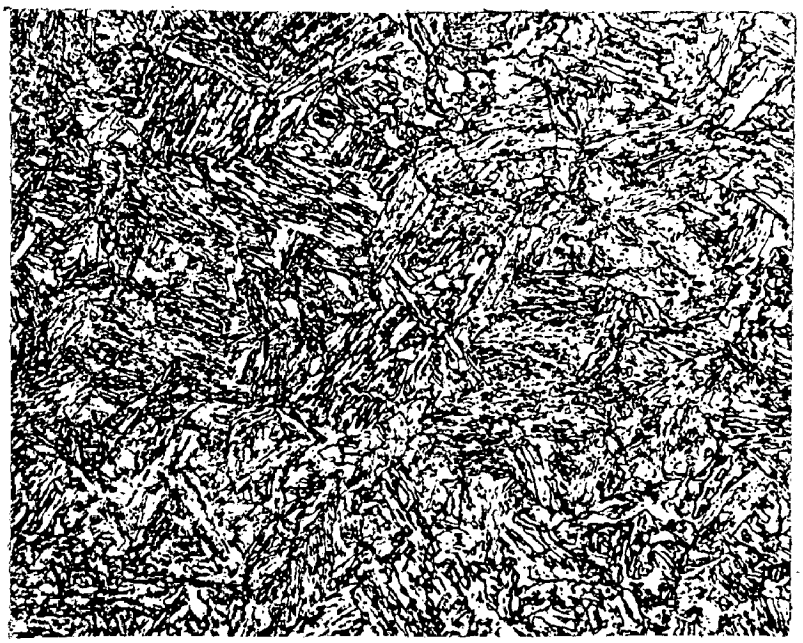

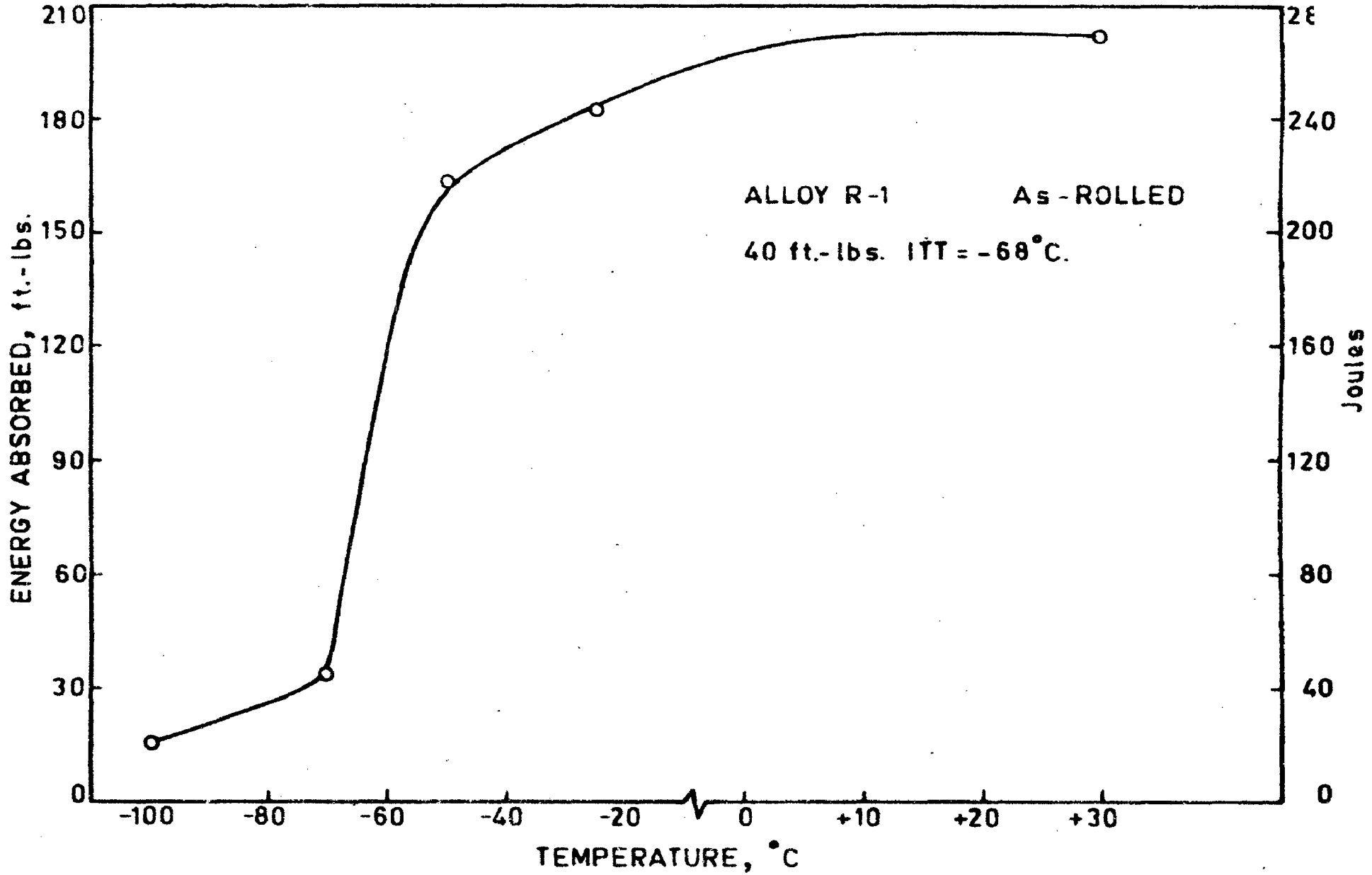

FIG.6.5 IMPACT TRANSITION CURVE FOR ALLOY R-1
(Standard Charpy specimen)

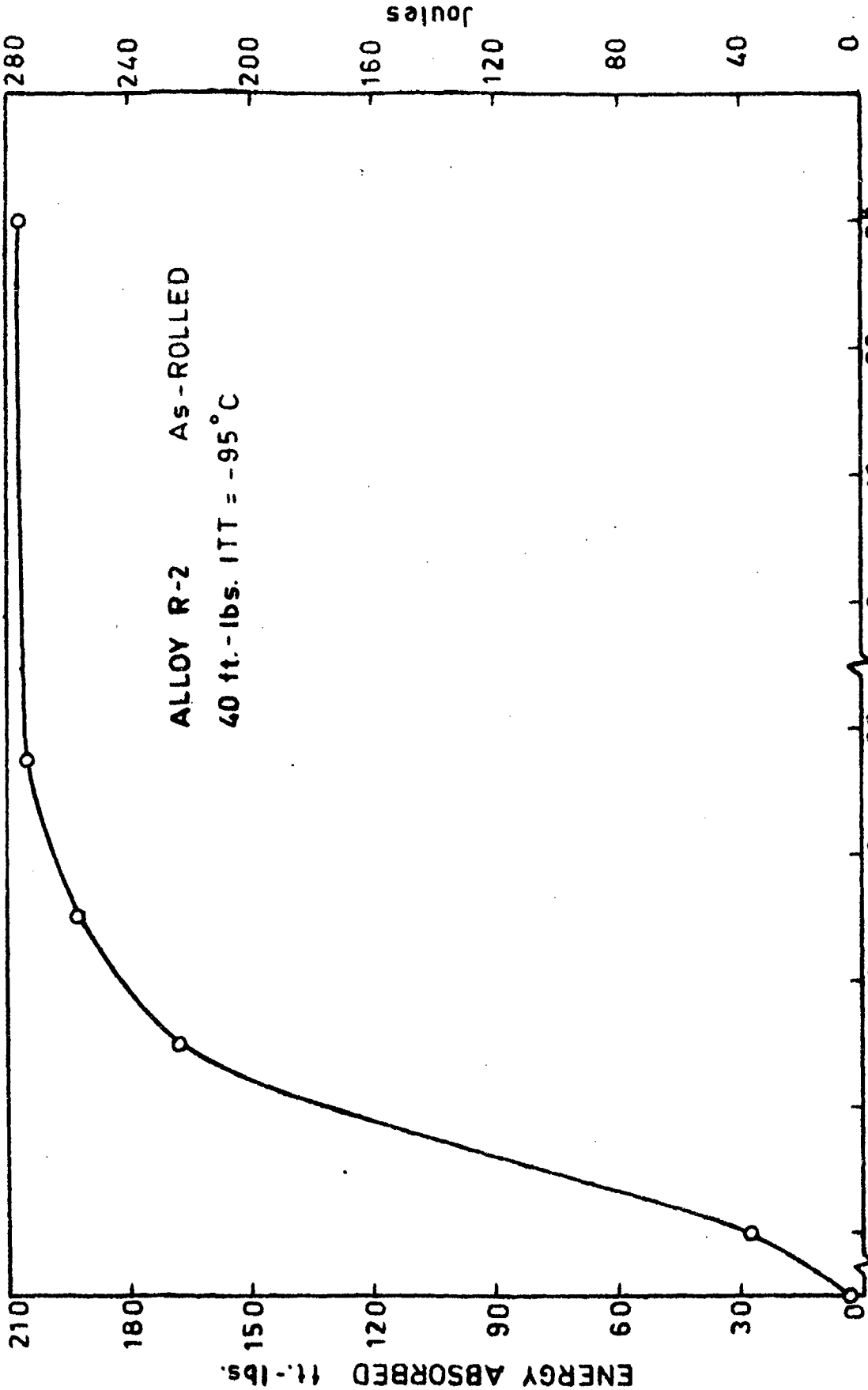

FIG. 6.6 IMPACT TRANSITION CURVE FOR ALLOY R-2
(Standard Charpy specimen)

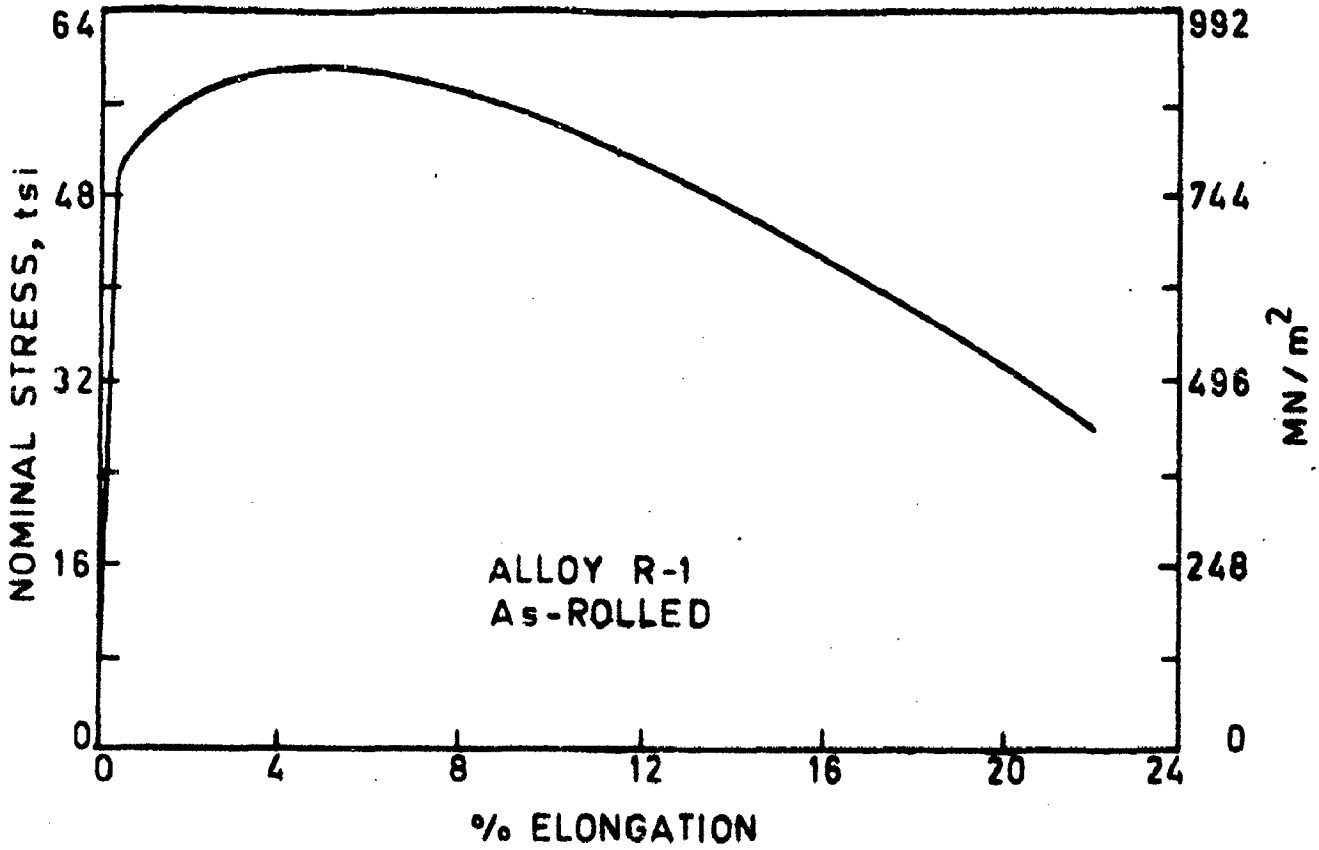

FIG.6.7 STRESS-STRAIN CURVE FOR ALLOY R-1

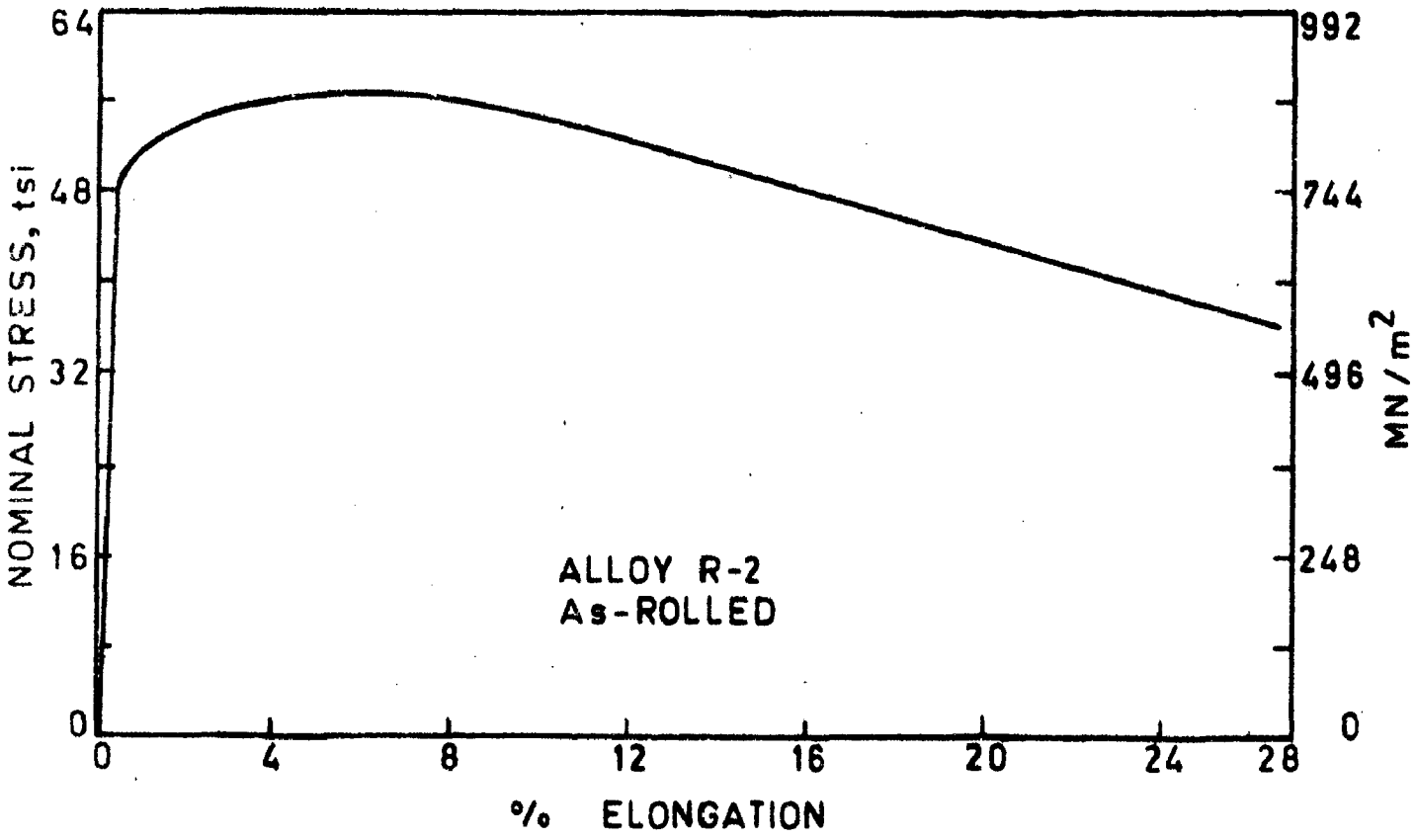

FIG.6.8 STRESS-STRAIN CURVE FOR ALLOY R-2

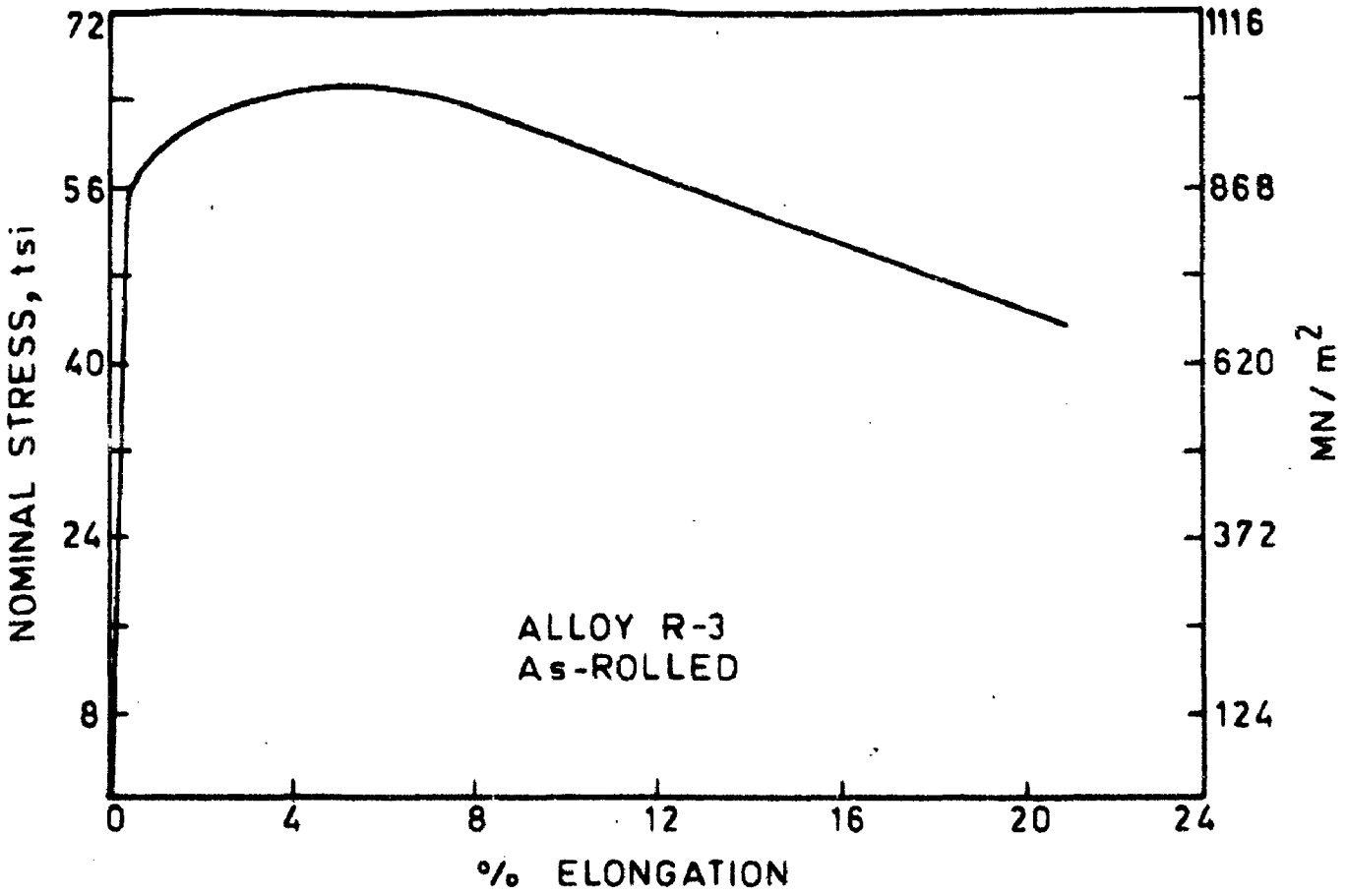

FIG. 6.9 STRESS-STRAIN CURVE FOR ALLOY R-3

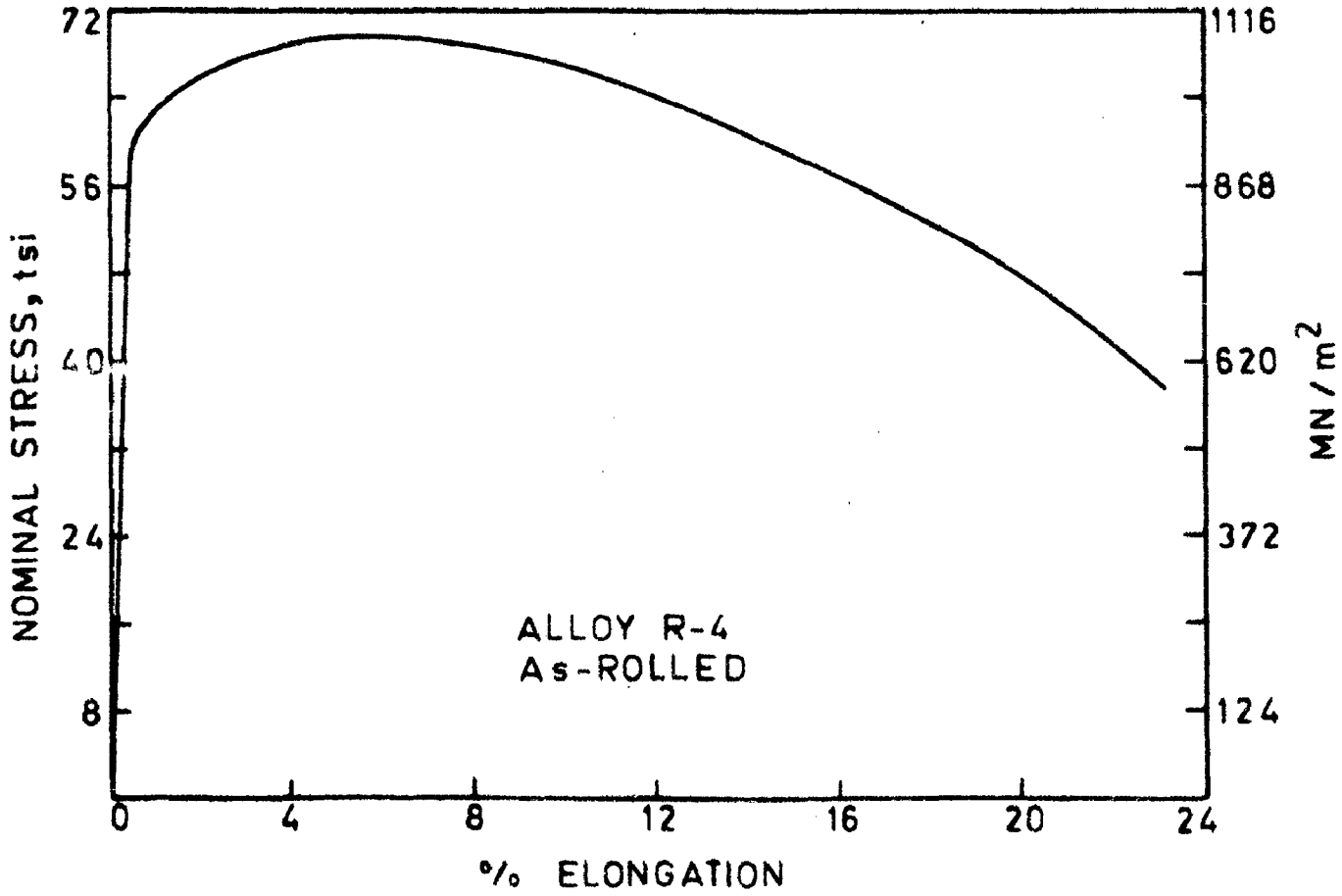

FIG. 6.10 STRESS-STRAIN CURVE FOR ALLOY R-4

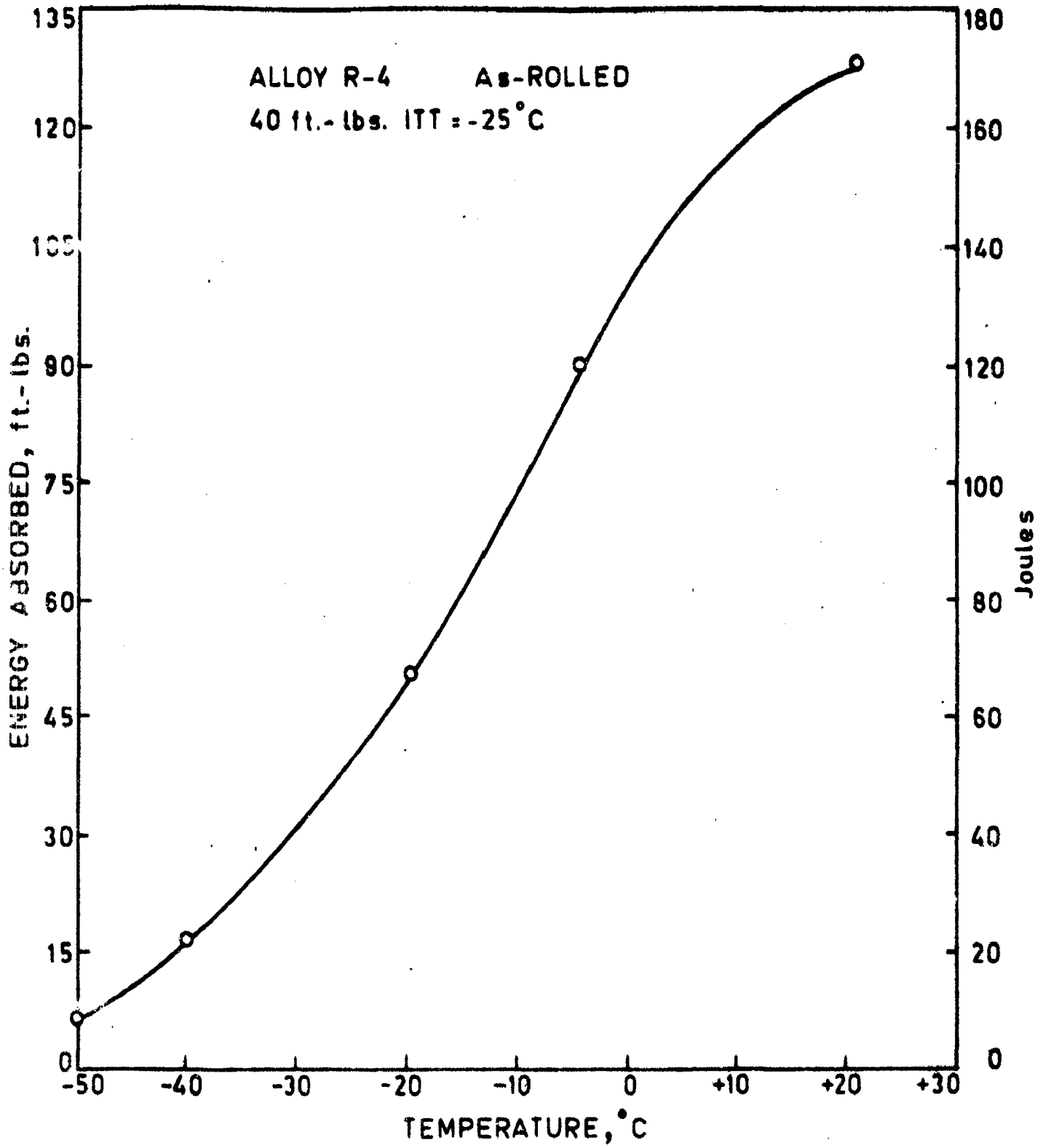

FIG. 6.11 IMPACT TRANSITION CURVE FOR ALLOY R-4
(Standard Charpy specimen)

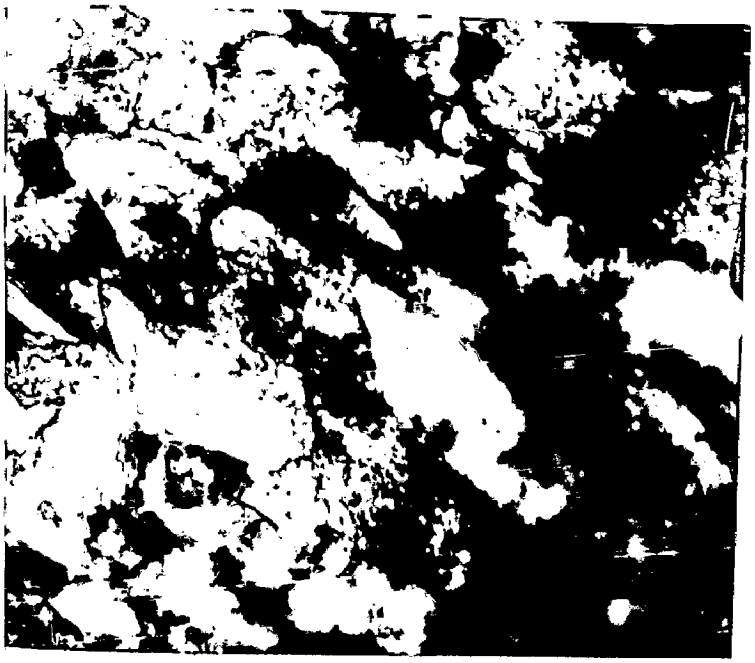


A
B
C

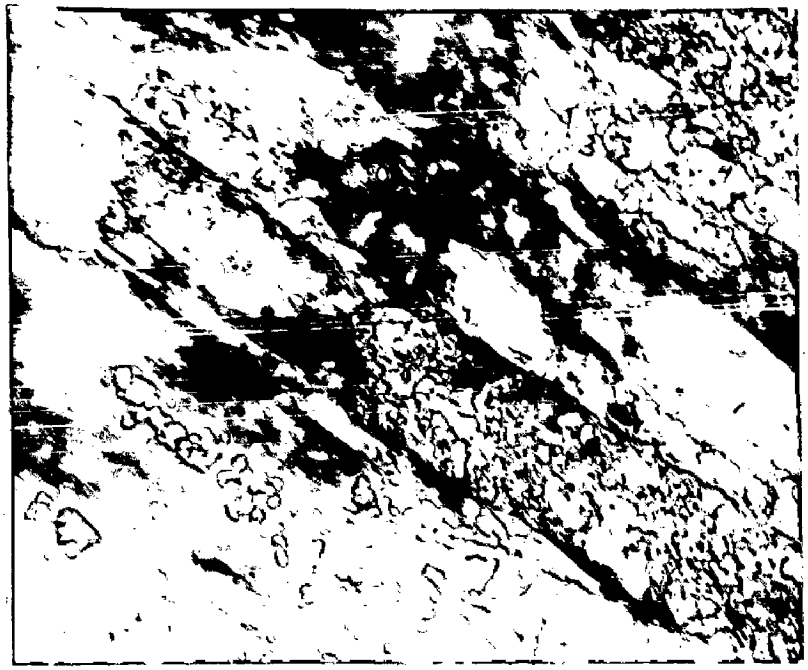

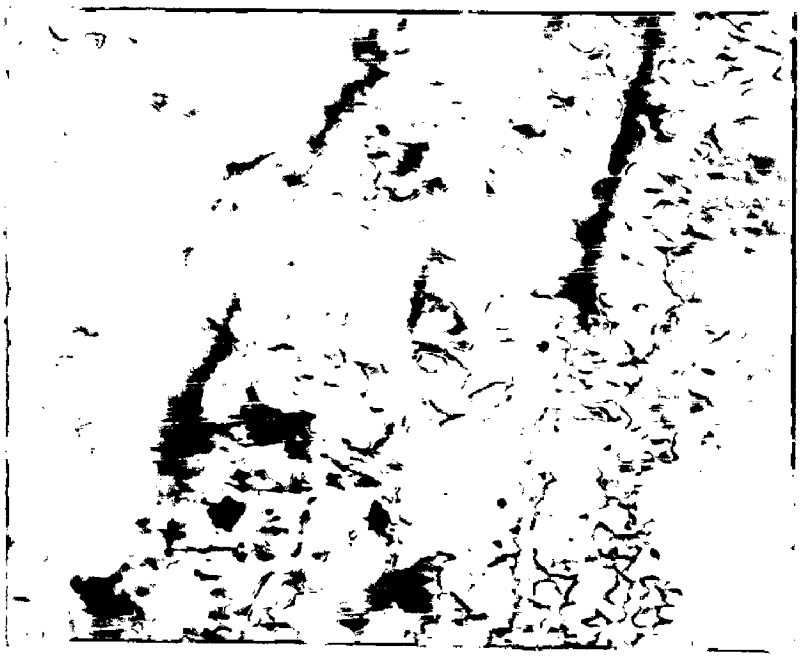

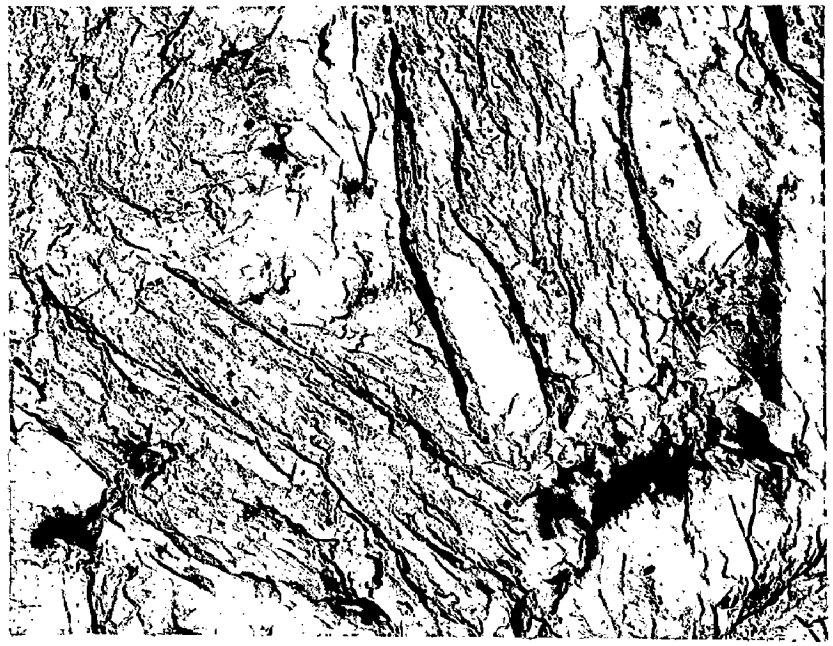

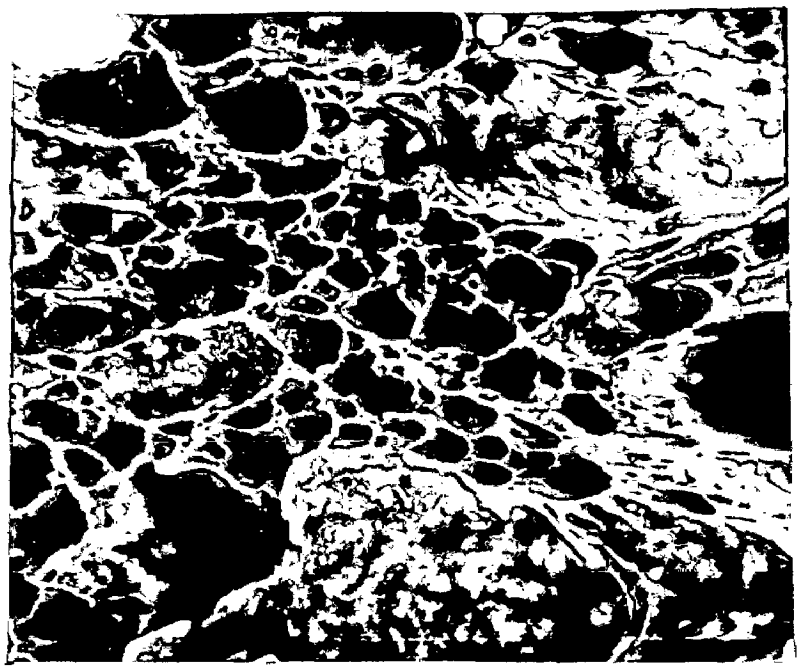

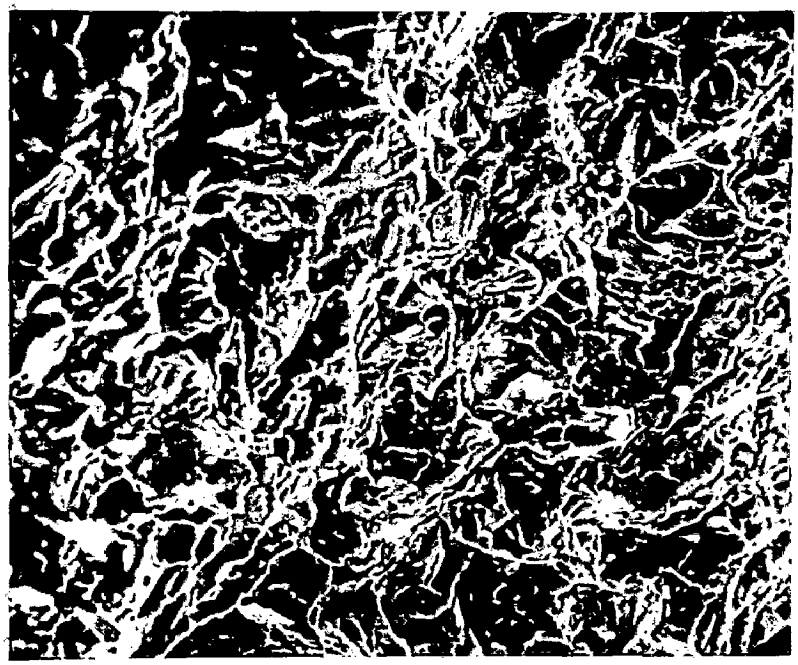

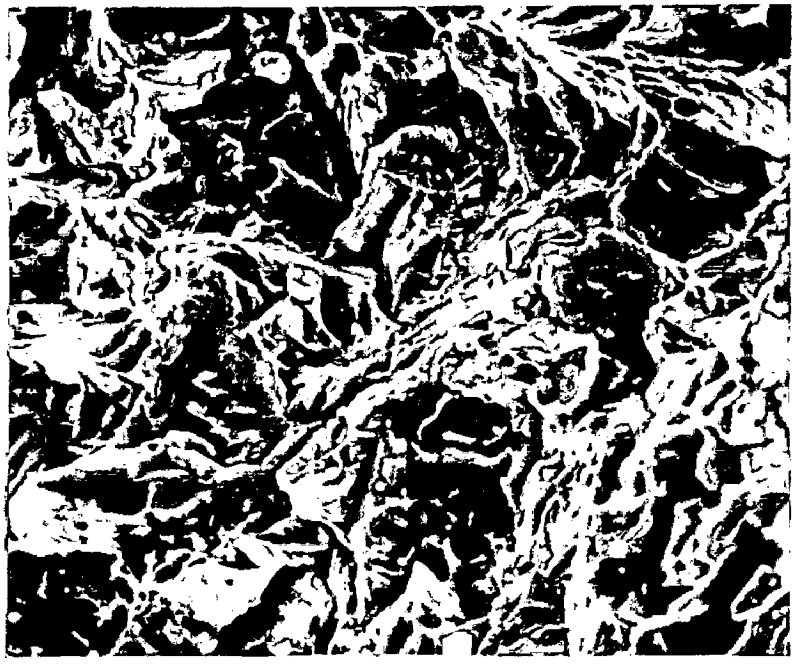

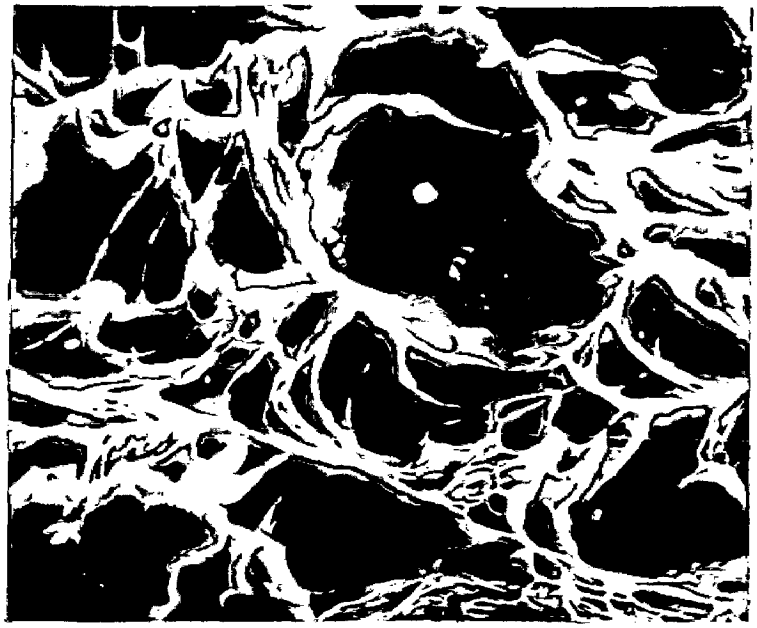

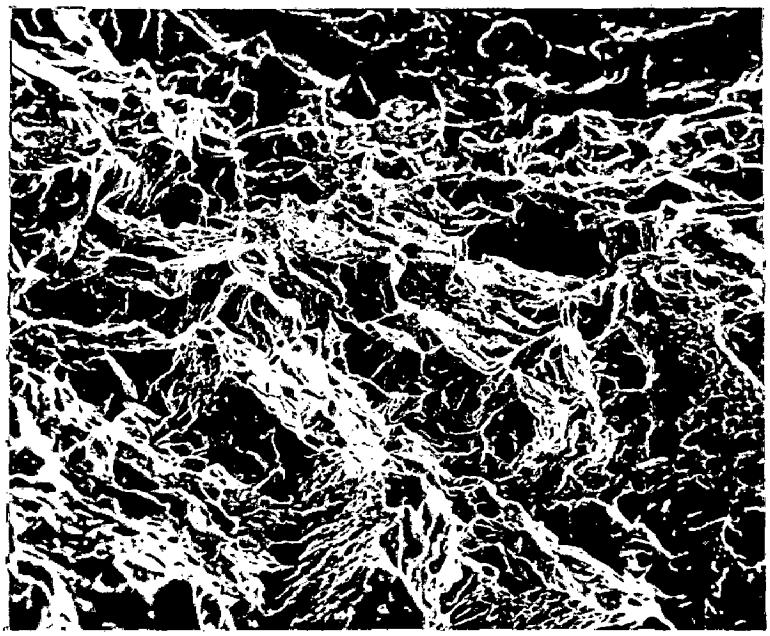

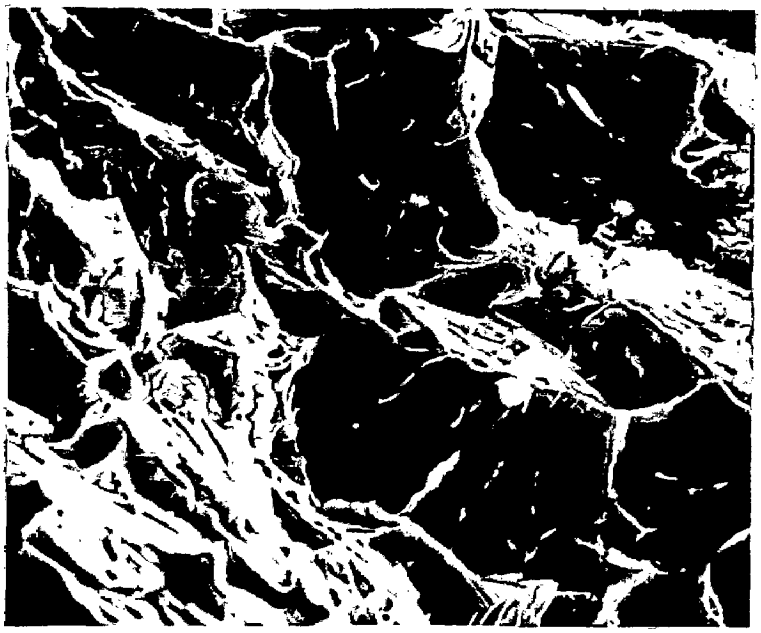

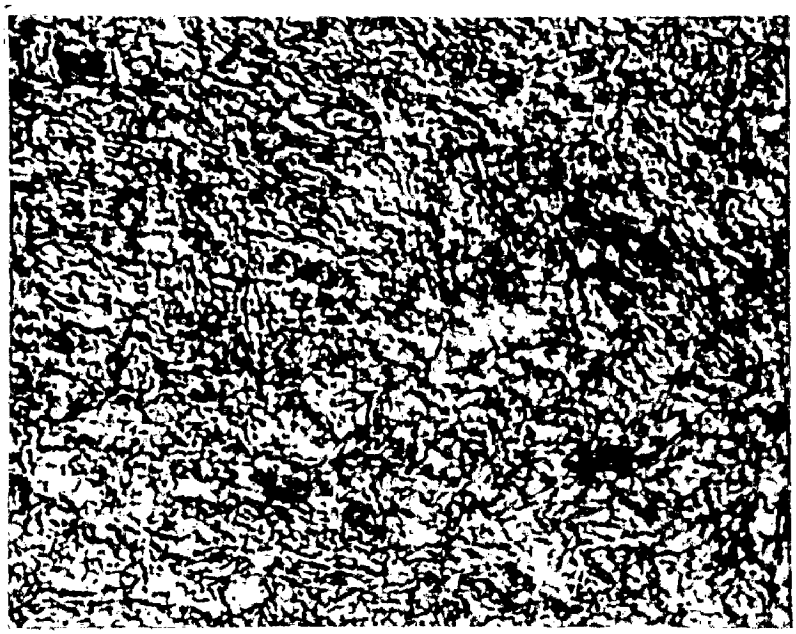

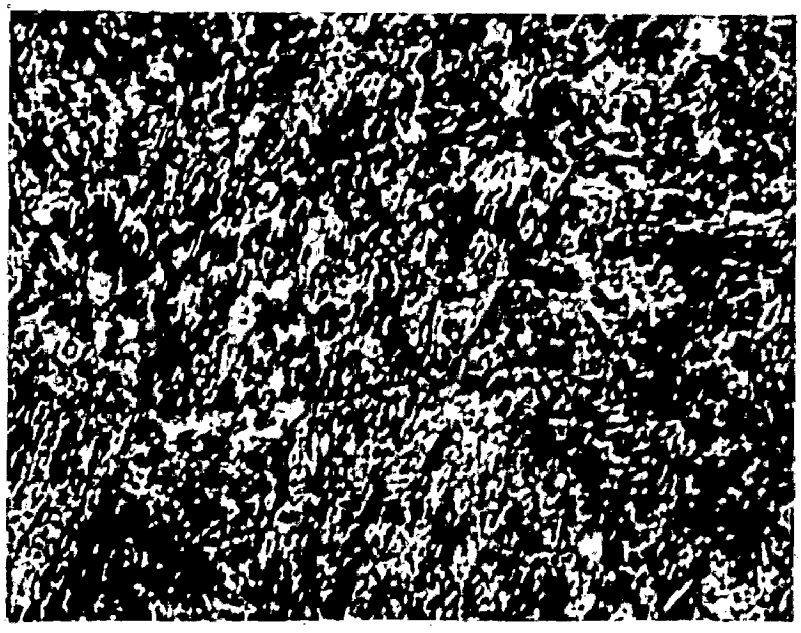

6.26
)

Alloy F ; Control Forged
Fine-grained
Lath-structure 100 x

6.26

Alloy F ; Forged with intermediate reheating
Finer grained
Lath-structure : 100 x

6.27

Representative structure of Alloy F, in the forged condition, at high magnification.
Lath-structure 1000 x

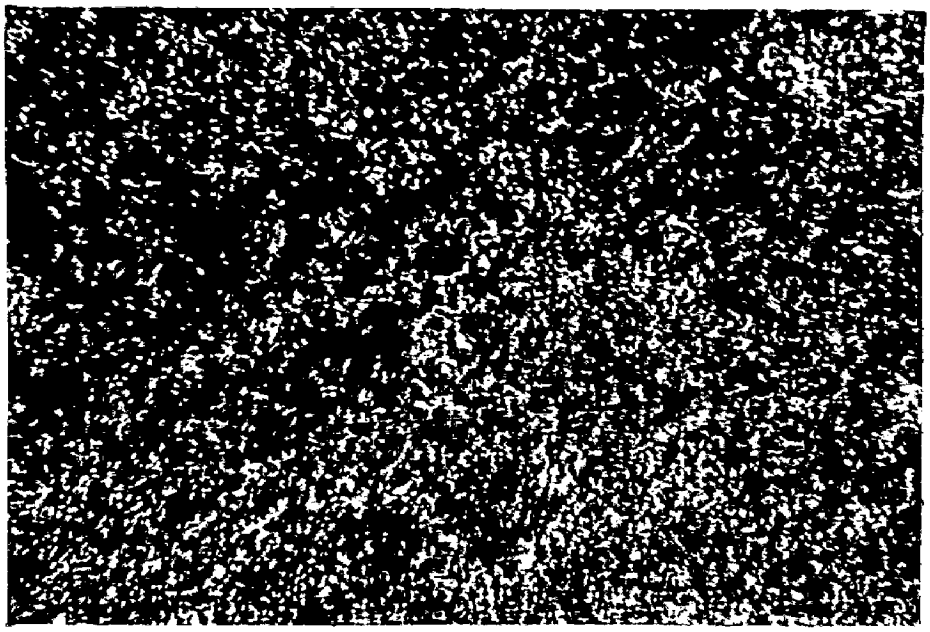

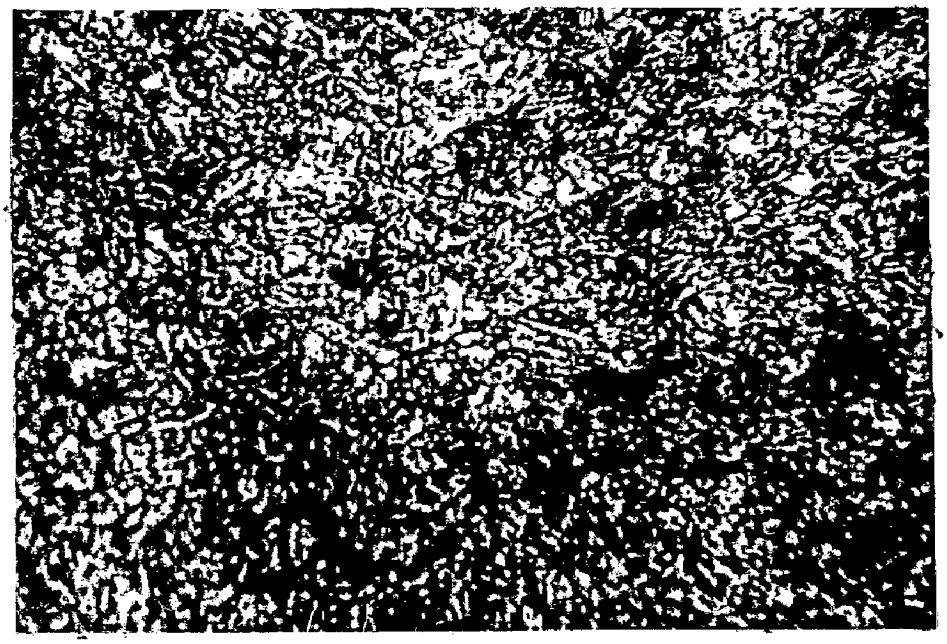

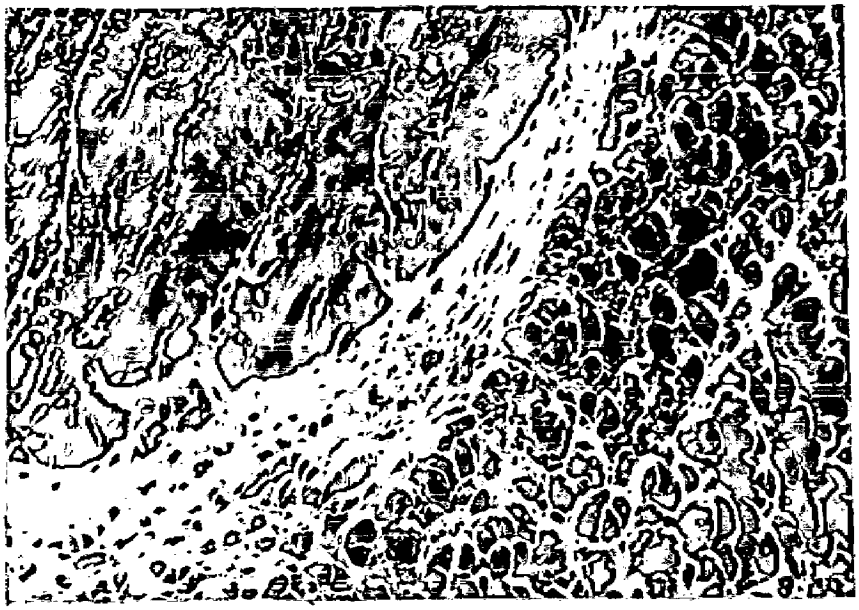

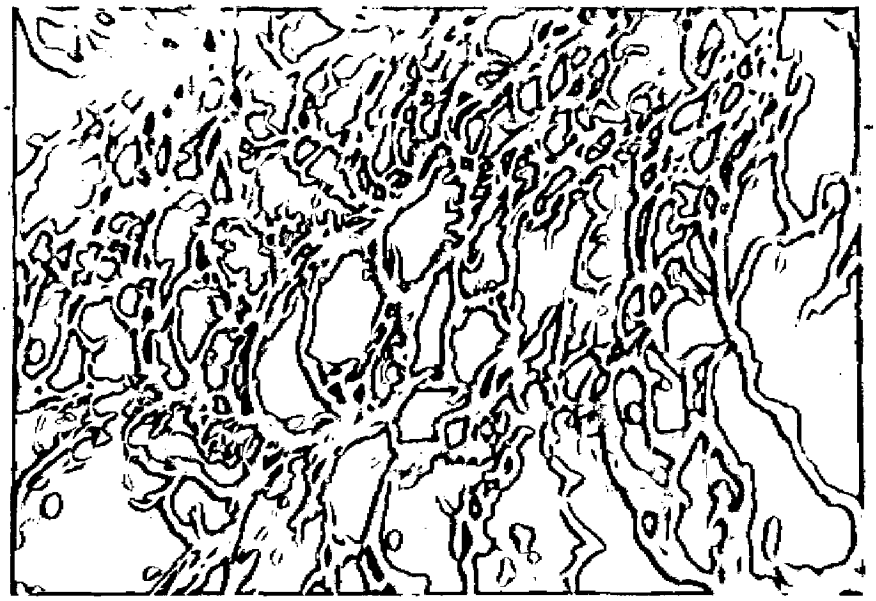

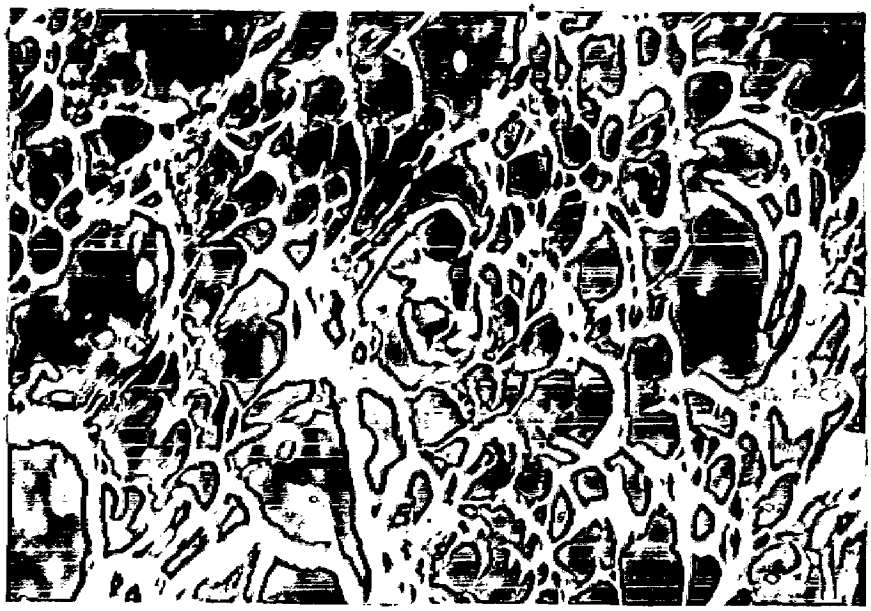

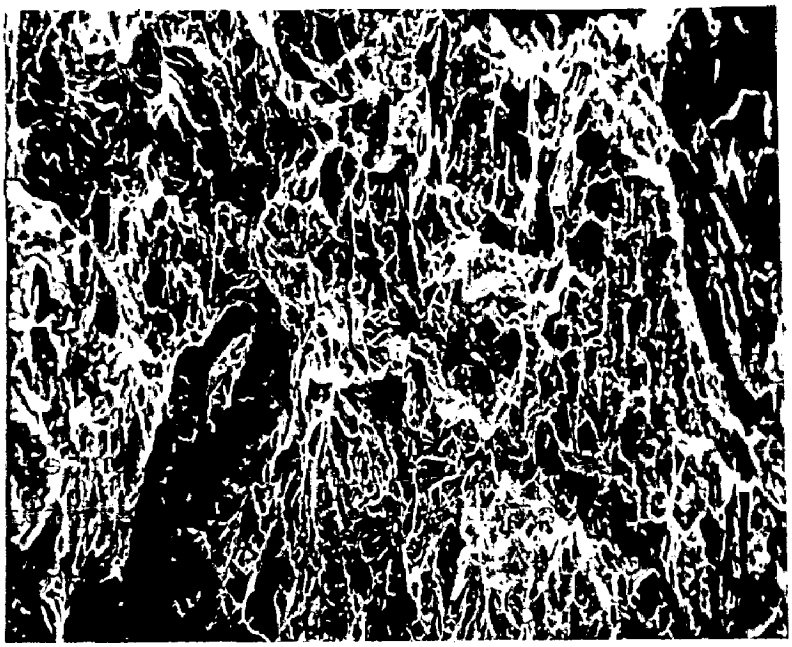

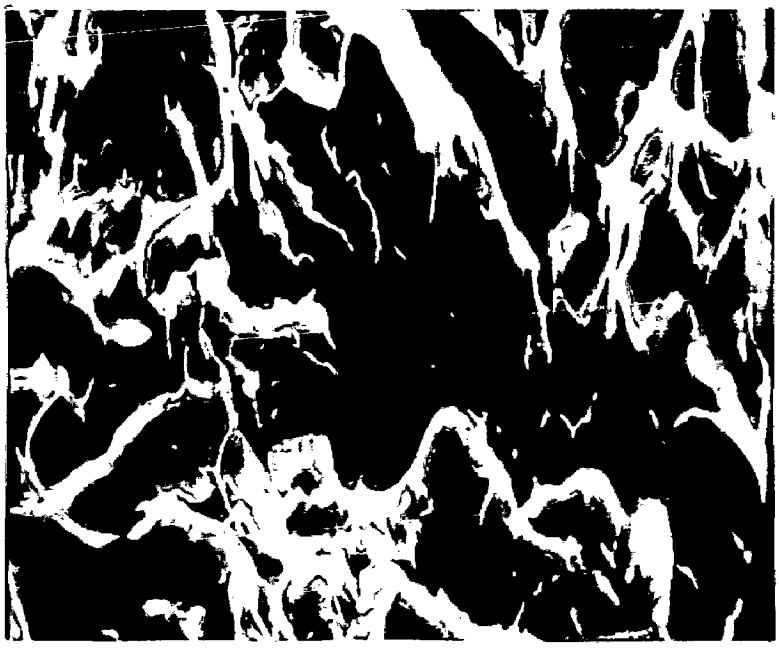

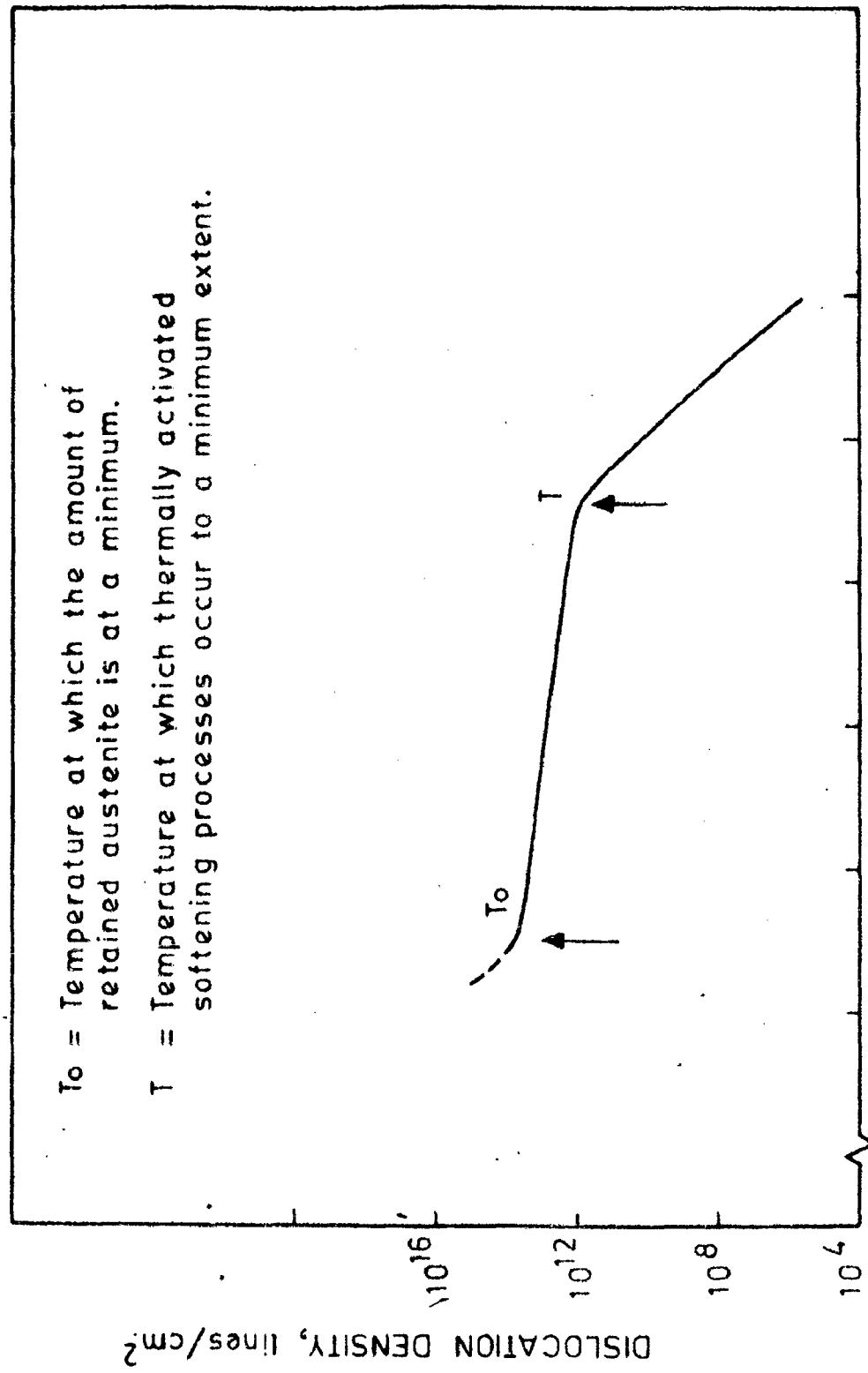

FIG. 7.1 PROBABLE VARIATION IN DISLOCATION DENSITY AS INFLUENCED BY TRANSFORMATION TEMPERATURE.